XN-AA2-750-A

RESEARCH AND DEVELOPMENT OF SOLAR-POWERED DESICCANT REFRIGERATION FOR COLD-STORAGE APPLICATIONS

(Grant No. DPE-5542-G-SS-4057-00)

Final Report

by

Prof. R. H. B. Exell
Professor

Dr. S. C. Bhattacharya
Associate Professor

and

Y. R. Upadhyaya
Research Associate

Asian Institute of Technology
P.O. Box 2754, Bangkok 10501
Thailand

1987

CONTENT

I. Requirement of Cold Storage in Thailand 1

1. Introduction 1
1.1 Requirement of Refrigeration and Cold Storage in Thailand 2

II. Summary of first year's work 5

2. Brief Summary 5
2.1 Occurrences of Natural Zeolites 6
2.2 Occurrences of Natural Zeolites in Japan 9

III. Zeolite-Water Solar Refrigerator 11

3. Introduction 11
3.1 Specifications 11
3.2 Experimentation, Test Results, and Conclusions 11

IV. Work carried out at AIT on Charcoal-Methanol Pair 18

4. Introduction 18

4.1 Experimental Setup and Procedure 18

4.2 Data Analysis and Results 20
4.2.1 Applications of Dubinin Equation 20

4.3 COP Calculations 29
4.3.1 Ideal Cycle 29
4.3.2 Heat Balances in the Cycle 36
4.3.3 Computation of COPs and Results 37

V. AIT Charcoal-Methanol Solar Refrigerator 41

5. Introduction 41

5.1 Design of the System 41
5.1.1 Heat Transfer in the Cycle 43
5.1.2 Design of Components 44
5.1.3 Pressure Drop in Connecting Tubes and Charcoal 49

5.2 Preparation for Tests 53
5.2.1 Calibration of Level Glass of Receiver/Evaporator 53
5.2.2 Overall Heat Loss Coefficient of Receiver/Evaporator Box 53
5.2.3 Leak-tightness Tests 56
5.2.4 Preparation of Charcoal for Test 56
5.2.5 Charging of the System 58
5.2.6 Instrumentation 58

5.3 Testing Procedure and General Observations 60
5.3.1 Solar Radiation 60
5.3.2 Ambient Temperature 60
5.3.3 Collector Temperature 60
5.3.4 Condenser Temperature 60
5.3.5 Receiver/Evaporator Temperature 65

5.4 Experimental Data Analysis 65
5.4.1 Initial Analysis 65
5.4.2 Detailed Analysis 67

5.5 Results and Conclusions 74

5.6 Cost and Economics of the System 74
5.6.1 Cost of the System 74
5.6.2 Economic Evaluation 74
5.6.3 Cost Comparison with Photovoltaic Refrigerators 77

5.7 Recommendations for the Future Work 77

REFERENCES 78

APPENDIX A

PHOTOGRAPHS

I REQUIREMENT OF COLD STORAGE IN THAILAND

1. Introduction

The need of refrigeration and cold/cool storage in the developing countries is mainly for the storage of foodstuffs such as for milk chilling, storage of fish, meat, fruits and vegetables and the storage of medical supplies.

Most of the rural areas of the world produce ample foodstuffs but losses are high due to lack of proper preservation facilities like refrigeration. The losses have been reported to be substantial and sometimes of the order of 50% in the interval between production and consumption (FAO, 1984). One of the acute needs of cold/cool storage is for the fruits and vegetables both in the temperate and tropical areas of the developing countries. In a temperate climate much of the production of the fruits and the vegetables is confined to short growing seasons and storage is essential to supply products after harvesting seasons. In a tropical climate the production can be extended but storage is still needed mainly due to the following reasons:

i. To remove the field heat immediately after harvesting to prevent overripening, deterioration and ultimate destruction of the fruits and vegetables.

ii. For short term storage around the production areas before being transported to big cold storages or for distribution.

iii. To extend the marketing period and increase the value of sales.

iv. To wait for a favorable market response.

Around two billion people, about half of the world population, live in the rural areas and villages of the developing countries. In most of the developing countries living conditions of the majority are poor and there is not only malnutrition but very high incidence of disease. Infant mortality is particularly high in the rural areas; it is surprising to note that in some countries, more than one-third of the children die before the age of four (Derrik and Durand, 1986). This is because from six months of age until the fourth year of life infections and parasitic disease play a significant role in the high infant and child mortality rate. Much of this can be controlled through mass immunisation before infection occurs. The vaccines for immunisation require refrigeration during transport and storage. According to WHO, vaccines for measles, yellow fever and oral polio has to be stored at a temperature between -15°C and -25°C, and others such as DPT, Tetanus Toxoid, DT and BCG need storage temepratures between

0°C and 8°C (EPI, 1986). But there is a great dearth of refrigeration systems in rural areas of the developing countries as they do not have access to mains electricity, and other sources of fuels are either scarce or expensive. This problem has been well recognised by World Health Organisation (WHO) for storage and transportation of vaccines for their Expanded Programme of Immunisation (WHO, 1981). They also have recognised the potential of solar refrigeration for vaccine Cold Chains in remote areas where solar energy is the only reliable source of energy. Most of the work to-date has been on the use of the photovoltaic refrigerator which unfortunately are expensive. A unit of photovoltaic solar refrigerator having capacity of four litres of vaccine storage costs more than US$ 6000 (Uppal and others, 1986). Moreover, in over 40% of the field tests done by WHO, breakdowns occurred and trivial repairs needed posed serious problems in remote areas due to lack of maintenance facilities. So there is a great scope for thermally powered systems which are reliable and available at lower cost.

1.1 Requirement of Refrigeration and Cold Storage in Thailand

Thailand is an agricultural country with a population of about 60 million. Agricultural crops, fish and meat are abundant in Thailand in comparison to the other developing countries of the world. Thailand is one of the largest fishing nations of the world and ranks third largest in the region after Japan and Peoples Republic of China. The most important fruit crops are mango, durian, pomeloes, custard apple, mangosteen, orange, lime, pineapple, water melon, lichee, papaya, banana, jackfruit, guava, tamarind and rambutan. The main vegetable crops of the country are shallot, chinese radish, tomato, cabbage, cucumber, pumpkin, white gourd, taro, etc.

The demand of the tropical and sub-tropical exotic fruits like mangoes, papayas, passion fruits, tamarinds, soursop, cashew apples, cherries, jackfruits, pineapples, lichees, longans, avocados, guavas, mangosteens is rising in several countries of the west (Vandendriessche, 1976). With its central location and favorable natural resources, Thailand has the potential to become a leading exporter of tropical and sub-tropical fruits of southeast Asia. The Royal Thai Government is very aware of this potential and intensive development of agriculture, and particularly increase of production of the cash crops to increase export earning and reduce the trade deficit is a prime element of Government policy.

The major fruit and vegetable producing area is the stretch of land west of Bangkok city but now the Government is incouraging this policy throughout the country. A particular emphasis has been given to the northern mountaineous region of Thailand under the Royal Northern Project, established in 1969 (Devapriya, 1984). This area is within the so called 'Golden Triangle' considered as one of the principal opium growing areas

of the world. This Project was established under Royal patronage to persuade the local hillpeoples to cease the practice of shifting cultivation and opium growing. The area under this project is approximately 40 square kilometres. Some of the replacement crops introduced are temperate-zone fruits and vegetables, and cut flowers which sell for relatively high prices in local markets (Boon-Long, 1983). After cutting and packing in the morning, the flowers must be kept cool at 0 -- 5°C before loading into refrigerated trucks for transportation from the hills in the afternoon or next day.

To evaluate the need for cold storages in Thailand a survey of the existing cold storages was carried out. There are altogether 46 cold storages in Thailand (Saisithi, 1982), of which 24 are situated at and around Bangkok and rest are scattered in the provinces. Most of the privately owned cold stores do not have 'cool stores' to store vegetables and fruits as they are designed for the storage of frozen meats and fish for export. The details of the activities of these private cold stores are not available. So informations were sought from the Government Cold Storage Organisation of Thailand.

The Cold Storage Organisation is a state enterprise under the control and supervision of the Ministry of Agriculture and Co-operatives. This organisation has altogether eleven plants at Bangkok and different provinces in the country. The cold stores in the provinces are located in the suburbs to make them accessible to producers of vegetables and fruits. The cold stores in provinces render freezing, cold and cool storage facilities to farmers and traders. The cool stores have temperature 0 to 10°C and relative humidity above 95%. The main products stored in the cool stores are fruits, vegetables, dried fresh water and marine fish, and dried lizard etc., for local consumption and export. The fresh fish is also stored temporarily in cool stores during an intermediate waiting period for better utilization of limited freezer capacity. According to Kasemsap, (1985), the Deputy Director of the organization, the market share of the organization is approximately 20%. The privately owned cold stores are generally small, having 30 to 100 ton holding capacities. According to him, there is a great need for small cool stores having storage temperature 0 to 10°C and relative humidity above 95% located close to the production areas. The holding capacities of these units can be of the order of 10 to 30 cubic metres. Such units should be available in the North, North-East, East and the central region of Thailand. These units would be used to store fruits and vegetables for retaining the freshness and quality for better distribution and sale in the local market, or as temporary store before being transferred to bigger stores for long term storage and distribution in a wider market or for export.

These units will be of great value for farmers in the mountaineous northern region of Thailand where vegetables, fruits

and flowers are grown as a part of crop replacement program to reduce deforestation and opium growing by hillpeoples. Emphasis has been placed on high-priced vegetables which could not be grown well or could be grown only during limited periods in the lowlands. But very heavy post-harvest losses have been reported mostly due to lack of proper storage conditions. Losses up to 75% on the route from Chiang Mai to Bangkok (a distance of 700 km) have been reported (Boon-Long, 1983). The major reason for this has been cited as lack of pre-cooling before transportation. So the small cool stores could be used as pre-coolers shortly after harvesting or a short term storage. These units might as well help in the proper utilization of 'cool store' capacities of the existing big plants, only 30 to 40% of whose total holding capacities are utilized at present.

To implement such projects in different parts of country government incentive is needed in terms of soft and sub-loans with the special purpose of developing rural areas. According to Kasemsap (1985) such loans could be channelled through the Government Cold Storage Organisation which has expertise and manpower to initiate and implement such projects.

The number of villages which had no access to mains electricity was about 47,725 during the year 1979, and in spite of the rural electrification programs of the Provential Electricity Authority this number is expected to increase to 55,000 by 1999 (Chantavorapap, 1979). The health posts of these villages are supplied with vaccines by the nearby hospitals or health centres with electricity and transported in ice boxes.

II SUMMARY OF THE FIRST YEAR'S WORK

2. Brief Summary

During the first year, a hybrid system which combines a solar powered intermittent ammonia-water absorption refrigeration cycle, a solid desiccant cooling cycle to cool the condenser, and positive ventilation with ice bank cooling to use the ice produced effectively, was studied.

The solid desiccant cycle can reduce the temperature of the condenser and increase the ammonia generation approximately by 50%. This also means increase in the yield of ice by the same proportion. The collector/generator of the ammonia-water system then operates at lower temperatures, which gives a better solar collection efficiency. Other indirect benefits of this system would be on the life of the collector/generator as it would be subjected to lower temperature and pressure induced stresses.

If the solid desiccant cycle is used to cool the condenser, the amount of ice increases, but at the cost of a lot of extra hardware like desiccant beds, solar air heaters, air blowers and the evaporative condenser. This system will have moving parts such as complex air switching arrangements which will need parasitic power. Such a system cannot be used in places which do not have an electricity supply.

Although the technology of the ammonia-water system is proved it has certain practical disadvantages: (1) the high pressure and consequent heaviness of the equipment, (2) the corrosiveness of the fluid, (3) the problem of rectification (removing water from the ammonia during generation), and (4) as the efficiency of the cycle decreases with a increased condenser temperature an air cooled condenser cannot be used, especially in hot countries.

These problems can be avoided by using solid adsorption systems. A literature survey of solid adsorption refrigeration revealed the development of the zeolite 13X-water systems in France(Meunier and Mischer, 1979). But this pair could only produce an evaporation temperature of $0^{o}C$ at heat sink temperatures of $50^{o}C$, typical of the air cooled condensers in tropical climate. For ice making, the zeolite 13X-CH_3OH pair was reported to be suitable and it was possible to achieve an overall COP of 0.13. Bechec and others (1981) reported the design of a system using zeolite 13X-CH_3OH pair. But a later study by Guilleminot and others(1981) found the above pair chemically unstable due to a catalytic reaction which forms dimethyl ether.

Synthetic zeolites such as zeolite 13X, zeolites 3A to zeolite 10 A have ordered crystalline structure, uniform pore size, and can be tailor-made to suit a particular use. But for solar refrigeration natural zeolites are preferred as the heat of

adsorption of water on zeolites is about 2791 kJ/kg compared to a value of about 4187 kJ/kg in the case of the synthetic zeolites. Moreover, natural zeolites are reported to be about ten times cheaper than the synthetic ones (Tchernev, 1978).

Dehydrated natural zeolites, especially chabazite crystals, rapidly adsorb many kinds of refrigerant gas, ranging from water vapour and ammonia to carbon dioxide, freons, methyl alcohol ethyl alcohol, and formic acid, etc. According to Tchernev (1984) the amount of any refrigerant adsorbed by the zeolites is about 30% by weight and the adsorption phenomenon is reversible especially in the case of chabazite and modernite.

The adsorption isotherms of the zeolites have an extremely non-linear pressure dependence while silica gel has almost linear pressure dependence (Tchernev, 1978). So the zeolites can adsorb large quantities of refrigerant vapour at ambient temperature and low partial pressures. When heated, they can desorb a large amount of the refrigerant vapour even at the high condenser temperatures, i.e. at the higher pressures in air cooled condensers. For the extreme condensation and evaporation pressures of 7.3 kPa and 0.5 kPa, respectively, the differential water loading of most natural zeolites is about 7% by weight between ambient temperature and 120°C, which is about the maximum temperature attainable with flat-plate collectors with a selective surface. The daily integrated efficiency of the zeolite water pair (total cooling/daily total solar radiation) has been experimentally found by Tchernev to be in the range 12 to 15% with a peak at 30%.

Considering the merits of zeolites in solar cooling, a survey of the availability of the natural zeolites was conducted to look for the possible sources for future use in this region.

2.1 Occurrence of Zeolite Minerals

Zeolites, generally occur in sedimentary rocks and in basaltic igneous and volcanic rocks. Selected examples of the sedimentary zeolites are tabulated in Table 2.1. The different natural zeolites with the countries of their occurrences are given in Table 2.2 (Breck, 1974).

Although there are more than thirty-four known zeolite minerals and about 100 types of synthetic zeolites, only a few have practical significance either because of the dehydration irreversibility, or because of structural collapse, or because they do not occur in sufficient quantities. Out of these thirty-four zeolite minerals only seven --- modernite, clinoptilolite, ferrerite, chabazite, erionite, phillipsite, and analcime --- occur in sufficient quantity and purity to be individually considered as viable mineral resources (Vaughan, 1978). Among the seven zeolite minerals, phillipsite is one of the more abundant mineral species in the earth. Over large areas of the

Table 2.1: Sedimentary Zeolite Deposits.

Age	*Location*	*Zeolites*	*Depositional Environment*
1 Some typical zeolites in deposits of saline, alkaline nonmarine environments			
Recent sediments	Lake Natron, Tanzania	Analcime	Sodium carbonate lake of high salinity
Recent-late Pleistocene	Teels Marsh, Nevada	Phillipsite, clinoptilolite, analcime	Sodium carbonate lake
Late Pleistocene	Owens Lake, California	Phillipsite, clinoptilolite, erionite, analcime	Saline, alkaline lake
Late Pleistocene	Olduvai Gorge, Tanzania	Analcime, chabazite, phillipsite	Playa Lake
Middle Pliocene to Middle Pleistocene	North Central Nevada	Erionite, phillipsite	Saline, alkaline lake
Pliocene	Central Nevada	Erionite, clinoptilolite, phillipsite	Saline, alkaline lake
Early and Middle Eocene	Wyoming	Analcime	Saline, sodium carbonate lake
Triassic	New Jersey	Analcime	Saline lake, soda-rich
Early Carboniferous	Tuva, Siberia	Analcime, laumontite	Saline and alkaline lake or lagoon
2 Zeolites deposited in marine and fresh-water environments			
Recent sediments	Gulf of Naples	Analcime	Shallow marine
Recent and Pleistocene	Pacific and Indian Oceans	Phillipsite, harmotome clinoptilolite, natrolite	Deep-sea floor
Recent and late Pleistocene	Atlantic Ocean	Clinoptilolite	Deep-sea floor
Late Miocene and Pliocene	Central Nevada	Clinoptilolite	Lacustrine
Oligocene to early Pliocene	North Central Nevada	Clinoptilolite	Lacustrine
Miocene	Northern Honshu	Clinoptilolite, mordenite	Marine and lacustrine
Oligocene	South Dakota and Wyoming	Clinoptilolite, erionite	Fluvial
Cretaceous	Ural Mountains	Mordenite	Marine
Cretaceous	New Guinea	Laumontite	Marine
Early to late Triassic	New Zealand	Analcime, heulandite, clinoptilolite, laumontite	Marine
Carboniferous	England	Analcime	Land surface
Early Paleozoic or Precambrian	Georgia, USA	Laumontite	Subaerial and subaqueous

Table 2.2: A List of Zeolite Minerals.

Name	*Structure Group*	*Year Discovered*	*Typical Occurence in Igneous Rocks*	*Examples of Occurence in Sedimentary Rocks*
Analcime	1	1784	Ireland, New Jersey	Extensive; Wyoming, etc. Deep sea floor
Bikitaite	6	1957	Rhodesia	
Brewsterite	7	1822	Scotland	
Chabazite	4	1772	Nova Scotia, Ireland	Arizona, Nevada, Italy
Clinoptilolite	7	1890	Wyoming	Extensive; Western U. S., Deep sea floor
Dachiardite	6	1905	Elba, Italy	
Edingtonite	5	1825	Scotland	
Epistilbite	6	1823	Iceland	
Erionite	2	1890	Rare, Oregon	Nevada, Oregon, U.S.S.R.
Faujasite	4	1842	Rare, Germany	
Ferrierite	6	1918	Rare, British Columbia, Italy	Utah, Nevada
Garronite	1	1962	Ireland, Iceland	
Gismondine	1	1816	Rare, Italy	
Gmelinite	4	1807	Nova Scotia	
Gonnardite	5	1896	France, Italy	
Harmotome	1	1775	Scotland	
Herschelite	4	1825	Sicily	Arizona
Heulandite	7	1801	Iceland	New Zealand
Kehoeite	1	1893	Rare, South Dakota	
Laumontite	1	1785	Nova Scotia, Faroe Islands	Extensive; New Zealand, U.S.S.R.
Levynite	2	1825	Iceland	
Mesolite	5	1813	Nova Scotia	
Mordenite	6	1864	Nova Scotia	U.S.S.R., Japan, Western U.S.
Natrolite	5	1758	Ireland, New Jersey	
Offretite	2	1890	Rare, France	
Paulingite	1	1960	Rare, Washington	
Phillipsite	1	1824	Ireland, Sicily	Extensive, Western U.S., Africa, Deep sea floor
Scolecite	5	1801	Iceland, Colorado	
Stellerite	7	1909		
Stilbite	7	1756	Iceland, Ireland, Scotland	
Thomsonite	5	1801	Scotland, Colorado	
Viseite	1	1942	Rare, Belgium	
Wairakite	1	1955	New Zealand	
Yugawaralite	1	1952	Japan	

Pacific Ocean sediments have been found that contain over 50% phillipsite (Breck, 1974).

Extensive deposits of various zeolites occur in North and Central America, Central and Southern Europe, Russia, Japan, Korea and New Zealand. A wide variety of the zeolite minerals like chabazite, thomsonite, natrolite, clinoptilolite and stilbite are reported to be available in abundance in Deccan Traps(specially Poona, India) by Wadia (1975) and Marel & Beutelspacher (1976). Small deposits of fibrous zeolites are reported to be found at Mount Wyatt, Upper River Madai, middle reaches of River Tingakayu, Salagan Island and abundant deposits have been found in Kalunpang in Simporna Peninsula of North Borneo (Kirk, 1962). Abundant high grade natural zeolites such as clinoptilolite, heulandite, mordenite, ferririte, erionite, analcinite, chabazite, mesolite, and natrolite are found in the Yeongil area, South Korea (Noh and Kim, 1986). Significant deposits of the natural zeolites of importance as given by Marel and Beutelspacher (1976) are given in Table 2.3.

Table 2.3: The countries having significant deposits of natural zeolites.

Zeolite Type	Country of Origin
Chabazite	Hungary, Faroe Islands, Ireland; Bohemia, Czechoslovakia; Global Station, Oregon, New Jersey and Nova Scotia.
Clinoptilolite	Hector, California.
Stilbite	Banat Csiklova, Roumania; Hanz, West Germany; Iceland, Faoer Islands, Nova Scotia.

2.2. Occurrences of Natural Zeolites in Japan

In this region, Japan, India and Korea are the likely potential sources for natural zeolites. Zeolite mineral was originally discovered in sedimentary rock in Japan (Ota and Sudo, 1979). The most commonly found zeolite tuffs (Zeolite having particle size smaller than 4mm in diameter), modernite and clinoptilolite, are both abundant in Japan. Both the modernite and the clinoptilolite-tuff are reported to show excellent adsorptive properties compared with commercial adsorbents, such as synthetic zeolites 5A, silica gel, and activated alumina. Because of high affinity for water, clinoptilolite-tuff is primarily used as a desiccant. About 5000 to 6000 tons of these

zeolites per month, are mined from the different open-pit mines in Japan. Some of the zeolite mines in Japan are listed in Table 2.4 (Minato, and Tamura, 1978).

Table 2.4: Zeolite Mines in Japan.

Mine	Prefecture	Amount of ore (t/month)	Zeolite
Osiyamambe	Hokkaido	100–200	Clinoptilolite
Futatsui	Akita	150–300	Clinoptilolite
Yasawagi	Akita	100–200	Clinoptilolite and mordenite
Itado	Akita	Spot (about 300 t)	Mordenite
Itaya	Yamagata	4000–5000	Clinoptilolite
Shiroishi	Miyagi	100–200	Mordenite
Ten'ei	Fukushima	100–200	Mordenite
Maji	Shimane	Spot (about 300 t)	Mordenite
Iwami mine	Shimane	50–100	Clinoptilolite

III Zeolite-Water Solar Refrigerator

3. Introduction

Some zeolite-water solar refrigerators were built and tested mainly in the cold countries like USA and France but none of them have been tested in a tropical climate. It is essential to evaluate the performance of such systems in this climate to find out their suitablity for possible future use. So, a zeolite-water solar refrigerator manufactured by Zeopower Company, USA was imported and tested at Asian Institute of Technology. This is a closed cycle intermittent adsorption type refrigerator which has natural zeolite as adsorbent and water as the refrigerant. A schematic diagram of this refrigerator is shown in Fig. 3.1. It consists of a selectively coated solar collector with a single glass cover. The solar collector is a rectangular copper pan with a lid, and contains about 25.63 kg of dehydrated natural zeolite about 50mm deep. The tilt angle of the solar collector is 14° which is almost equal to the latitude of AIT. This system consists of an air cooled condenser placed under the solar collector. A glass bottle graduated in BTU's, and housed in an insulated box acts as the receiver/evaporator. These components are connected by copper tubes. This system operates below the atmospheric pressure, so it was evacuated, leak tested, filled with about 8.4 kg of water and hermetically sealed before being shipped for testing at AIT. The specifications supplied by the Zeopower Company, USA are as follows:

3.1 Specifications of the refrigerator

Type: Liquid with Solid/Gas Adsorption System.
Model : SR-4
Gross Collector Dimensions : 29" x 47" = 0.8786 m^2
Net Collector Absorbing Surface Area : 25" x 43" = 0.6935 m^2
Overall Dimensions:

Height	46 1/4"	(1.175 m)
Width	30 1/2"	(0.7742 m)
Depth	48 1/2"	(1.232 m)

Refrigeration Capacity : 4 Cubic feet = 0.112 m^3
Ice Making Capacity : 15 lbs or 6.803 kg per day.
Storage Capacity : Three days of bad weather after collector surface has been exposed to a series of three or more sunny days.
Maintenance Requirements : None.
Moving Part : None except the door of the refrigerator box.
Total Weight : 215 lbs (97.505 kg).

3.2 Experimentation, Test Results and Conclusions

During intial testing, the refrigerator was instrumented with a few calibrated k-type temperature sensors which were attached to the top and bottom of the condenser, top and bottom of the

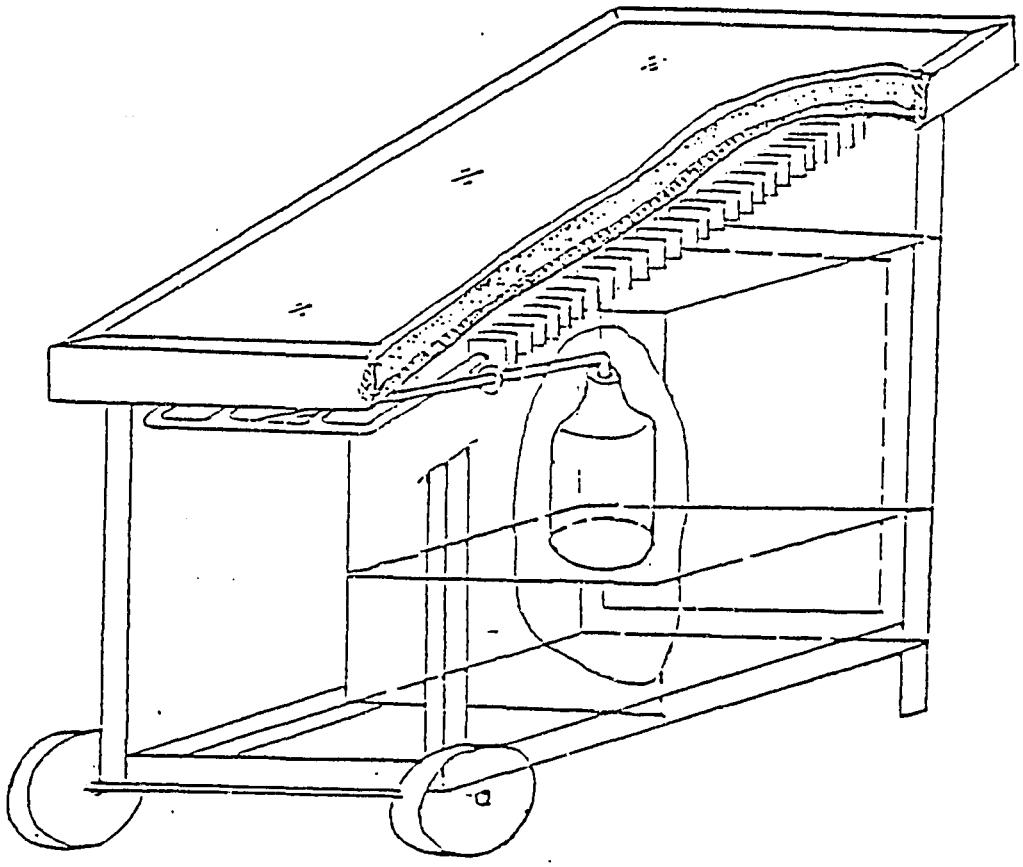

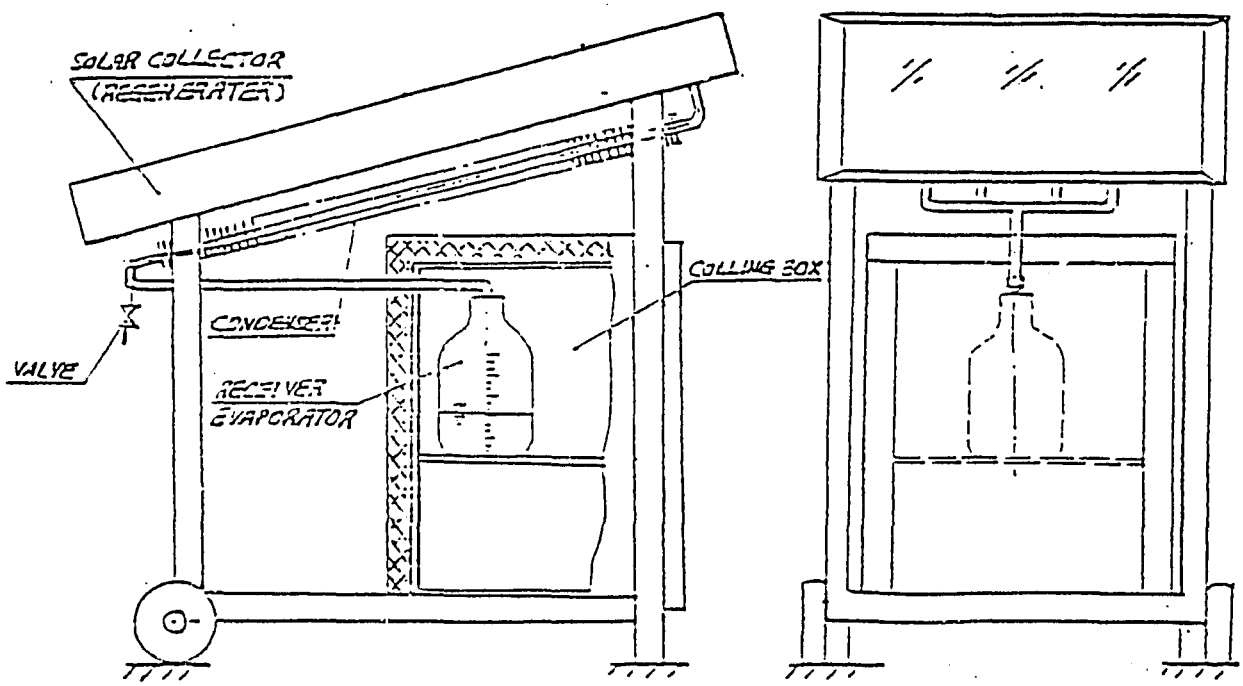

Fig. 3.1: Schematic diagram of the Zeolite-Water Refrigerator.

glass bottle (receiver/evaporator), and one senser was left hanging in the cooling chamber. These temperature sensors were connected to a Fuji Chart Recorder and values were recored continuously. Integrated and the instanteneous values of solar radiation incident on the surface of the collector were measured by a calibrated diffused type pyranometer with integrator, and hourly values were read from a digital display. The amount of heat rejected by the condensing water during desorption was estimated by taking the difference of water level in the morning and late afternoon from the glass bottle, calibrated in BTU's by the manufacturer. Similarly, the difference of readings between late afternoon and the early morning gives the net cooling produced by evaporation of water from the glass bottle during night. The water level in the receiver/evaporator bottle was read every hour until 24:00 hours.

The refrigerator was in transit for a couple of weeks and the zeolite had adsorbed approximately 7.9 kg of water (30.71 wt. %, dry basis) out of about 8.37 kg charged into the system. During the days of average insolation, water started to desorb between 10:00 and 11:00 hours and the desorption continued until the peak temperature for the day was reached generally by 15:00 hours. The zeolite, although, starts to adsorb water immediately after peak collectr temperature but noticeable change in water level was observed only after 18:00 hours. During first few days comparatively large quantities of water desorbed as the zeolite was saturated with water during transit, but only a fraction of desorbed water was adsorbed during subsequent nights. The system took several days to achieve near equilibrium condition as could be seen comparing the amount of heat rejected and cooling produced from Table 3.1. The cooling produced during night varied from 316 to 844 kJ. It was observed that the condenser temperature was very high and reached up to 57°C. During 5, 6, and 7 November 1986 two blowers were used to cool the condenser. Although the use of blowers did not help to reduce the condenser temperature significantly but the average condenser temperature was lower and the integrated efficiency or Solar COP (cooling produced/total daily incident solar radiation) was between 6.1% and 6.7% which are higher.

As stated by the manufacturer, the system should be able to produce about 6.8 kg of ice during a clear day. To produce that much ice the system should cycle more than 1 kg of water. But even after several days of operation, the receiver/evaporator bottle contained only about 2.45 kg of water (estimated by the measurement of the external dimensions of the glass receiver/evaporator); and only a fraction of this(approximately 130 to a maximum of 360 gm of water) was readsorbed during cooling period. The system was not able to produce ice and the sensor attached to the bottom of the glass bottle recorded temperatures always above 4°C. Moreover, the condensation starts in the glass bottle, as it is the coldest and it continues

Table 3.1: The summary of test results of Zeolite-Water Solar Refrigerator (22 Oct. 1986 -- 16 May 1987).

Date d/m/y	Ambient Temp. Max. (C)	Ambient Temp. Min. (C)	Evaporator Temp. Minm. (C)	Zeolite Temp. Max. (C)	Zeolite Temp. Min. (C)	Condenser Temp. Max. (C)	Heat Rejected (kJ/day)	Cooling Produced (kJ/day)	Solar Radiation (MJ/day)	Solar COP (%)	Remarks
22/10/86	31.0	27.5	7.2	--	--	48.0	3166.2	527.0	12.029	4.4	
23/10/86	30.6	27.7	7.2	--	--	48.7	369.3	485.5	7.520	6.5	
24/10/86	33.4	27.7	7.2	--	--	55.9	1224.3	580.5	11.122	5.2	
25/10/86	33.0	28.3	7.1	--	--	47.4	52.8	527.7	6.002	8.8	Initial
26/10/86	33.0	28.3	5.8	--	--	55.0	949.9	580.5	11.561	5.0	Testing
27/10/86	31.3	28.5	6.6	--	--	57.0	369.4	527.7	8.568	6.2	without
28/10/86	34.1	27.3	5.8	--	--	51.0	527.7	527.7	9.172	5.8	any
30/10/86	28.4	25.8	5.1	--	--	47.0	527.7	316.6	9.612	3.3	modifications.
31/10/86	29.9	26.4	6.4	--	--	45.1	316.6	369.4	9.030	4.1	
1/11/86	32.0	27.3	7.2	--	--	52.0	949.8	474.9	11.918	4.0	
2/11/86	31.7	27.0	3.7	--	--	52.0	633.2	633.2	12.248	5.2	
3/11/86	33.7	27.7	4.1	--	--	61.0	738.8	633.2	11.726	5.4	
4/11/86	33.7	25.9	3.8	--	--	57.0	686.0	686.0	13.099	5.2	
5/11/86	33.4	23.5	6.0	--	--	50.0	633.2	791.5	11.754	6.7	Tests
6/11/86	36.2	23.8	6.0	--	--	52.0	791.6	738.8	12.029	6.1	with
7/11/86	32.7	24.1	5.1	--	--	48.0	897.1	844.3	12.173	6.9	two blowers.
9/12/86	29.6	21.0	8.8	105.0	26.3	46.6	622.1	400.9	11.369	3.5	
10/12/86	29.0	18.7	6.6	109.0	22.8	48.1	506.4	316.5	12.056	2.6	Tests after
23/12/86	32.0	18.6	10.6	109.0	21.8	49.9	422.0	316.5	11.232	2.8	the loss of
24/12/86	32.1	19.7	9.3	111.0	24.8	50.8	527.5	422.0	11.946	3.5	Inert Gas.
25/12/86	34.6	19.4	8.8	112.0	24.3	54.1	474.8	474.8	12.221	3.9	
15/5/87	36.2	24.7	10.2	114.0	26.8	44.2	1022.5	279.1	10.661	2.6	With mirror
16/5/87	37.5	26.1	8.0	127.0	29.0	40.9	930.4	325.6	14.056	2.3	boosters

Note:

1. Heat rejected by the condenser is equal to the latent heat of water condensed in the receiver.

2. The Zeolite temperature was assumed equal to mean container temperature.

3. Cooling produced at night is equal to the heat extracted by the evaporation of water, while the latent heat of evaporation of water is 2326 kJ/kg (Tchernev, 1979).

until the temperature of the bottle reaches the ambient temperature. This has serious consequences as the ice produced by the system is not removable and part of the cooling produced during night will be used to condense the water vapour.

After this initial testing, some sensors were attached to the top and bottom of the absorber plate to measure the approximate collector and zeolite temperatures. During this modification due the defective valve in the supplied system, some air leaked into the system which was evacuated immediately after the pressure gauge and isolation valves assembly was soldered. The temperature of the zeoloite panel(collector) during a clear day having total incident solar radiation between 18 and 19 MJ/m^2-day reached up to 105°C; even then it was not high enough to give significant desorption. The amount of water cycled was found less than 1%. Since the performance of the system became worse, it was decided to evacuate the system as completely as possible and recharge again. The system was further modified and tested by Zhu (1987). In one important modification, two mirror boosters each having about 0.812 m^2 area were attached along the length of the system (Fig. 3.2). The solar collector was heated using mirror boosters and evacuated during late morning until late afternoon almost for a month. The minimum concentration of water in the zeolite reached about 16.5% from 31.71 wt. % initially charged into the system. Then the system was charged with a small quantity of water in steps over of sevaral days. The charging system with isolation valves is shown in Fig. 3.3. The performance of the recharged system (water content in the zeolite about 21.4 wt. %, dry basis) is shown in Table 3.1 (8-16 May, 1987). During these days, the average collector temperature was found higher than the average found earlier as there was less water charged into the system, but the amount of water cycled was less and surprisingly zeolite did not adsorb more than 22 wt.%, (dry basis) in subsquent charging. It is seen from Table 3.1 that the solar COP of the recharged system varied between 2.3 and 2.6%, which is lower than the unmodified system. We came to know about a small amount of inert gas initially charged into the system the supplier (Worek, 1986) which unfortunately escaped during first modification. Since, no further information about the type and the quantity of the inert gas was available, and since the system did not perform as well when the inert gas was intact, no further tests were carried out.

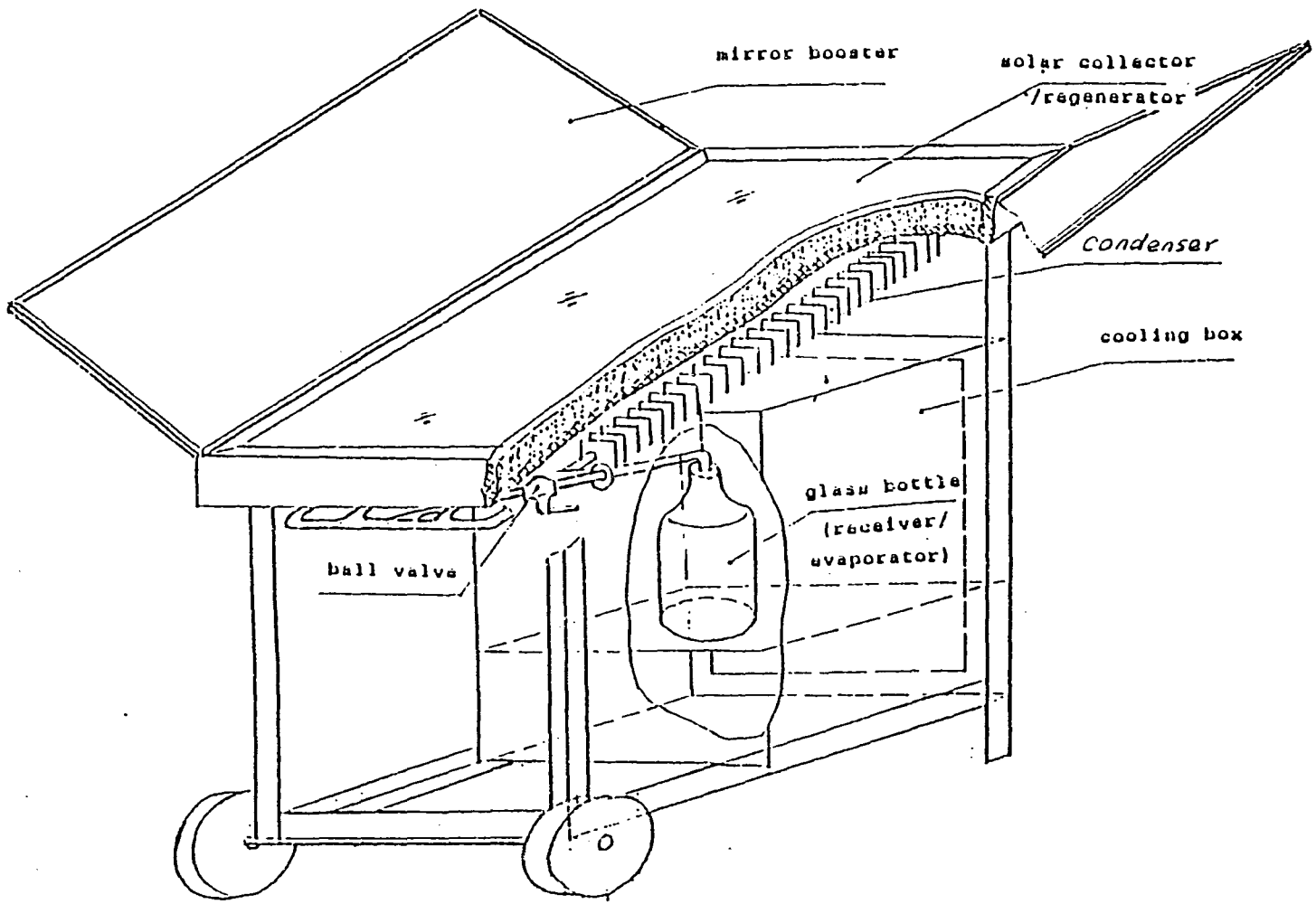

Fig. 3.2: Modified Zeolite-Water Refrigerator.

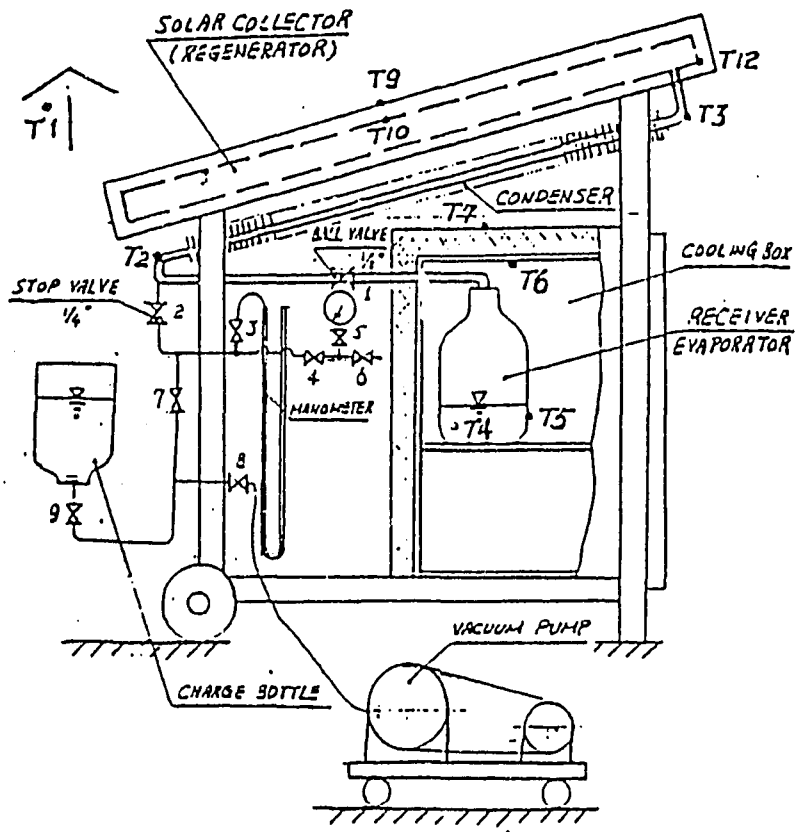

Fig. 3.3: Modified Charging System.

IV Work Carried out at AIT on the Charcoal-Methanol Pair

4. Introduction

The performance of the zeolite-water solar refrigerator was found not very promising during the initial testing and further research was done to investigate other pairs.

The comparison of synthetic zeolite 5A, 13X and activated charcoal(AC) with different refrigerants R11, R12, R22, and R114 done by Critoph and Vogel (1986) proved charcoal as the preferable adsorbent for solar cooling. We also became aware of the study done by Grenier and Pons(1983), Meunier and others (1986) on synthetic zeolite-methanol and the charcoal-methanol pairs. Their study revealed that charcoal-methanol gives a better COP generally, but that when the night-time ambient temperature-evaporating temperature is particularly high then a zeolite-water combination is better. However this will require a higher generating temperature from the solar collector during the day. The comparison of zeolite 13X-water and AC 35-methanol done by Meunier and others(1986) suggest that zeolite combinations will only be superior when the temperature lift (difference between adsorption and the evaporating temperatures) exceeds 45°C. The COP is based on heat input to the adsorbent rather than the solar collector and so the reduced solar collector efficiency at higher temperatures may actually make charcoal-methanol combinations superior even at higher temperature lifts.

The others reasons for preferring activated charcoal are as follows:

1. Activated charcoals are cheaper than zeolites.
2. Activated charcoals can be made with properties to suit particular applications by varying the activation time and temperature, etc.
3. Activated charcoals (particularly coconut shell charcoal) can be manufactured in the country of origin and use.

Because of above advantages and the encouraging French results it was decided to investigate the methanol-charcoal system under the terms of the USAID contract.

The properties of the activated charcoals such as porosity, pore size, and surface area for adsorption depends upon the raw material used, the activation process and the degree of activation. Accordingly, we carried out tests to investigate the adsorption properties of some imported and locally available charcoal samples for their possible use in solar refrigeration.

4.1 Experimental Setup and Procedure

The test rig (Fig. 4.1) used to determine the equilibrium data has a brass container A which was filled with a known quantity of a activated charcoal sample (usually 100 gms), a

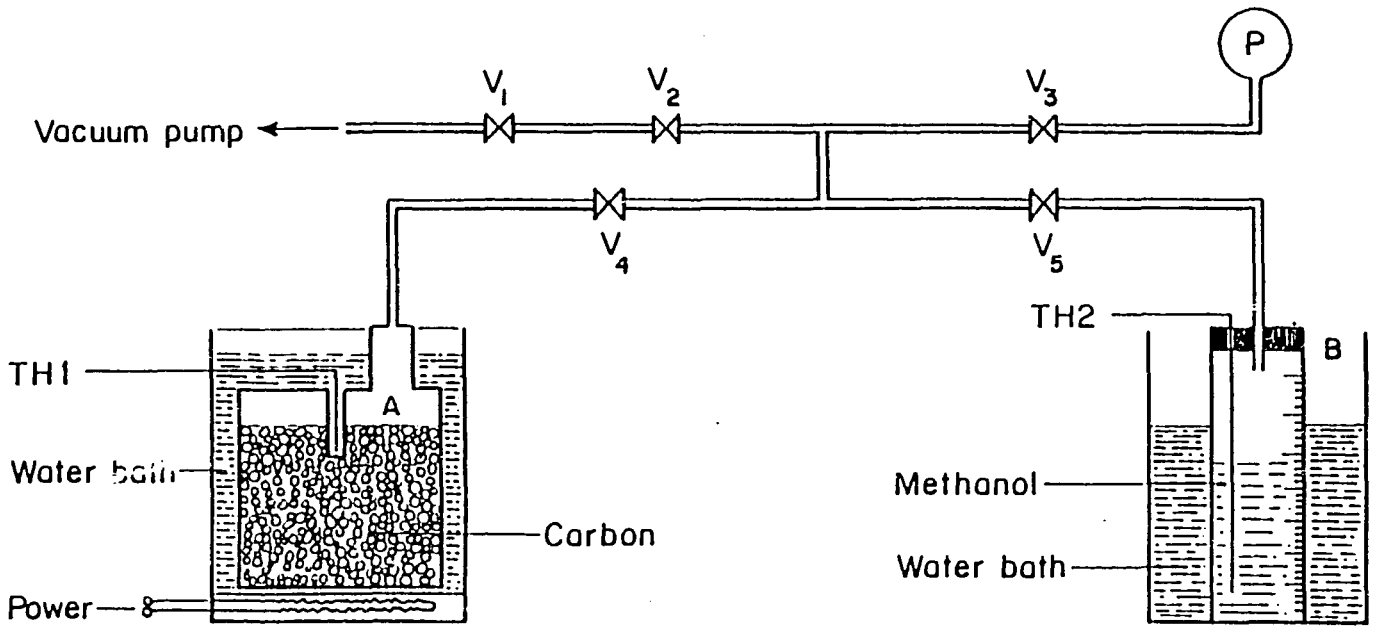

A — Activated carbon container
B — Methanol receiver cum evaporator
P — Vacuum gauge
TH1 — Thermocouple conn. for carbon temp.
TH2 — Thermocouple conn. for methanol temp.
V_1.....V_5 — Isolation valves.

Fig. 4.1: Schematic of the Experimental Setup.

graduated glass vessel B for containing methanol, and a vacuum gauge P. The methanol level can be read from the graduations of B and the quantity of methanol in the charcoal can thus be calculated at any time. The temperatures of the charcoal and methanol can be read from two calibrated k-type thermocouples TH1 and TH2. The components A, B, and P were separated by isolating valves V1 through V5 to facilitate evacuation of each components separately and checking leaks. The piping was of 1/4" soft copper and all valves were soldered to successfully maintain the system vacuum tight.

The activated charcoal was degassed over at least two days by heating the charcoal at about 100°C and continuously evacuating it. This was done to drive out impurities present in the deep pores before actual adsorption/desorption takes place. Similarly, methanol contained in vessel B was separately evacuated and a small amount of methanol was allowed to boil out to ensure no dissolved air remains in the methanol. Equilibrium data were obtained along two isobars (0.13 bar and 0.04 bar) keeping the methanol in B at constant temperature while varying charcoal temperatures. To obtain the desorption data, charcoal saturated with methanol at about 30°C was heated in steps of 10°C approximately to 100°C. Sufficiently long time was allowed to reach the near equilibrium and at each step pressure, temperature and concentration were measured. Similarly adsorption data were obtained cooling the charcoal in the steps of 10°C back to 30°C. For each sample, to get the better data points, up to three such adsorption/desorption cycles were repeated at each isobar. In case of slight deviation, the latest data were taken as correct.

In total, eight samples of activated charcoal, six imported and two local were tested. The specifications for the charcoals supplied by the manufacturers are listed in Table 4.1.

4.2 Data Analysis and Results

The data obtained along two isobars can be used easily, when plotted on a ln P versus -1/T graph, for applications like refrigerations etc. The ideal cycle, which consists of two isobars and two isosters can be easily traced in such diagrams. Since we can determine the state points on this diagram, the performance of such systems can be determined. Moreover, the slopes of the straight lines (isosters) directly give the heat of adsorption/desorption. The pressure-temperature-concentration (p-T-x) diagrams for charcoals tested are shown in Fig. 4.2 through Fig. 4.6. For three charcoals the p-T-x diagrams are not presented, due to lack of consistent data points at both the pressures.

4.2.1 Applications of the Dubinin Equation

The best established description of adsorption in activated

Table 4.1: Manufacturer's Data.

SUTCLIFFE CARBONS CO. LTD., U. K.

COCONUTSHELL BASED CARBONS

GRADE	SURFACE AREA m^2/g B.E.T. N2	*BULK DENSITY g/cc	CTC %	ASH %
203C	700 — 800	0.55 — 0.59	20 — 30	1.0 — 2.0
205C	900 — 1000	0.53 — 0.57	35 — 45	2.0 — 2.5
207C	1100 — 1200	0.49 — 0.53	50 — 60	2.5 — 3.0
208C	1200 — 1300	0.47 — 0.51	60 — 70	3.0 — 4.0
† 607	1100 — 1200	0.49 — 0.53	50 — 60	0.5 — 1.0
610	1300 — 1500	0.40 — 0.44	80 — 90	3.0 — 4.0

† Type 607 is a specially prepared acid washed carbon with low ash and high ignition temperature for use in solvent recovery or condensate de-oiling.

* The bulk density is carried out on dry base carbon with nominal mesh size 7-18BSS.

IMPREGNATED & MISCELLANEOUS SPECIAL CARBONS

207E3(EXTRUDED)	1100 — 1200	0.45 — 0.49	55 — 65	4.0 — 8.0
207E4(EXTRUDED)	1100 — 1200	0.45 — 0.49	55 — 65	4.0 — 8.0

UDP CHEMICAL CO. LTD., BANGKOK.

TYPICAL APPLICATIONS : MD-G 7746

MD-G 7746 is designed for removal of odourous atmosphere in industrial processes and in air conditioning systems, including a variety of purification and separation processes in the chemical industries.

GENERAL SPECIFICATIONS AND PROPERTIES

Mesh Sizes	4×6
Iodine Number Min.	1050
Methylene Blue Number Min.	200
Abrasion Number Min.	80
Hardness Number Min.	90
Moisture as packed Max. %	3
Residue on Ignition, Max. %	3
pH	8–9
Surface Area (N_2-B.E.T.)	1100-1200
Bulk Density, g/cc.	0.40-0.45

TYPICAL APPLICATIONS : MD-W 7830

MD-W 7830 is recommended for water purification both in municipal and industrial use. It is also popular in a variety of separation and purification processes in the organic chemical industries.

GENERAL SPECIFICATIONS AND PROPERTIES

Mesh Sizes	8×30
Iodine Number Min.	1050
Methylene Blue Number Min.	220
Abrasion Number Min.	80
Hardness Number Min.	90
Moisture as packed Max. %	3
Residue on Ignition, Max. %	3
pH	8–9
Surface Area (N_2-B.E.T.)	1150-1250
Bulk Density, g/cc.	0.50-0.55

UDP. CHEMICAL CO., LTD.

776 SOI KLONGNONGYAI SUKHAPIBAN 1 RD. BANGKAE PASRICHAROEN BANGKOK 10160
[illegible] TELEX [illegible] UCHEM TH

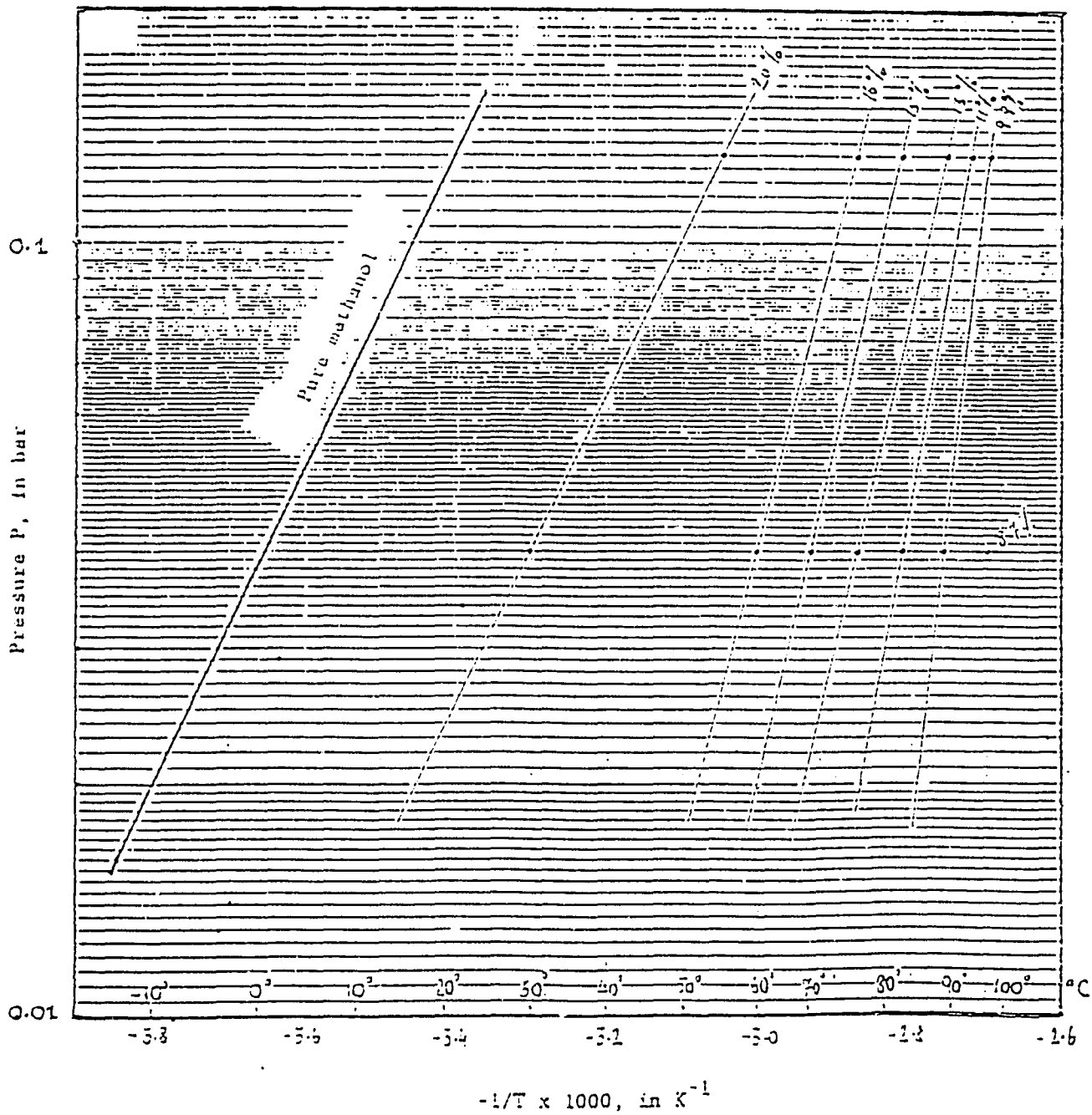

Fig 4.2: Experimental isosteres on a ln P versus -1/T plot.

(a) Carbon 207C

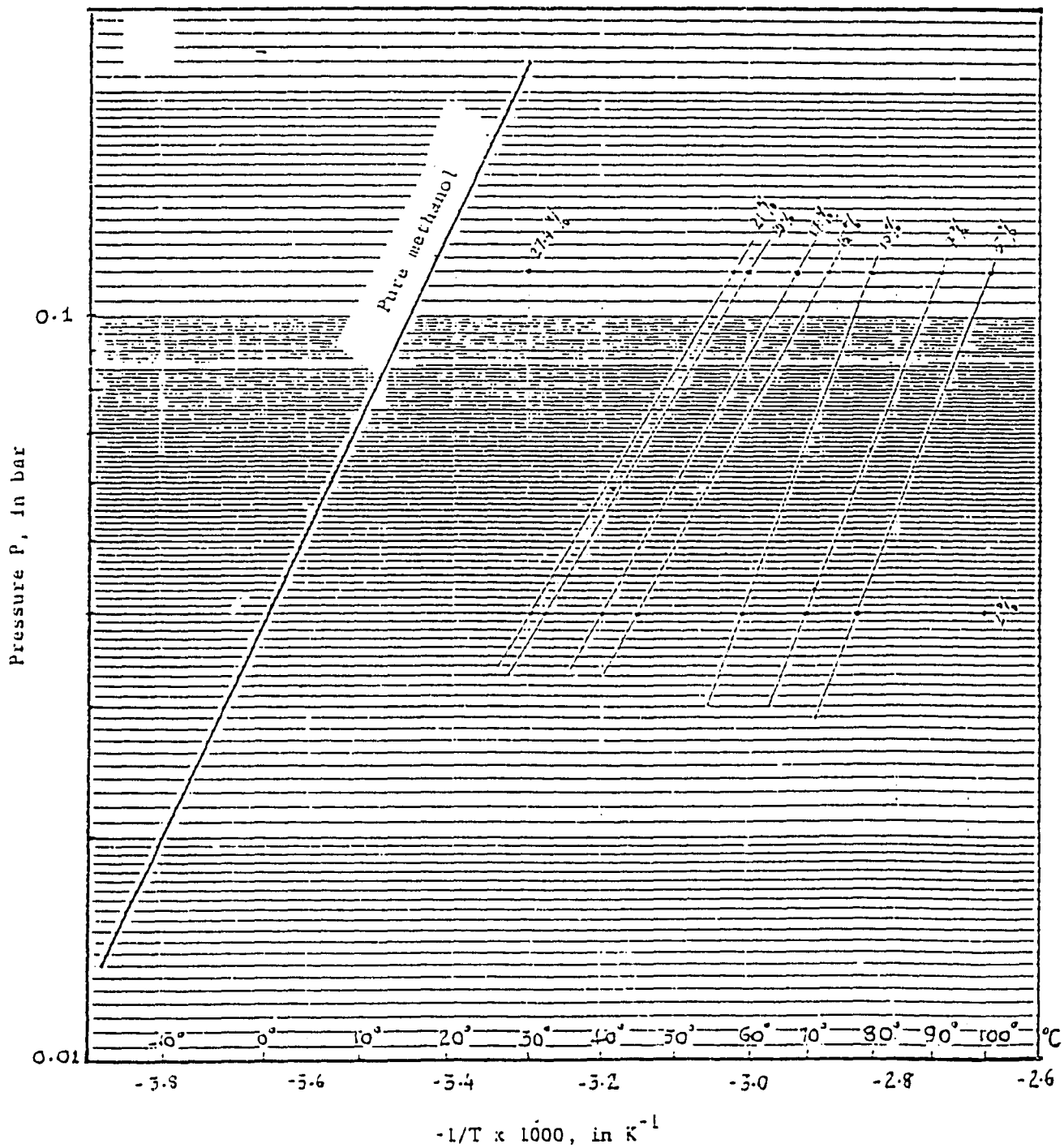

Fig 4.3: Experimental isosteres on a ln P versus -1/T plot.

(b) Carbon 207E

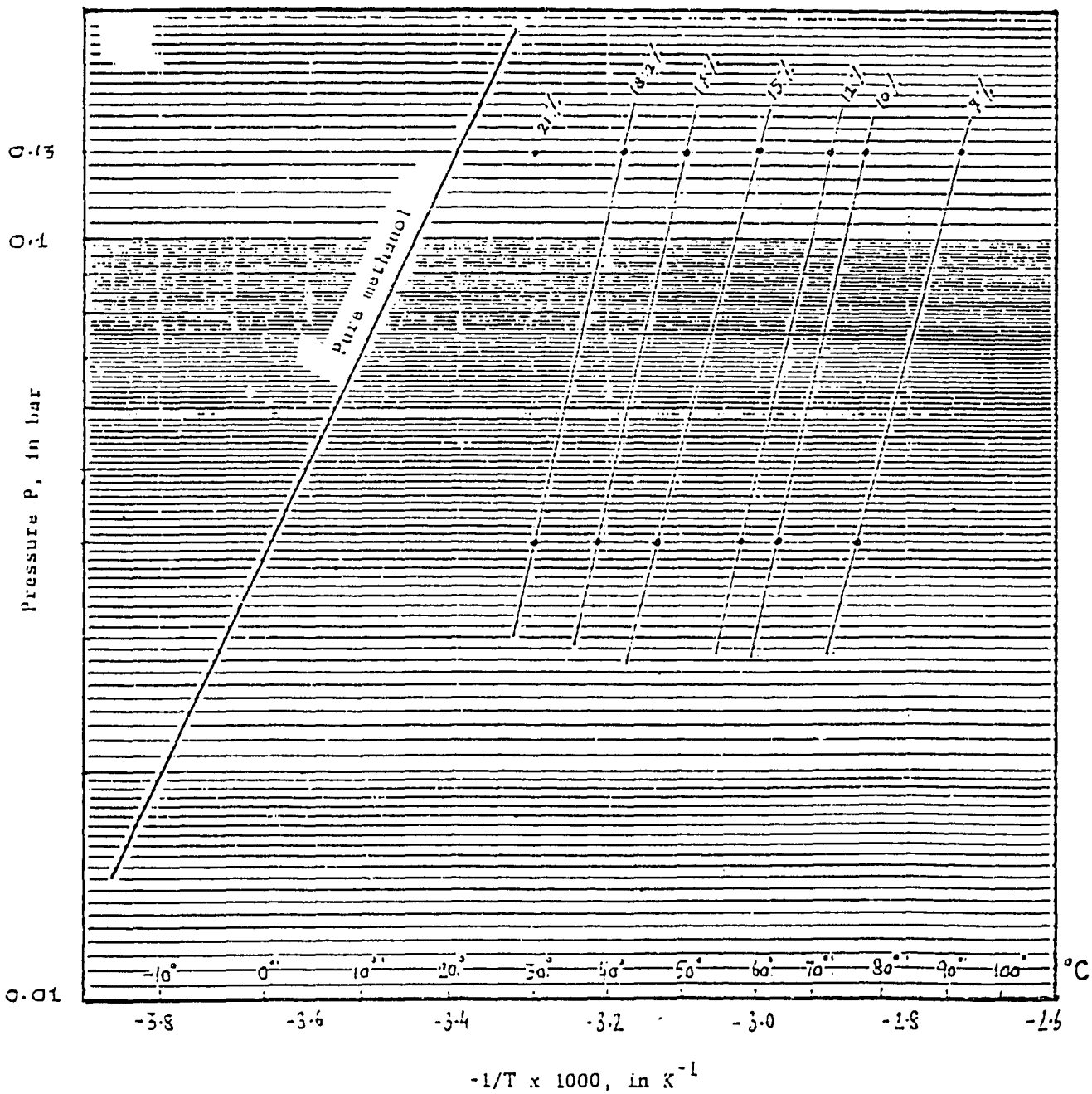

Fig 4.4: Experimental isosteres on a ln P versus -1/T plot.

(d) Carbon 610

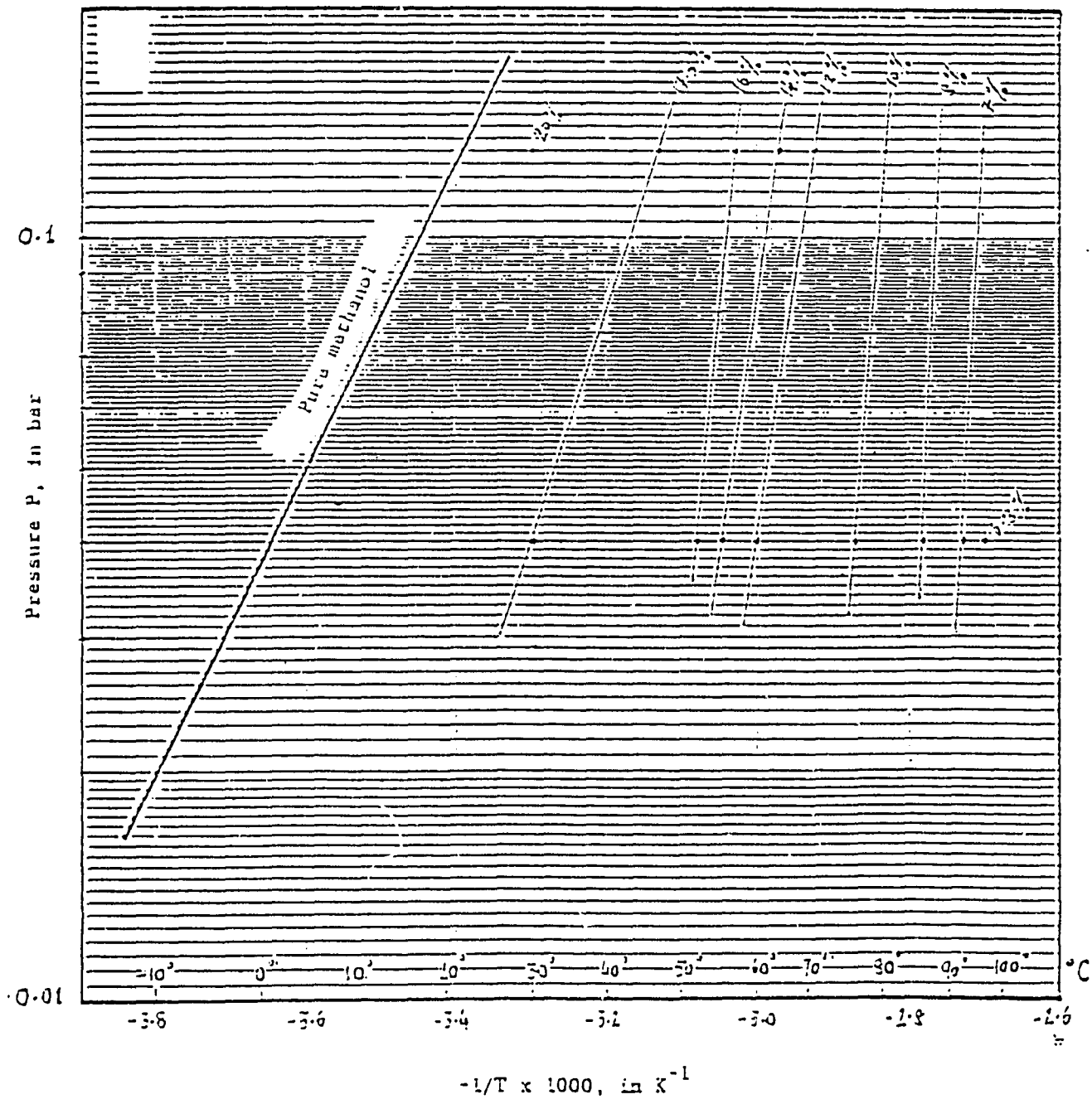

Fig 4.5: Experimental isosteres on a ln P versus -1/T plot.

(e) Carbon THAI-1

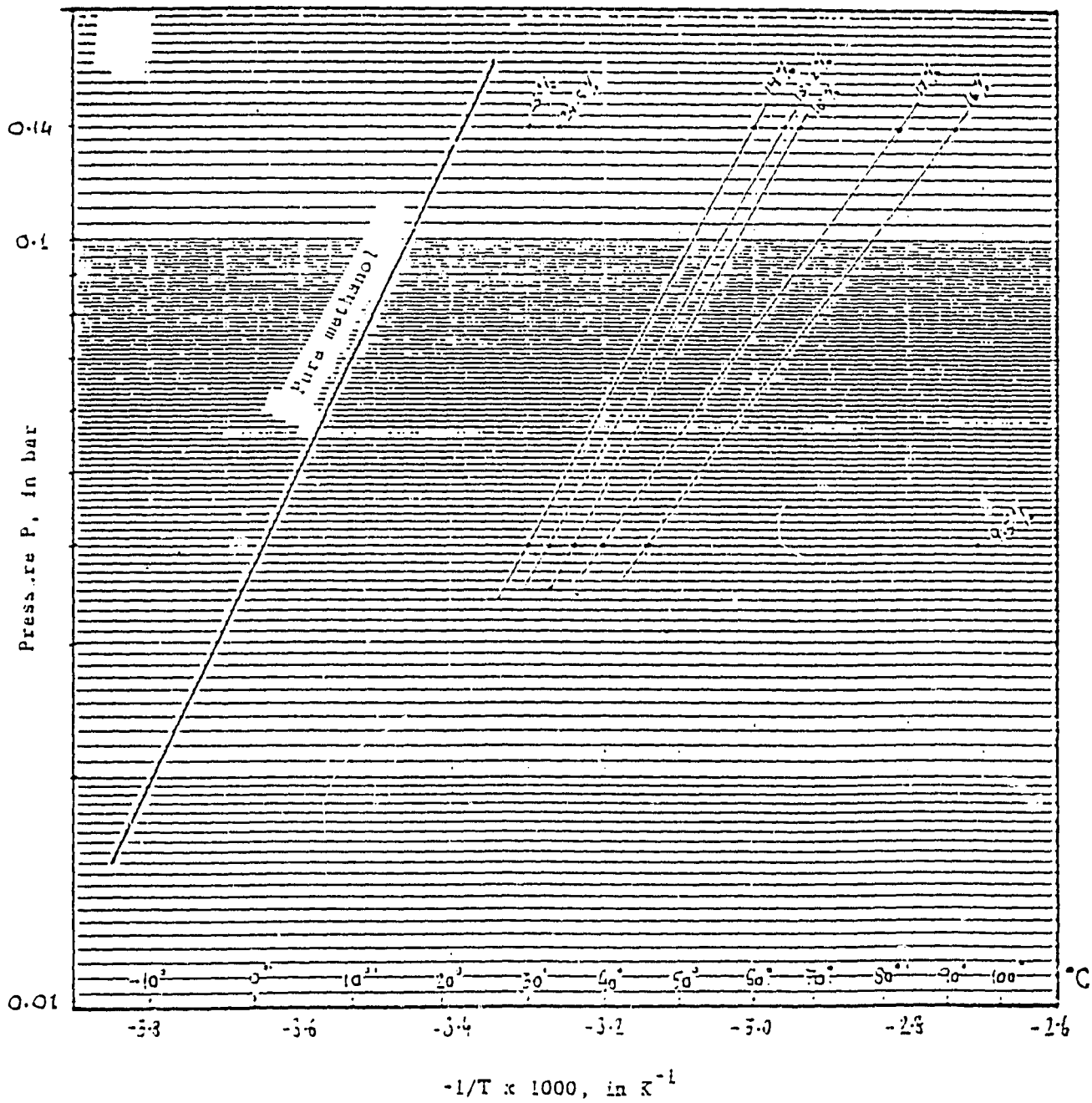

Fig 4.6: Experimental isosteres on a ln P versus -1/T ploc.

(f) Carbon THAI-2

charcoal as proposed by Polayani(1970) is based on the potential theory. But the analytical form for the adsorption isotherm was by given Dubinin(Smisek, and Cerny, 1970). This theory of volume filling of micropores applies over a large range of relative pressures, and the fundamental equation originally proposed by Dubinin and Radushkevich(D-R equation) can be expressed as (Smisek and Cerny, 1970):

$$W = W_o \exp(-k\ (RT \ln P_s/p)^2) \qquad (4.1)$$

where

- W = Volume filled by the adsorbate,
- W_o = Maximum volume of the adsorption space,
- k = A parameter which primarily depends upon the number and size distribution of micropores and also upon the adsorbate, as adsorbents have different affinities for different adsorbates,
- R = Gas constant,
- T = Absolute temperature,
- Ps = Saturated vapour pressure of adsorbate at temp. T,
- P = Equilibrium pressure.

The above equation is valid for temperatures sufficiently below the critical temperatures T_c ($T < 0.8\ T_c$ or $T < T_{b.p.}$). If we consider k' is the same parameter for the standard vapour whose affinity coefficient β is equal to 1 , then $k = k'/\beta^2$. Thus k now will be function of the structure of the adsorbent only and its value will not depend on the adsorbate as the difference in adsorption properties of different vapours from those of the standard vapour (normally benzene) is accounted by β; which is a function of adsorbate only. The D-R equation can thus be written as:

$$W = W_o \exp(\ -\ B\ (\ T/\beta \ln P_s/P)^2) \qquad (4.2)$$

where B is a function of the adsorbent microstructure, the more the microporous the charcoal is, the smaller is B.

The density of the adsorbed phase in the above case can be assumed to be same as that of liquid adsorbate at the same temperature provided that temperature is well below the critical temperature.

The usefulness of this equation lies in the separation of adsorbate and adsorbent properties, since affinity coefficient which is the ratio of adsorbate molar volume at T to that of reference gas at the same temperature T, can easily be determined. The affinity coefficient of different adsorbates on activated charcoal is given in Table 4.2(Smisek and Cerny, 1970). The two parameters Wo and B can be determined by plotting the experimental data in the linear form. Unfortunately, some deviations from linearity were observed by Marsh and Rand (1970). So, the Dubinin and Astakhov (D-A) equation (1970), which

Table 4.2: The Affinity Coefficient β for some vapours on Charcoal.

	β		β
Benzene	1.00	Dichloromethane	0.66
Cyclobenzane	1.04	Ethyl Chloride	0.76
Toluene	1.25	Ethyl Ether	1.09
Propane	0.78	Acetone	0.88
n-Butane	0.90	Formic acid	0.61
n-Pentane	1.12	Ammonia	0.28
n-Hexane	1.35	Nitrogen	0.33
n-Heptane	1.59	Carbon Disulphide	0.70
Methanol	0.40	Acetic acid	0.97
Ethanol	0.61	Xenon	0.50
Methyl Chloride	0.57	Krypton	0.37
Methyl Bromide	0.56	Chloroform	0.86

introduces a third variable n in the parameter to improve the fit of the experimental data, is given as:

$$W = W_o \exp(- D \{ T \ln P_s/P)^n) \quad (4.3)$$

Writing this in the linear form we obtain:

$$\ln W = \ln W_o - D (T \ln P_s/P)^n \quad (4.4)$$

When n = 2, the D-A equation is equivalent to the D-R equation.

The p-T-x data when plotted in the D-R form gives a straight line if adsorption follows the theory of volume filling of micropores. Thus plotting ln W versus $(T \ln P_s/P)^2$ the values of Wo and D can be determined. The D-R plots for the different charcoals tested are shown in Fig. 4.7 through 4.10.

If the D-R equation applies, the experimental points determined at two isobars theoretically merge to a single straight line. But over some part of the experimental range distinct disagreement has been observed as seen from the D-R plots. This has been attributed to the not so sophisticated experimental setup and also due to presence of mesopores in some charcoals. In some cases the data obtained along one of the two isobars was found inconsistent even when it was repeated to several cycles and the D-R plots are for the data points along one isobar. But most of the charcoals tested showed results close to ideal ones, and linear plots having correlation coefficient r between 0.96 and 0.97 were obtained with the exception of Thai-2 which has the correlation coefficient equal to 0.87. The values of Wo, D and correlation coefficient r are given in Table 4.3. It is seen that charcoal 607 has the highest value for Wo followed by 207E3, which means their adsorption capacities for methanol are larger. Other charcoals have also shown significant adsorption capabilities expect for Thai-2 which showed the lowest value, although Thai-1 and Thai-2 were from two different batches from the same manufacturer. This might be due to different degrees of activation in different batches.

4.3 COP Calculations

Since we know the constants for the Dubinin equation Wo and D, the relationship between p, T, x is known, where x is the concentration of the refrigerant adsorbed (kg/kg of charcoal). Once this relation is known, with the knowledge of any two parameters the third can be calculated, and thus the coefficient of performances (COPs) for different applications can be calculated.

4.3.1 Ideal Cycle

The ideal cycle operating this type of system consists two

(a)

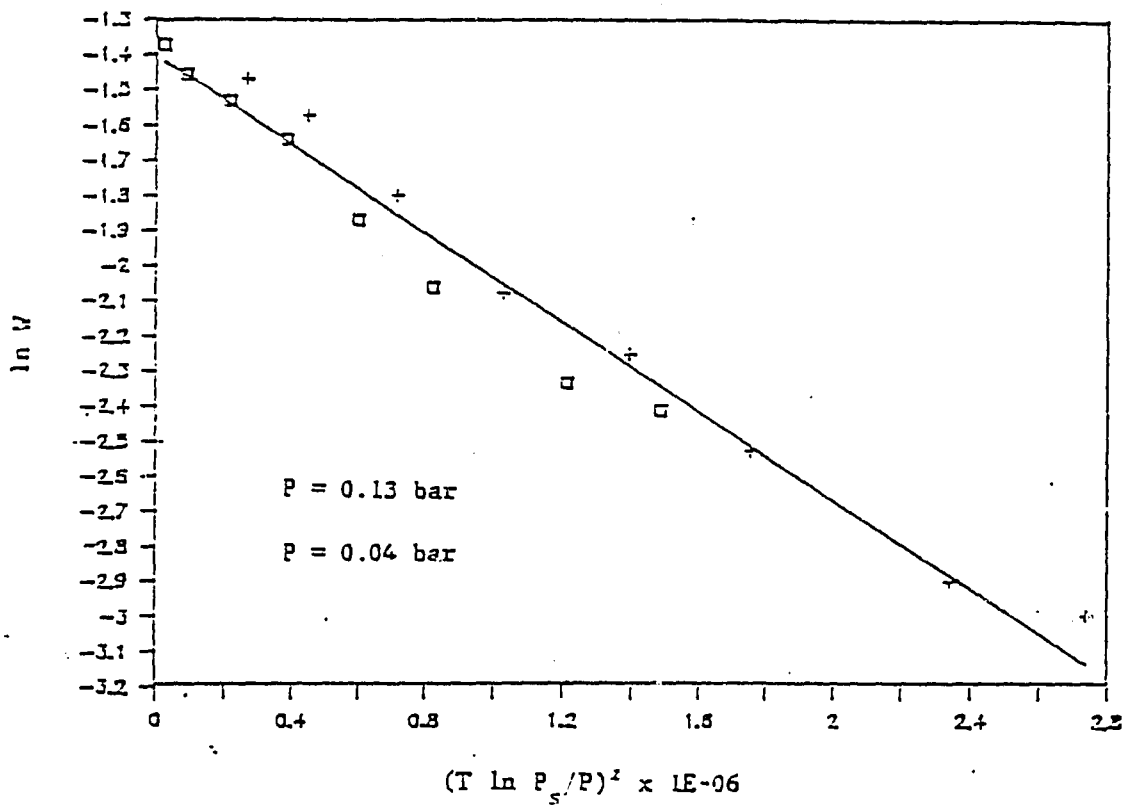

(b)

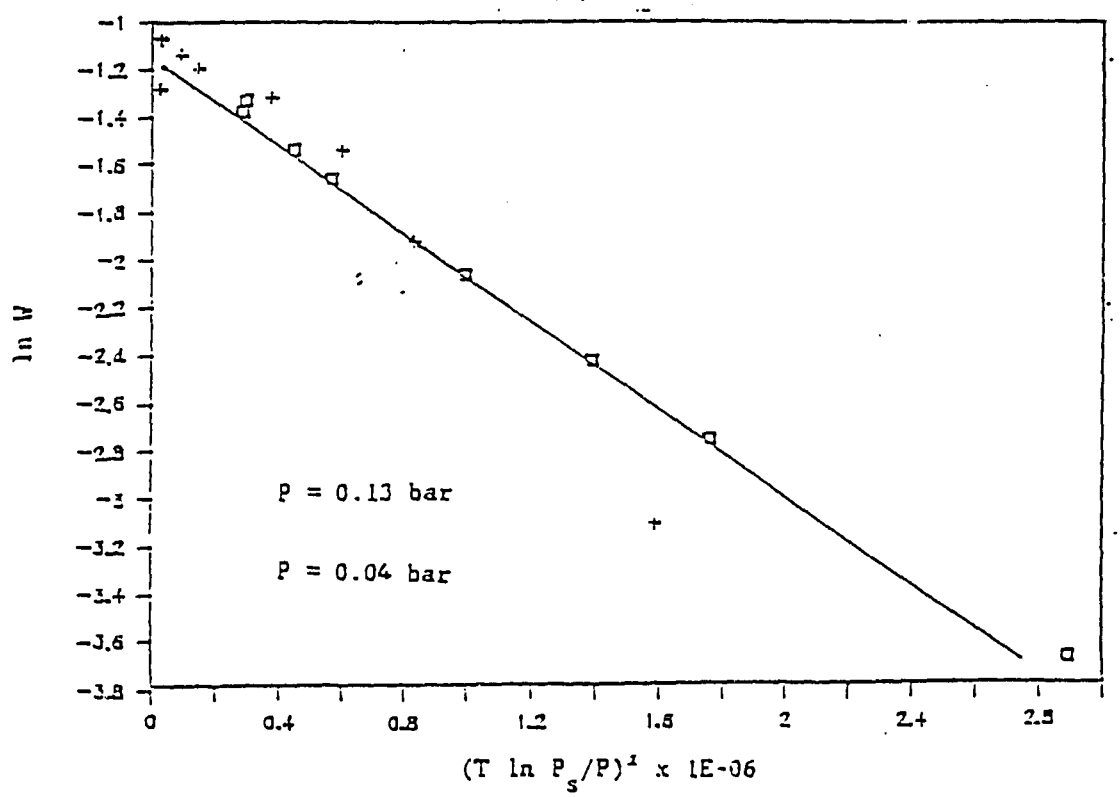

Fig 4.7: Characteristic curve obtained on a D-R plot.
(a) Carbon 207C (b) Carbon 207E

(c)

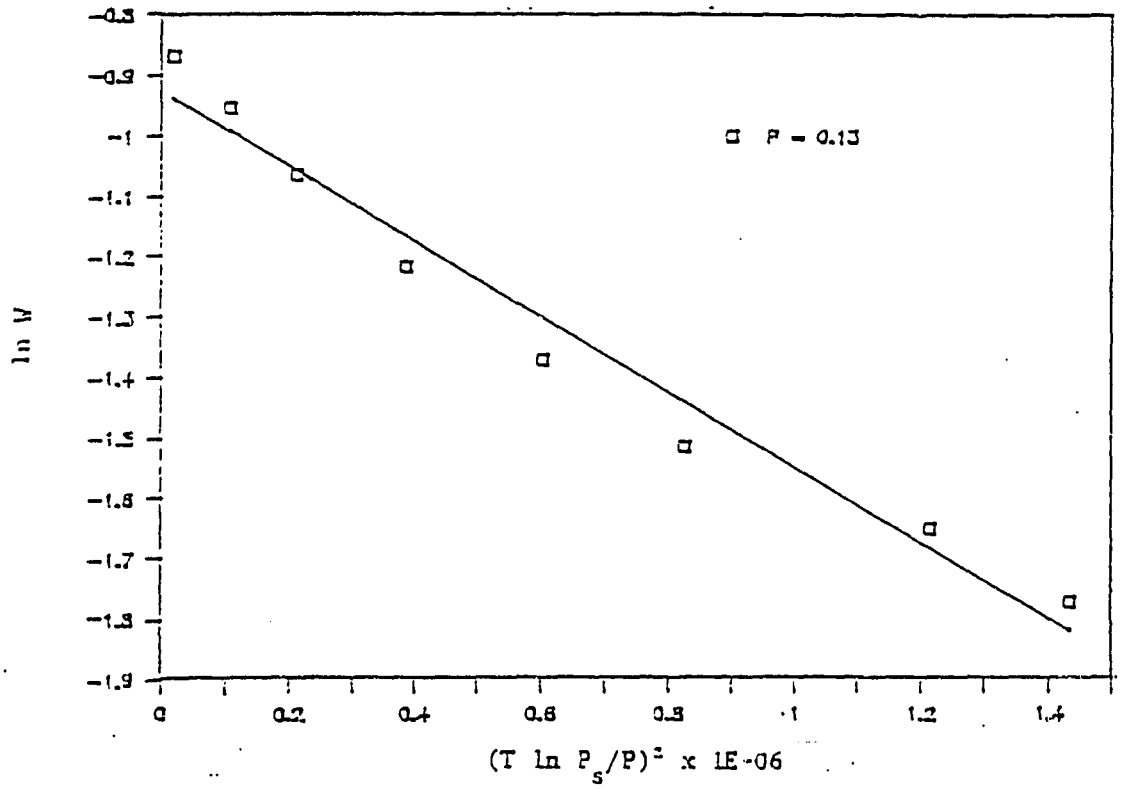

(d)

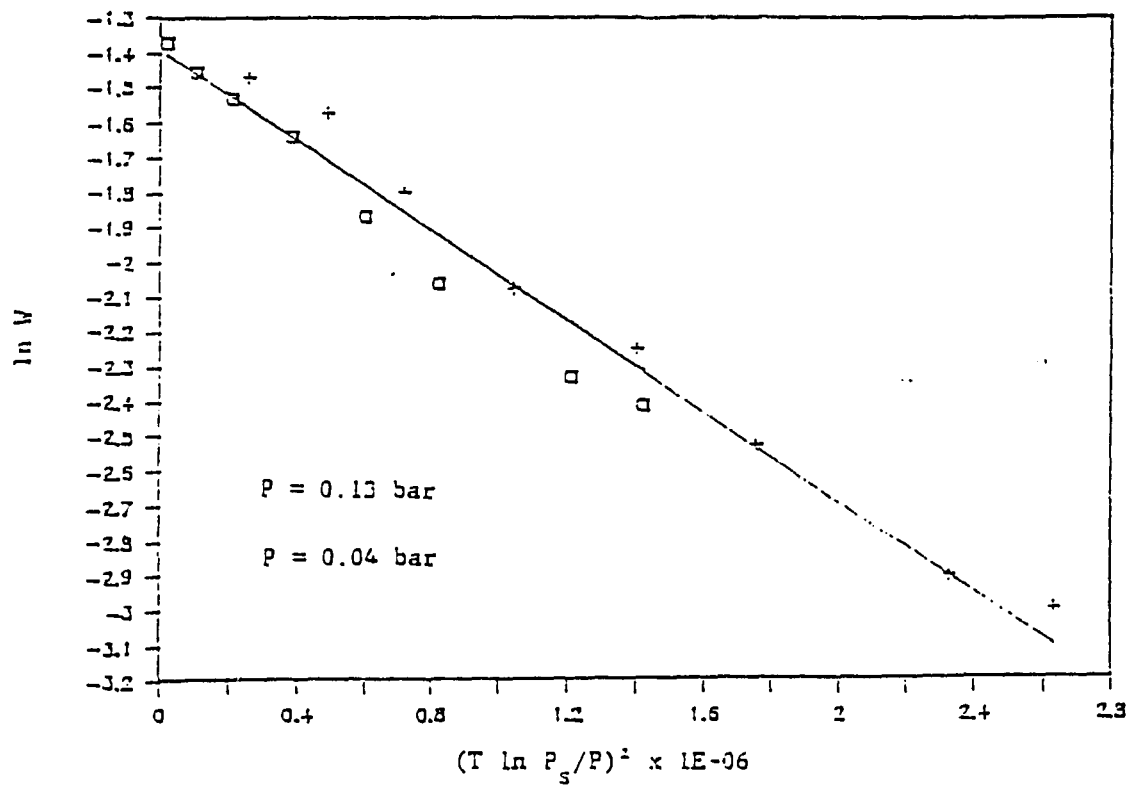

Fig. 4.8: Characteristic curve obtained on a D-R plot.
(c) Carbon 607C (d) Carbon 610

(e)

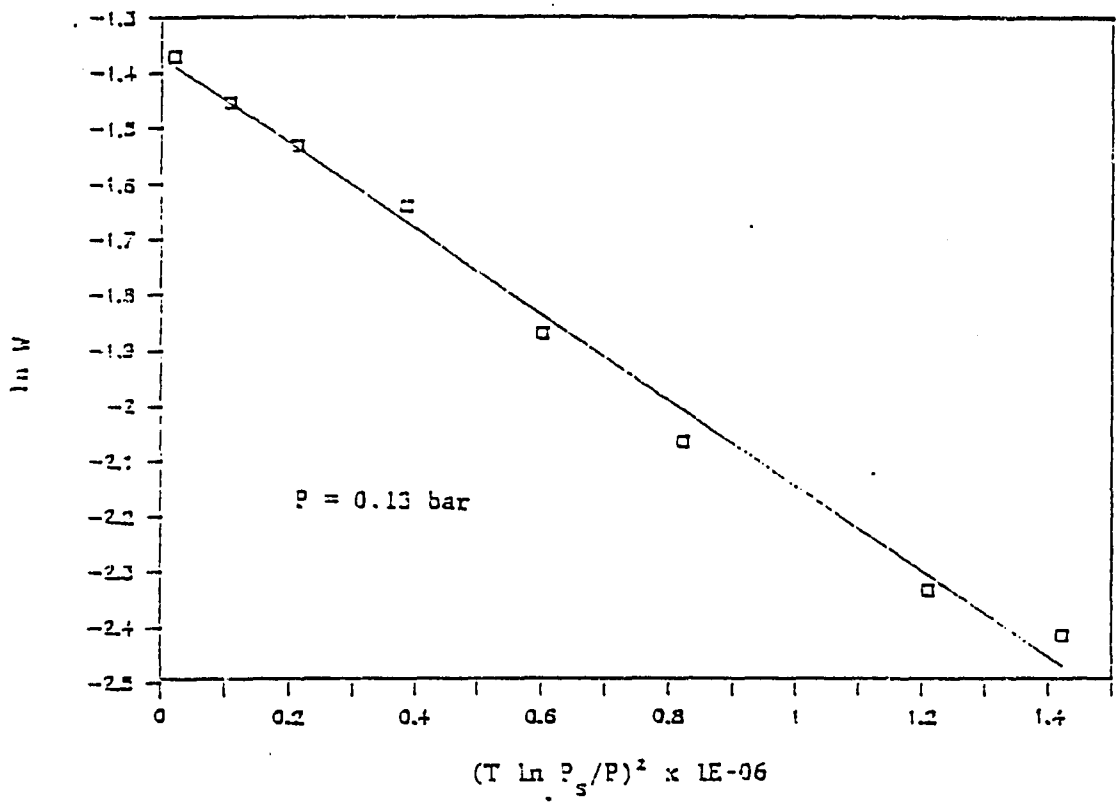

(f)

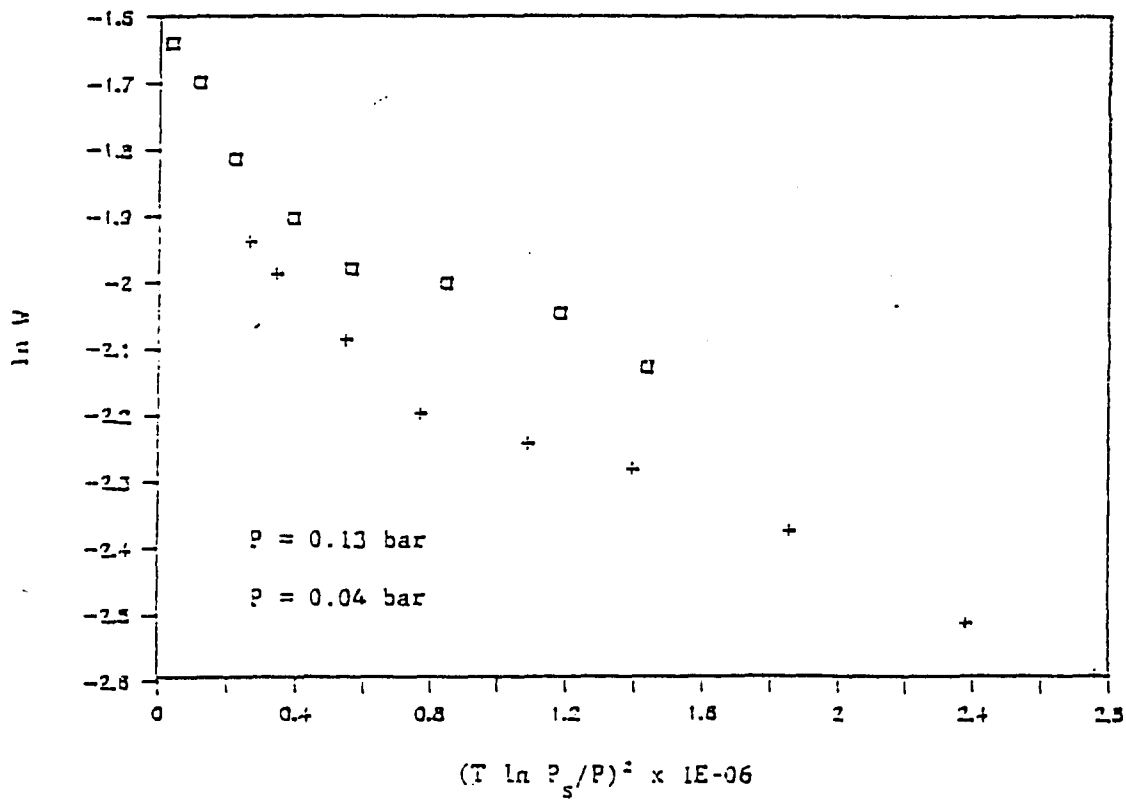

Fig 4.9: Characteristic curve obtained on a D-R plot.
(e) Carbon THAI-1 (f) Carbon THAI-2

(g)

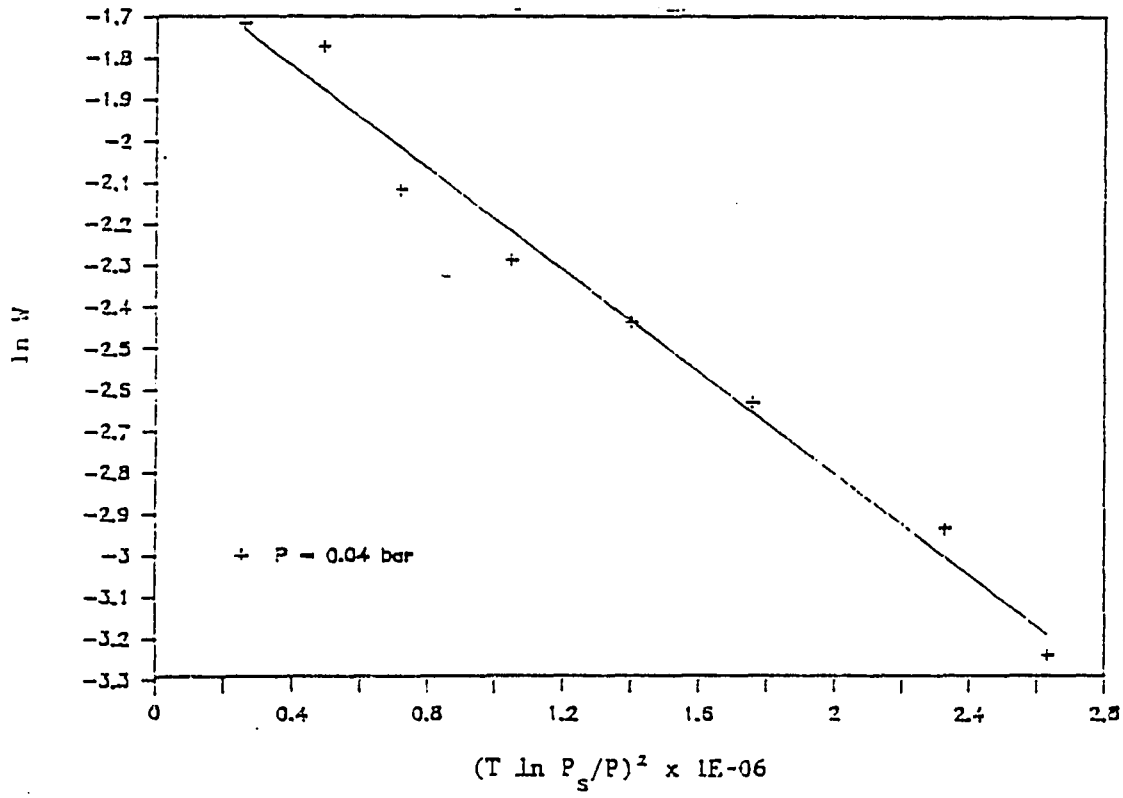

(h)

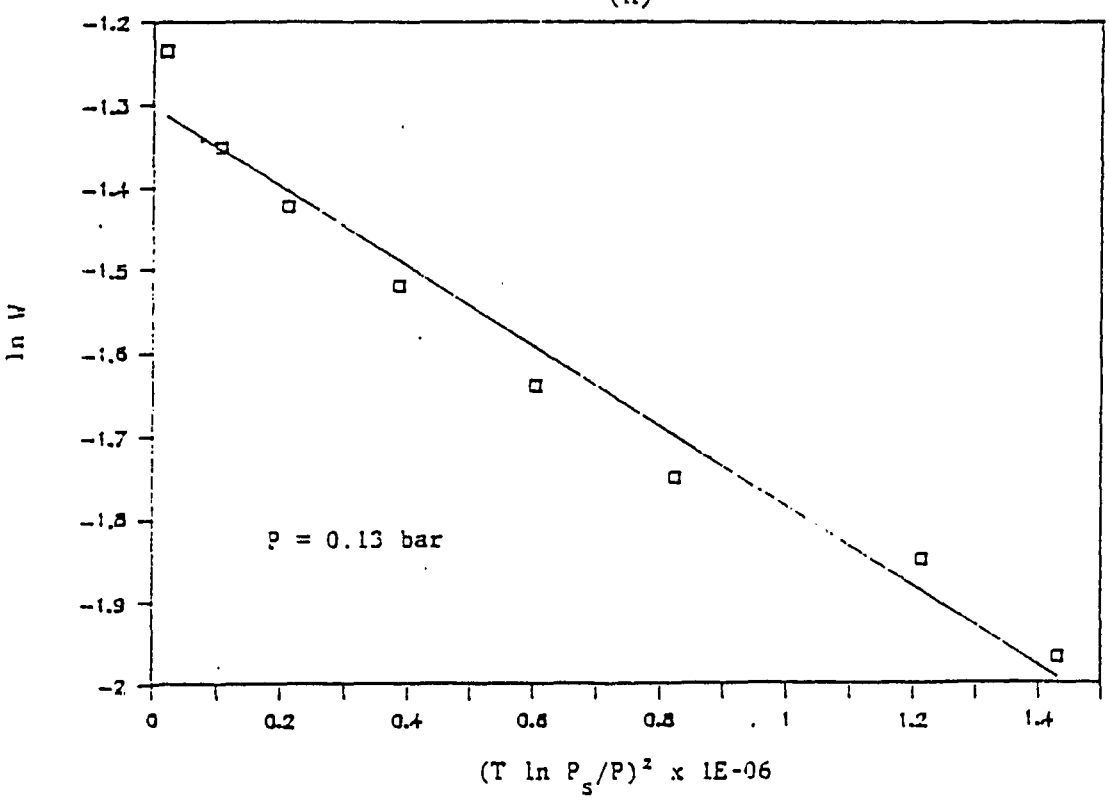

Fig 4.10:Characteristic curve obtained on a D-R plot.
(g) Carbon 203C (h) Carbon 205C

isosters and two isobars. The sensible heating and sensible cooling before and after generation follow two isosters; and the

Table 4.3: Values of W_o, D and r in the D-R Equation for the Charcoals Tested.

Charcoal	W_o (lit/kg)	D x 1E+06	Correlation Coefficient (r)
207E	0.3339	0.9645	0.96
207C	0.2458	0.6329	0.97
203C	0.2060	0.6134	0.98
205C	0.2710	0.4820	0.97
607	0.3962	0.6258	0.97
610	0.2485	0.6502	0.97
THAI-1	0.2531	0.7731	0.99
THAI-2	0.1666	0.3064	0.87

generation and the adsorption processes follow the isobars. The cycle can best be illustrated in the p-T-x diagram of Fig. 4.11.

a. Sensible Heating 1-2

The process starts at point 1, where the charcoal adsorbs the maximum amount of adsorbate, the concentration is x_{max} at temperature T_1. Starting in the morning, charcoal having a rich concentration of adsorbate is heated from temperature T_1 till the pressure P_2 (condenser pressure) is reached. Since no desorption has taken place yet, and the concentration being the same at x_{max}, T_2 can be evaluated.

b. Generation Process 2-3

Desorption starts at point 2 at a constant pressure corresponding to the condenser temperature and the adsorbent becomes more and more dilute. This continues until the maximum temperature attainable, T_{max} for the day is reached. Since we know the pressure and the temperature T_{max}, the new concentration x_{min} at point 3 can be calculated.

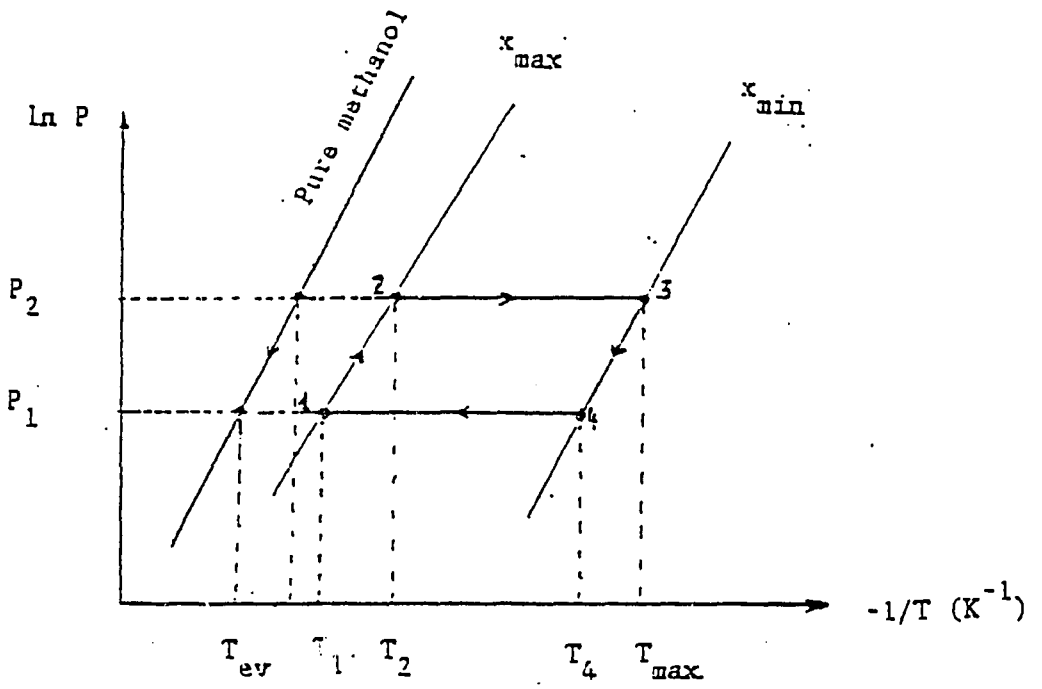

Fig 4.11: Adsorption Cycle.

c. Sensible Cooling 3-4

Cooling of the collector/generator takes place, at constant concentration x_{min} from 3 to 4 till the evaporator pressure P_1 is reached. Since P_1 and x_{min} are known, we can calculate T_4.

d. Adsorption 4-1

Adsorption starts at point 4 and continues until the concentration of refrigerant in the adsorbent reaches its maximum value x_{max}. Thus the cycle is complete.

4.3.2 Heat Balances in the Cycle

Process 1-2

The total heat used during this part of cycle is the sensible heating of the adsorbent and adsorbed refrigerant:

$$Q_{1-2} = (CP_a + CP_r\, x_{max})\ (T_2 - T_1) \qquad (4.5)$$

where

CP_a, CP_r are the specific heats of the adsorbent and the refrigerant respectively,
Q_{1-2} is the sensible heat during the process from state point 1 to 2.

Process 2-3

The heat supplied during the process consists of (i) sensible heating of the adsorbent from T_2 to T_3, (ii) sensible heating of the mean mass of the adsorbate from T_2 to T_3; and (iii) the heat of desorption.

$$Q_{2-3} = (CP_a + CP_r\ (x_{max} + x_{min})/2.)\ (T_3 - T_2) + (x_{max} - x_{min})\ H_{des}, \qquad (4.5)$$

where the heat of desorption/adsorption H_{des} is the average value of the two extreme values calculated from the slope of the two isosters calculated using the Clausius-Clapeyron equation:

At x_{max},

$$H1_{des} = (R/M)\ \ (\ln P_2/P_1)\ /\ (1/T_1 - 1/T_2),$$

Similarly, at the isoster, x_{min},

$$H2_{des} = (R/M)\ (\ln P_2/P_1)/(1/T_4 - 1/T_3),$$

where R is the universal gas constant,
M is the molecular weight of the adsorbate.

Thus the average heat of desorption $H_{des} = (H1_{des} + H2_{des})/2$.

Cooling Produced

Assuming the refrigerant first cools from temperature T_1 to the evaporator temperature T_{ev}, and then evaporates, and also assuming the latent heat of evaporation L is constant, the cooling produced is:

$$Q_c = (x_{max} - x_{min}) \ (L - CP_r \ (T_1 - T_{ev})), \tag{4.7}$$

and the coefficient of performance is

$$COP_{th} = Q_c/(Q_{1-2} + Q_{2-3}). \tag{4.8}$$

4.3.3 Computation of COPs and Results

Based on the type of application the evaporator temperature will be fixed, and the condenser temperature can be assumed known based upon the type of condenser used. The values of specific heats of the adsorbent CP_a and CP_r are known. The heat of adsorption/desorption H_{des} can be calculated, knowing condenser and evaporator temperatures, latent heat of evaporation L for an adsorbate can be calculated. Thus the COPs can be calculated.

It is clear from the heat balances that the thermal mass of the container has not been taken into account and the heat input is directly to the adsorbent and the refrigerant. A computer program written in Fortran Language was used to compute the COPs of the different charcoal samples tested. This computer program utilizes the data determined for charcoal-methanol adsorption presented in Section 4.2. The possible cases investigated include evaporator temperatures of -10°C and 5°C, typical for ice-making and cool storage respectively. The condenser temperatures modeled in above cases are 35°C and 25°C. The results of this computer simulation are shown in Figs. 4.12 through 4.15.

Charcoal 607 has shown the best performance with methanol for ice-making followed by Charcoal 207E3; but at lower condenser temperatures and higher evaporator temperatures, Charcoal 207E3 is better. The COPs for Charcoal 207E3 at a generation temperature of about 110°C, condenser temperatures of 35°C and 25°C, and evaporator temperature of -10°C were 0.41 and 0.52 respectively. The COPs for the local samples THAI-1 at the above temperatures were 0.36 and 0.47; while for THAI-2 were 0.25 and 0.35 (Sridhar, 1987). Similarly, Charcoals 607 and THAI-1 have been paired with other refrigerants for ice making purposes (T_{evap} = -10°C, T_{con} = 35°C) shows better COPs compared to methanol (Figs. 4.16 and 4.17). But other practical difficulties, such as high pressure and corrosion, in the case of ammonia must be considered.

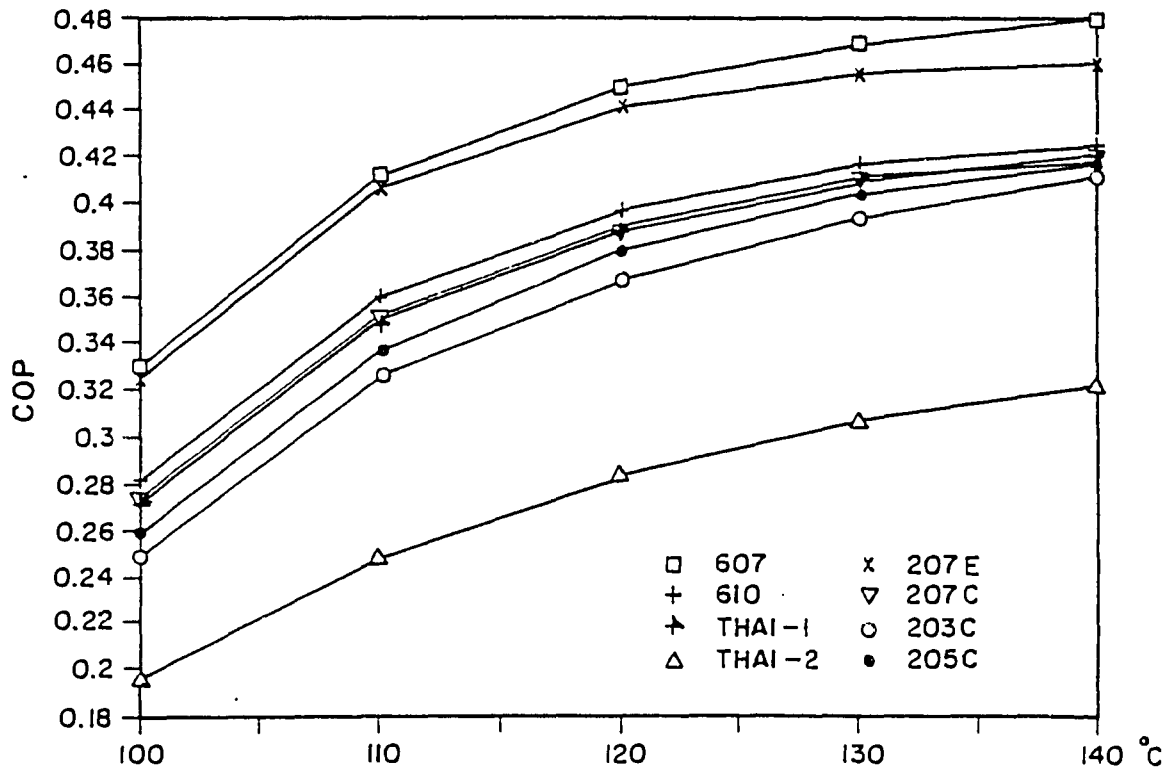

Fig.4.12: COP versus maximum temperature for the different carbons $T_{evap} = -10°C$; $T_{cond} = 35°C$.

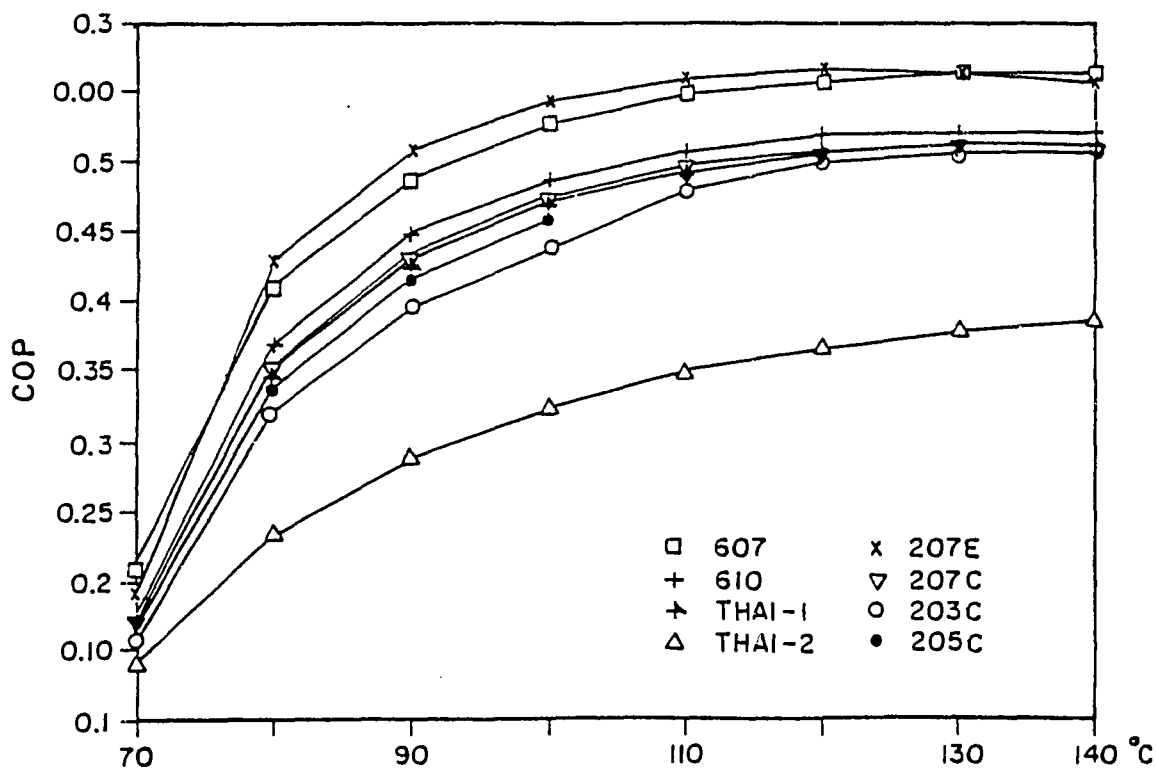

Fig.4.13: COP versus maximum temperature for the different carbons $T_{evap} = 5°C$, $T_{cond} = 35°C$.

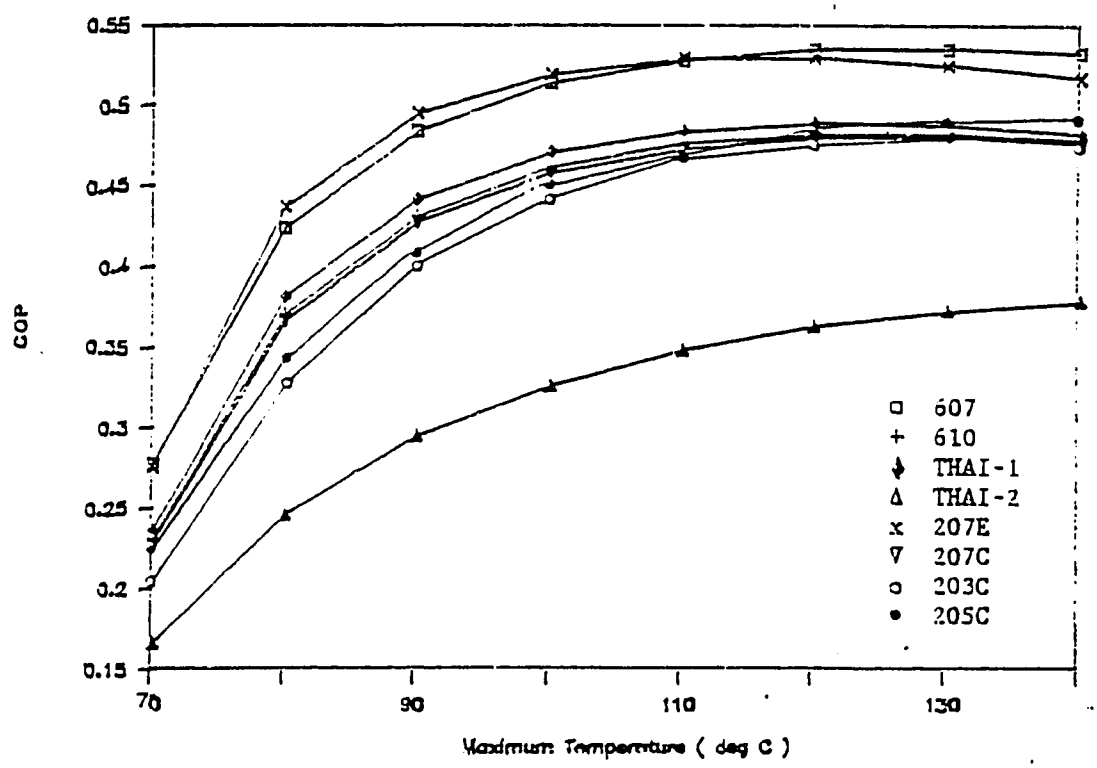

Fig 4.14. COP versus maximum temperature for the different carbons
T_{evap} = -10°C; T_{cond} = 25°C

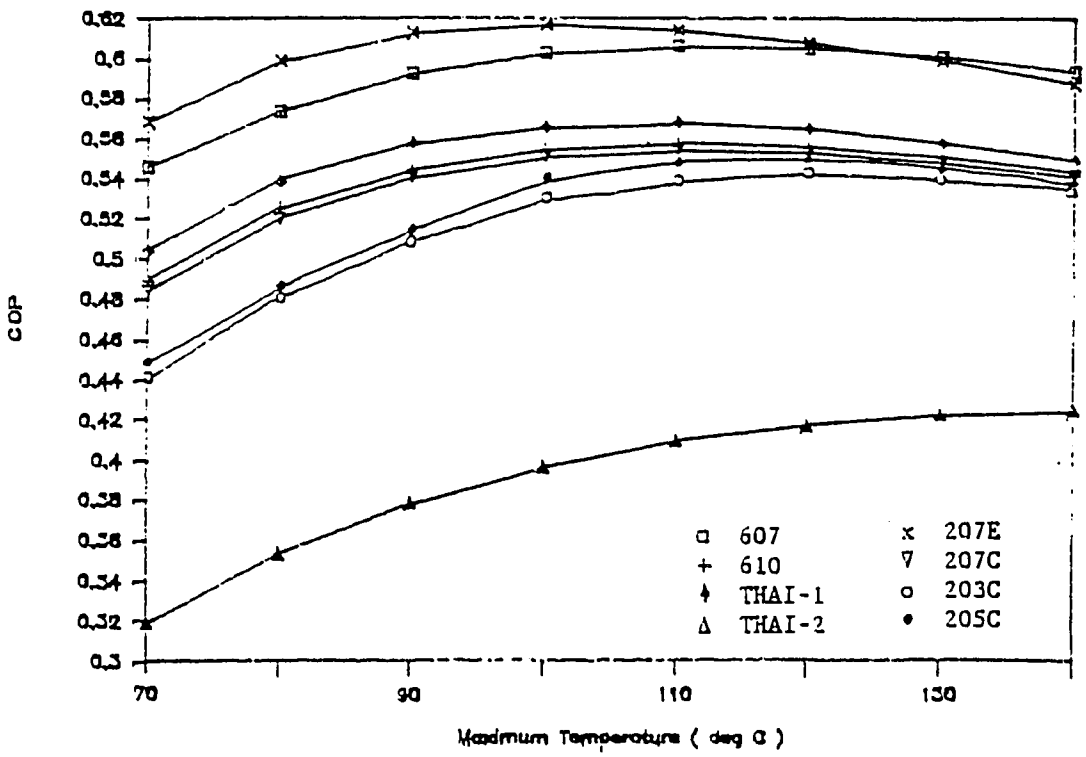

Fig 4.15: COP versus maximum temperature for the different carbons.
T_{evap} = 5°C; T_{cond} = 25°C

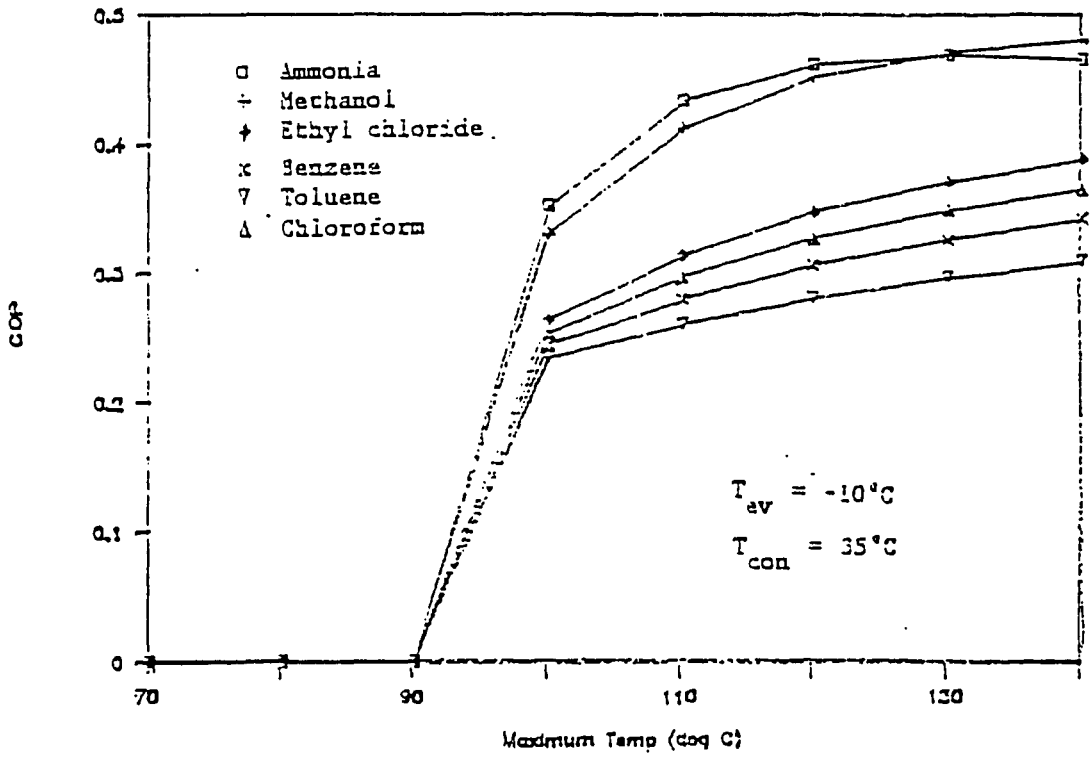

Fig 4.16: Carbon 607C with different refrigerants.

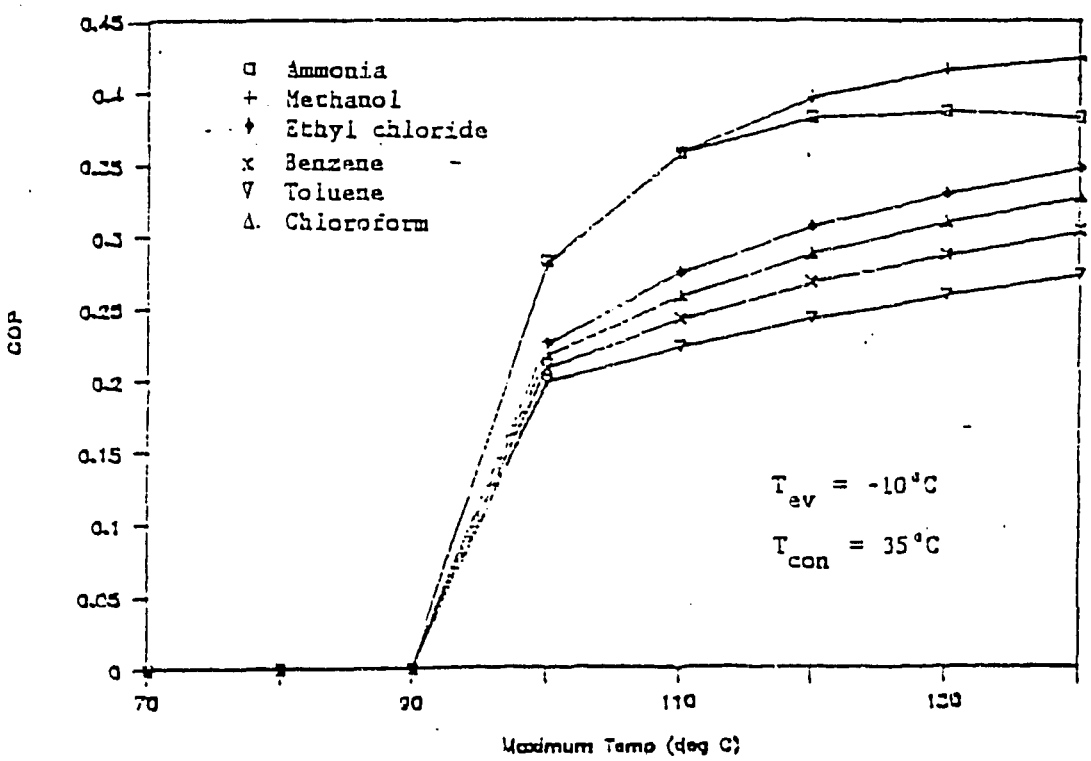

Fig 4.17: Carbon THAI-1 with different refrigerants.

V AIT Charcoal-Methanol Solar Refrigerator

5. Introduction

An intermittent solar activated charcoal-methanol adsorption refrigerator has been designed and tested at AIT. The design of the system is based on p-T-x data determined with our laboratory measuring equipment for one of the eight charcoal samples, (extruded type 207E3) from Sutcliffe Speakman Carbons Ltd., U. K. Two samples of the activated charcoal from a local factory in Thailand were also tested. Those samples were able to adsorb and desorb methanol, but large hysteresis was observed during adsorption and desorption especially at low evaporator pressure. So, the local charcoal was not used in this system.

5.1. Design of the System

The ideal cycle plotted on an Ln P versus -1/T chart for the selected charcoal is shown in Fig. 5.1. The following is the method used to trace the state points on this diagram.

The evaporation temperature T_{ev} depends on the applications; for ice production it has to be in the range of -10°C. T_{con} is the condensing temperature which should be as near to the ambient temperature as heat transfer and economics will allow. Similarily T_1 should be as low as possible so that the rich concentration x_{max} is as high as possible. This maximizes the concentration change thus minimizing the quantity of charcoal that must be (wastefully) heated and cooled with the adsorbed refrigerant. But T_1 depends on the night-time ambient temperature and also the heat transfer characteristics of the collector. For design calculations it has been assumed equal to 30°C. Thus the point corresponding to the evaporation temperature of -10°C and adsorber temperature of 30°C fixes point 1 in the p-T-x diagram. The concentration corresponding to it is about 15% by weight. This system has a water cooled condenser and condensing temperature assumed equal to 30°C. By following the 15% isoster and condensation pressure corresponding to 30°C, point 2 can be located, which corresponds to the generator temperature of 86°C. Assuming a generator temperature T_3 equal to 100°C, typical of the flat-plate solar collector and condensation at 30°C, point 3 can be located. Thus the final concentration of the methanol remaining in charcoal is 7%. This gives a concentration change of 8 wt. %. Similarly the generator has to be sensibly cooled down until it reaches the point 4, corresponding to temperature equal to 60°C, before the adsorption starts at a pressure corresponding to the evaporation at -10°C. This adsorption process starts late at night and continues until next morning. This fixes the ideal cycle on which the design is based.

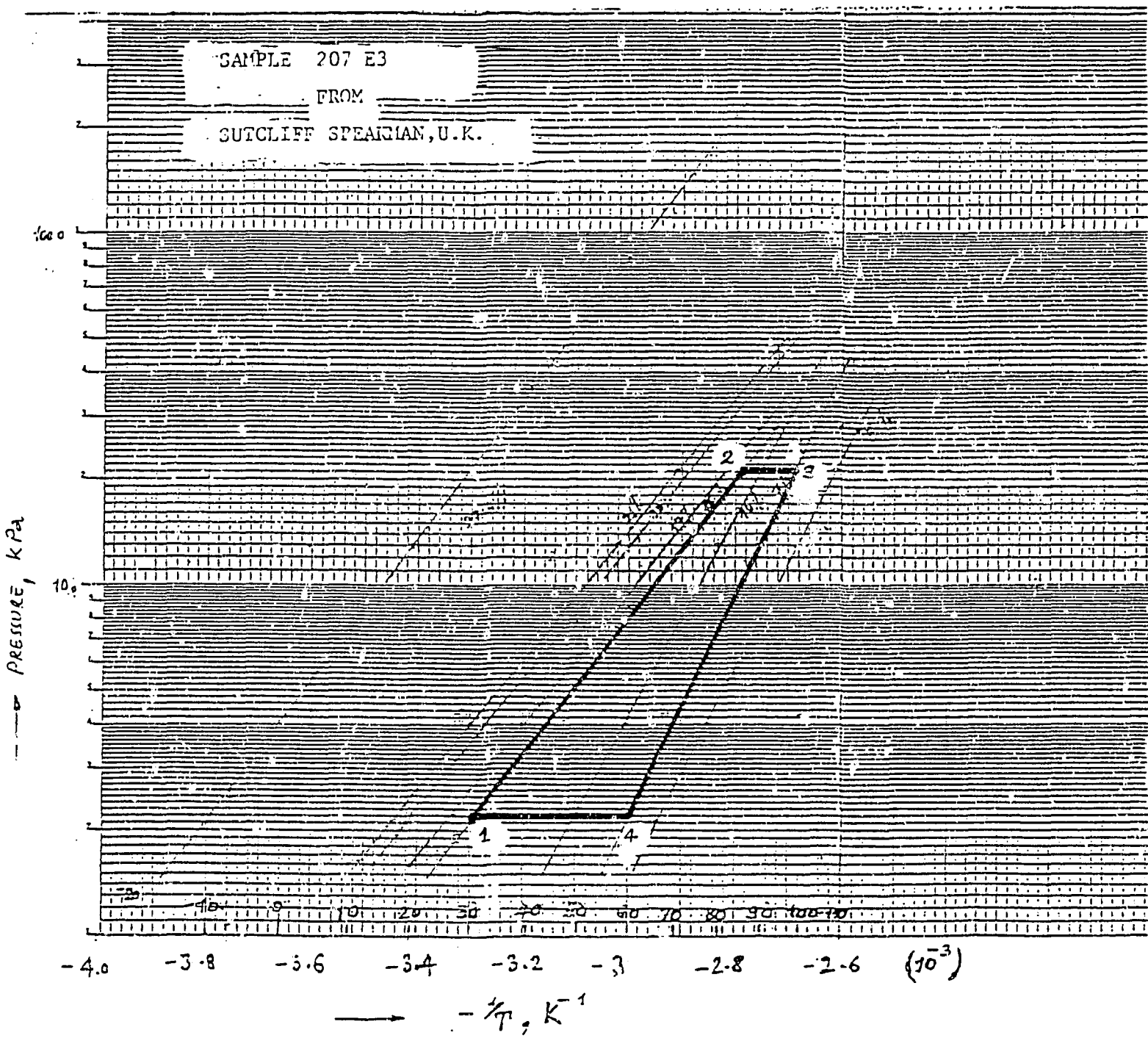

Fig. 5.1: Ideal Cycle in Ln P v. 1/T diagram.

5.1.1 Heat Transfer in the Cycle

Let m_c and m_a be the mass of the collector/generator and adsorbent (charcoal) contained in the collector respectively. Let CP_c and CP_a be the respective specific heats of the collector material and the charcoal. The specific heat of the adsorbed phase has been assumed equal to that of the liquid phase and denoted by CP_r. Assuming the collector, charcoal and the adsorbed phase are at the same temperature, the heat to be supplied during the sensible heating Q_{1-2} from temperature T_1 to T_2 can be estimated as:

$$Q_{1-2} = (m_c\ CP_c + m_a\ CP_a + m_a\ x_{max}\ CP_r)\ (T_2 - T_1). \qquad (5.1)$$

where X_{max} is the rich concentration (kg of methanol/kg of charcoal).

The desorption or generation process starts once the temperature reaches T_2 and continues until the highest temperature of the day T_3 is reached. After this, heat loss from the collector becomes greater than the heat input and generation stops. Thus heat supplied during the generation process includes sensible heating of the collector grid, charcoal, the adsorbed phase and also the heat of desorption. Assuming the specific heat of the adsorbed phase is equal to that of the liquid phase and sensible heating of the desorbed phase is equal to that needed to raise the mean mass of the adsorbate during desorption to the final temperature T_3, the heat needed to be supplied Q_{2-3} can be approximated as:

$$Q_{2-3} = (m_c\ CP_c + m_a\ CP_a + m_a\ (X_{max} + X_{min})/2)\ CP_r)\ (T_3 - T_2) + m_a\ (X_{max} - X_{min})\ H_{des}. \qquad (5.2)$$

where X_{min} is the weak concentration at the end of generation, and H_{des} is the heat of desorption which has been assumed equal to the heat of adsorption.

The total heat that has to be supplied during the sensible heating and the generation process is approximately the sum of the quantities given by equations (5.1) and (5.2).

The heat that has to be lost from the collector during the sensible cooling process T_3 to T_4 can be calculated as:

$$Q_{3-4} = (m_c\ CP_c + m_a\ CP_a + m_a\ x_{min}\ CP_r)\ (T_3 - T_4). \qquad (5.3)$$

The heat needed to be rejected by the collector during adsorption process Q_{1-2} can be approximated as:

$$Q_{4-1} = (m_c\ CP_c + m_a\ CP_a + m_a\ (x_{max} + x_{min})/2\ CP_r)\ (T_4 - T_1) + m_a\ H_{Ads}\ (X_{max} - X_{min}). \qquad (5.4)$$

The useful cooling Q_c that can be produced by this system

during night can be approximated as:

$$Q_c = m_a (x_{max} - x_{min}) (L - CP_r (T_{con} - T_{ev})). \quad (5.5)$$

where L is the average latent heat of the refrigerant liquid leaving the evaporator (kJ/kg).

Thus the thermal coefficient of performance of the system is given as follows:

$$COP_{th} = Q_c / (Q_{1-2} + Q_{2-3}). \quad (5.6)$$

Since this calculation is based on the heat used by the collector, the overall coefficient of performance the the system will be equal to the thermal coefficient of performance multiplied by efficiency of the solar collector/generator.

5.1.2 Design of the Components

(a) Solar collector

The solar collector consists of an array of 15 copper tubes $2^1/8$"(53.97 mm O.D.), 0.528" (1.47mm)thick and 1.2 m long. This configuration provides an effective collection area of about 1 m^2. Although calculations were done on the different materials such as brass, stainless steel, aluminum tubings and also aluminum sections, M-type copper tube was chosen for the following reasons:

- availability of the material and fittings,
- ease of fabrication such as by soft soldering, silver brazing etc.,
- low specific heat but high conductivity of the material of the tubing.

Each copper tube contains a centrally placed perforated gauge tube of 3/8" diameter which is connected to the common header at the bottom of the collector. This was done to ensure even distribution of the methanol vapour in the charcoal and to reduce the pressure drop. Once the charcoal was filled, the top ends of the collector tubes were sealed by soldering brass plates. The lower ends of collector tubes have flare joints which can be assembled to the bottom header. The arrangement is shown in Fig. 5.2. The collector as fabricated has 38 kg of copper in tubes containing charcoal, header and gauge tubes, the 3.85 kg of brass in end caps, nipples, and flared joints. The total weight of the collector grid is 59.6 kg and contains 17.8 kg of charcoal.

The collector has a single glass cover, 4mm thick at a distance of 32 mm from the top surface of the collector tubes. One glass cover was choosen based on the previous experience at AIT (Exell and Kornsakoo, 1981). The top surface of the collector array is covered with selective Maxorb Solar Foil (Inco

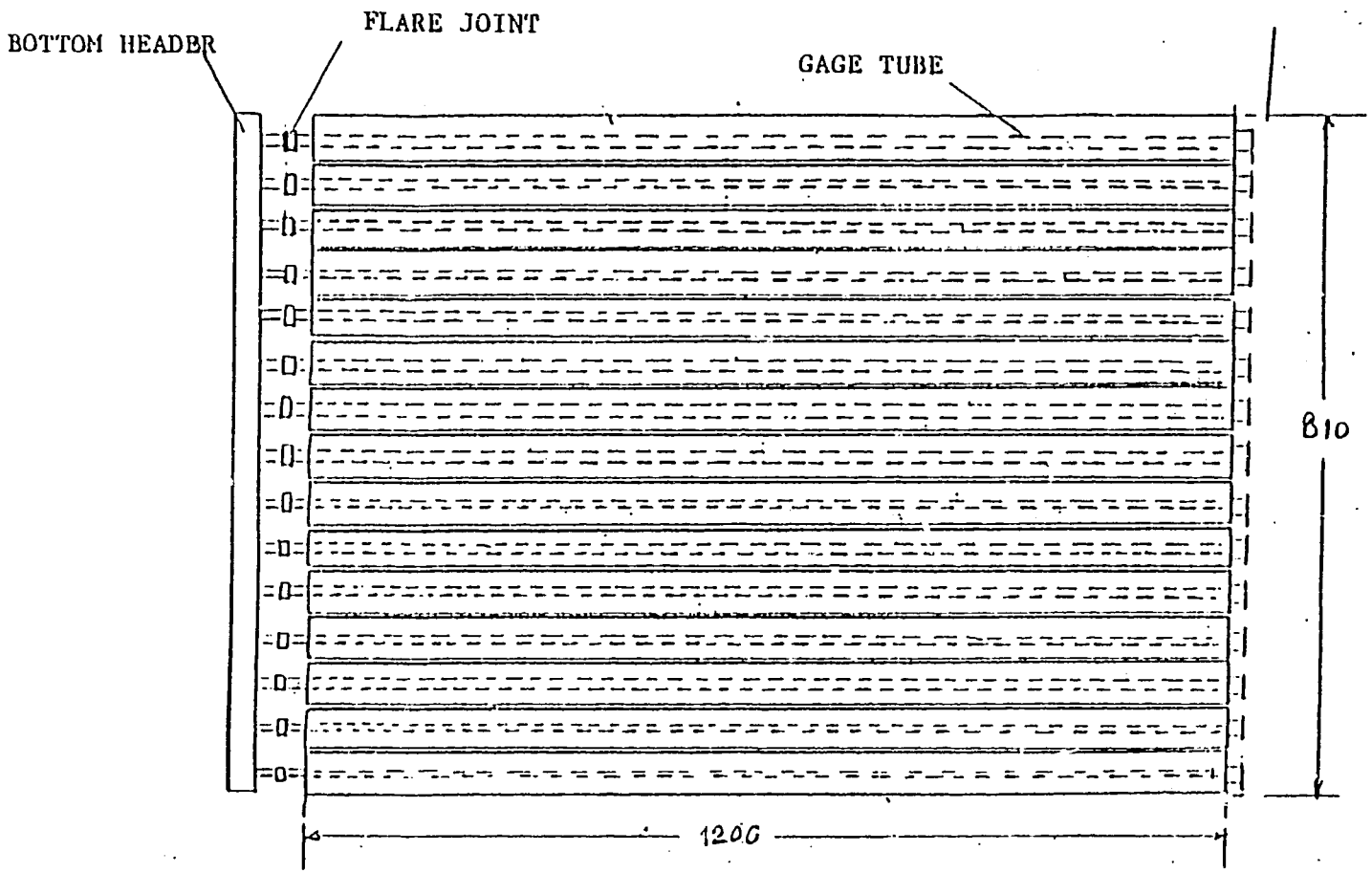

Dimensions are in mm.

Fig. 5.2: Solar Collector Grid.

200

Selective Surfaces, U.K.) coated with a special pressure-sensitive adhesive which can be used at high temperatures.

The assembly is housed in a galvanized iron sheet case of size 1.5m x 1 m. Polyurethane foam is used for insulating the pipes. The insulation fills in the casing and forms a mould about 90 mm thick. The back insulation of the collector can be opened by lowering the back of the casing which is hinged at the bottom and bolted in position at the top. The panel is tilted at an angle of 14° facing south. This collector at 30 to 35% collection efficiency can provide heat needed to desorb approximately 1.4 kg of methanol and has sufficient area to dissipate the heat of adsorption when the back of the collector is lowered. The properties of the materials used are given in Table 5.1 and the detailed calculations are given in appendix.

Table 5.1: Properties of different materials used in the design.

Methanol Properties		
Average Specific Heat of Liquid	2.55	kJ/kg-K
Average Density of Liquid	791.00	kg/m^3
Average Latent Heat of Evaporation of Methanol Vapour	1200.00	kJ/kg
Average Heat of Adsorption/Desorption	1500.0	kJ/kg
Charcoal Properties		
Bulk Density	500.0	kg/m^3
Average Specific Heat	0.7	kJ/kg-K
Other Properties		
Average Specific Heat of Copper	0.380	kJ/kg-K
Average Specific Heat of Brass	0.385	kJ/kg-K

(b) Condenser

The design of the condenser is based on the condensation of 1.4 kg of methanol vapour at 30°C to methanol liquid at the same temperature. The total amount of heat to be released in the condenser can be calculated as follows:

From the methanol property tables (Liney, 1982), the enthalpy of the methanol vapour at 30°C is 1776.5 kJ/kg and the enthalpy of the methanol liquid at the same temperature is 613.85 kJ/kg. So, a total of 1627.7 kJ has to be released in the condenser. Supposing condensation takes place during the period of four

hours, the heat rate is 113.03 W.

The heat transfer area for the condenser can be calculated as:

$$A_{con} = 113.03/(U\ \Delta t),\ m^2 \qquad (5.7)$$

where U is the overall heat transfer coefficient in W/m^2-K and Δt is the temperature difference in degrees.

The overall heat transfer coefficient by natural convection in the static water tank with some fouling was estimated to be 170 W/m^2-K from previous experience (Exell and Kornsakoo, 1981). Assuming a 2°C temperature difference between the vapour and the cooling water, a heat transfer area of 0.332 m^2 is required. The condenser, fabricated from 1/2" and 1 3/8" hard copper tubing is shown in Fig. 5.3. This configuration has about 0.35 m^2 heat transfer area.

Since the total heat to be released in the static water tank is about 1627.7 kJ, and allowing a temperature rise of 1.5°C, the amount of water needed in the tank is 260 kg. The water tank is made from of mild steel sheets and has dimensions 1m x 0.7m x 0.4m; it can contain 279 kg of water.

(c) Receiver

The methanol is contained in a brass container 150mm in diameter and 180mm long, and it can hold about 3 litres of methanol liquid. The tubing connecting the receiver and the evaporator, and the evaporator together can hold about 0.5 litre of methanol. So, the total methanol that can contained in the assembly is about 3.5 litres which is approximately 15.6 wt. % of the methanol cycled. The total weight of receiver is about 2 kg.

(d) Evaporator

The design of the evaporator is based on the following assumptions:

1. The amount of methanol to be evaporated is 1.4 kg.
2. The refrigeration process takes 12 hours.
3. The evaporator temperature is -10°C.
4. The average latent heat of evaporation of the methanol vapour between 30 to -10°C is 1200 kJ/kg.
5. The conductivity of the ice layer is 2.2 W/m-K.
6. The average specific heat of methanol liquid is 2.55 kJ/kg-K.

It follows from the above assumptions that the maximum amount of ice that could be produced by this system (neglecting the thermal mass of the container and the heat leak to the ice

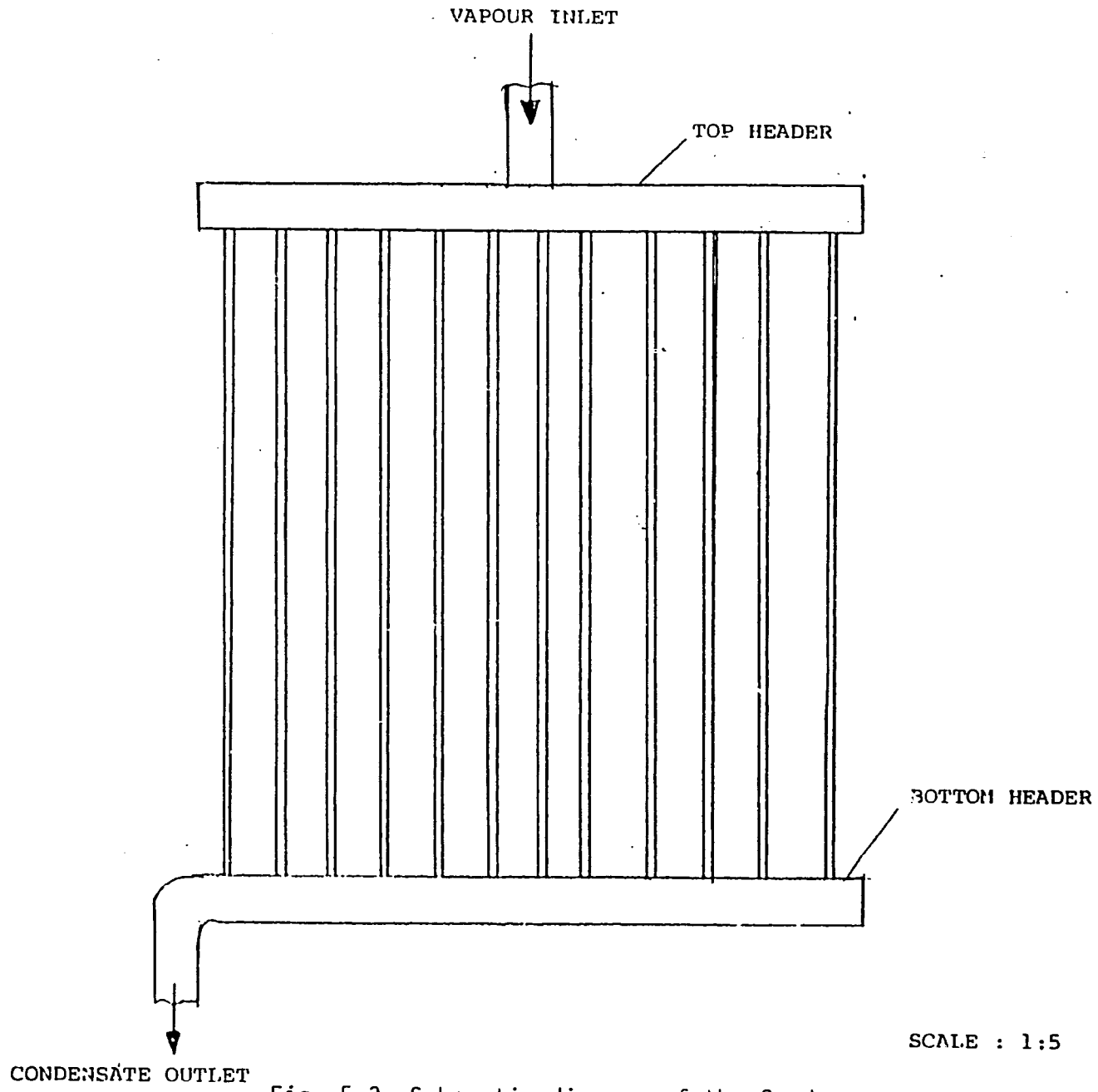

Fig. 5.3: Schematic diagram of the Condenser.

box) from water initially at 30°C is about 3.35 kg. The total cooling produced is 1537 kJ and the heat flow rate required is 35.6 W. This heat flow rate must be maintained by the freezing water until the last bit of ice is formed in the cycle. Thus,

$$35.6 = 2.2\ A_{ev}\ \Delta T/x, \tag{5.8}$$

where

A_{ev} = Heat transfer area of the evaporator, m^2,
ΔT = Temperature difference between evaporator and water surrounding the evaporator 10°C,
x = Thickness of ice, m.

From equation (5.8), $A_{ev}/x = 1.62$ m. (5.9)

The specific volume of ice at 0°C is 0.001091 m^3/kg and the total volume of 3.35 kg of ice is 0.00365 m^3 which gives:

$$A_{ev}\ x = 0.00365\ m^3. \tag{5.10}$$

Solving equations (5.9) and (5.10), gives the surface area of heat transfer equal to 0.077 m^2, and the maximum thickness of the ice is 47.5 mm. After several trials a trapezoidal section has been selected for the evaporator. This section provides an effective surface area of about 0.131 m^2, and from equation (5.10) the effective thickness of ice reduces to 27.8 mm. The evaporator was made out of the brass sheet and has a total mass of 2.0 kg, including the copper tubing connecting receiver and the evaporator. Moreover, this configuration allows easy removal of ice. The receiver/evaporator assembly is shown in Fig. 5.4, and the sectional view of the refrigerator is shown in Fig. 5.5.

5.1.3 Pressure Drop in Connecting Tubes and Charcoal

The worst possible case that might be encountered is a temperature of 260 K (-13.15°C) during evaporation, the specific volume of methanol vapour at this temperature is 39.49 m^3/kg and the corresponding pressure is 1700 Pa. Since the total amount of vapour to be cycled is about 1.4 kg in twelve hours, the average mass flow rate is 3.24×10^{-5} kg/s. The average velocity of the methanol vapour V can be calculated as:

$$V = \dot{m}\,\nu / A_f \tag{5.11}$$

where,

m = Methanol vapour rate, kg/s,
ν = Specific volume, m^3/kg,
A_f = Cross-section area of flow, m^2.

To keep the pressure drop in the connecting pipe low a smooth drawn 1 3/8" (32.8 mm I.D.) copper tube has been choosen. This tube has a flow area of 0.0008296 m^2 and the average

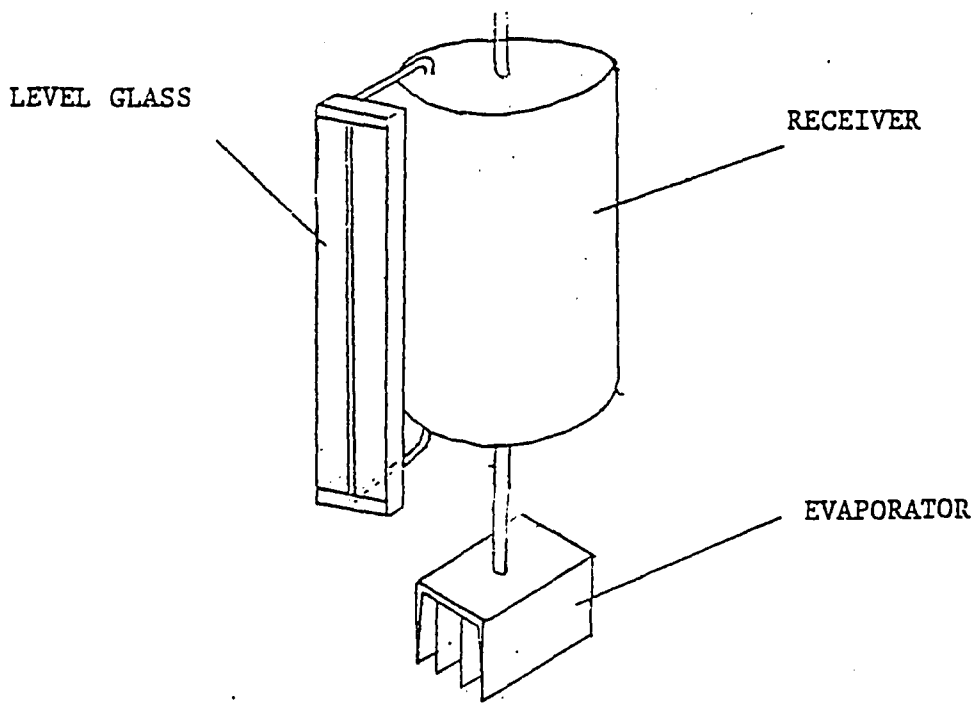

Fig. 5.4: Receiver/Evaporator Assembly.

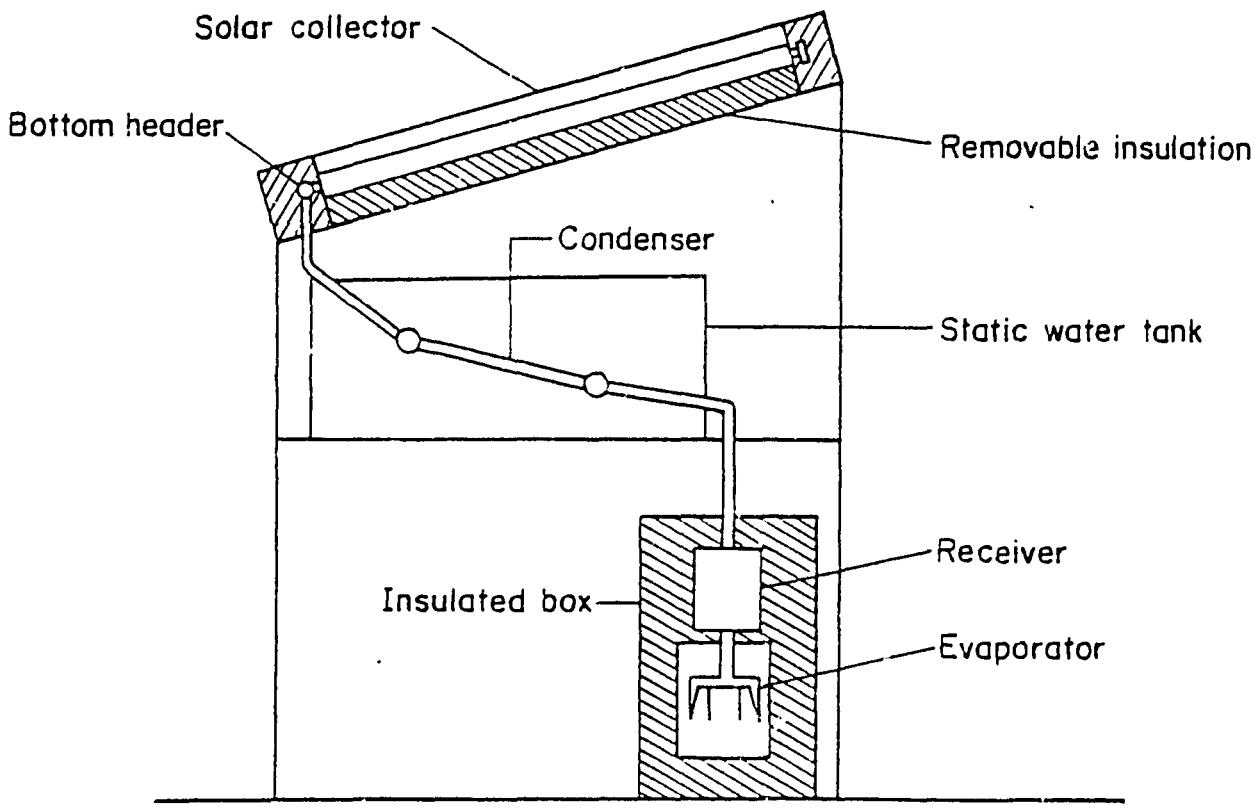

Fig. 5.5: The sectional view of the Solar Refrigerator.

velocity of vapour flow in the tube is 1.54 m/s. Assuming the average viscosity of the methanol vapour μ is equal to 10.1 x 10^{-6} Ns/m^2, the Reynold's number R_N is given as:

$$R_N = 4\,\dot{m}\,/(\pi D_i\,\mu) \simeq 126 \qquad (5.12)$$

where

D_i = Internal diameter of vapour transport tube(m).

Since the Reynold's number is less than 2000, the flow is laminar and the Fanning's friction factor f is equals to $16/R_N$ (Perry and Chilton, 1973), and the pressure drop ΔP (Pa/m) in the connecting tubes can be calculated as:

$$\Delta P = 1/2\,(f\,\rho\,V^2)\,/D_i \qquad (5.13)$$

For the 1 3/8" connecting tubes, the pressure drop is equal to 0.1161 Pa/m and the pressure drop in gauge tubes is 1.9 Pa/m, which is satisfactory.

The flow is laminar and the pressure drop in the bends is small but the bends and sudden changes in the internal diameter of flow have been kept to minimum.

Since gauge tubes have been used in this system, the effective thickness of charcoal in the tube in the radial direction is only 21 mm and the pressure drop in the charcoal will be negligible.

5.2 Preparation for Tests

5.2.1 Calibration of Level Glass of Receiver/Evaporator

The receiver/evaporator assembly consists of a level glass to measure the liquid level inside the receiver. The level glass was calibrated by filling a known quantity of water into the receiver/evaporator in small increments. The volume V of the liquid in the receiver can be calculated from the level glass reading as follows:

$$V = 34.17 + 192.16\ H - 0.55\ H^2,\ cm^3 \qquad (5.14)$$

where H is the level glass reading (cm) and the above equation is valid for $3 \leqslant H \leqslant 19.1$.

The lowest value that can be read from the level glass is 3 and the highest level is 19.1 cm. The evaporator and the tube connecting the evaporator and the receiver contains about 600 cm^3 of methanol liquid.

5.2.2 Overall Heat Loss Coefficient of Receiver/Evaporator Box

The receiver/evaporator is housed in a box (700 mm x 460 mm x 460 mm) well insulated by polyurethane foam. To determine the overall heat loss coefficient of the box, the receiver/evaporator was filled with ice-cold water and the temperatures at different points (Fig. 5.6) were recorded continuously.

TR_1 = Receiver top temperature, ^oC
TR_2 = Receiver bottom temperature, ^oC
TR = Mean receiver temperature, ^oC
TE_1 = Temperature of the tube connecting receiver/evaporator, ^oC
TE_2 = Evaporator temperature, ^oC
TE = Mean evaporator temperature, ^oC
TW = Water temperature, ^oC
TC = Mean cover temperature, ^oC.

and,

$m_R\ C_R$ = Thermal mass of the receiver, kJ/kg-^oC,
$m_E\ C_E$ = Thermal mass of the evaporator, kJ/kg-^oC,
$m_W\ C_W$ = Thermal mass of water filled in the receiver/evaporator, kJ/kg-^oC.

The heat balance of the receiver/evaporator can be written as:

$$m_R\ C_R\ dTR/dt + m_E\ C_E\ dTE/dt + m_W\ C_W\ dTW/dt =$$

$$3.6\ U\ A_C\ (TC - (TR + TE)/2) \qquad (5.15)$$

where,

U = Overall heat loss coefficient with respect to outside surface area of the cold box, W/m^2-^oC,
A_C = Total outside heat transfer area of the cold box, m^2.

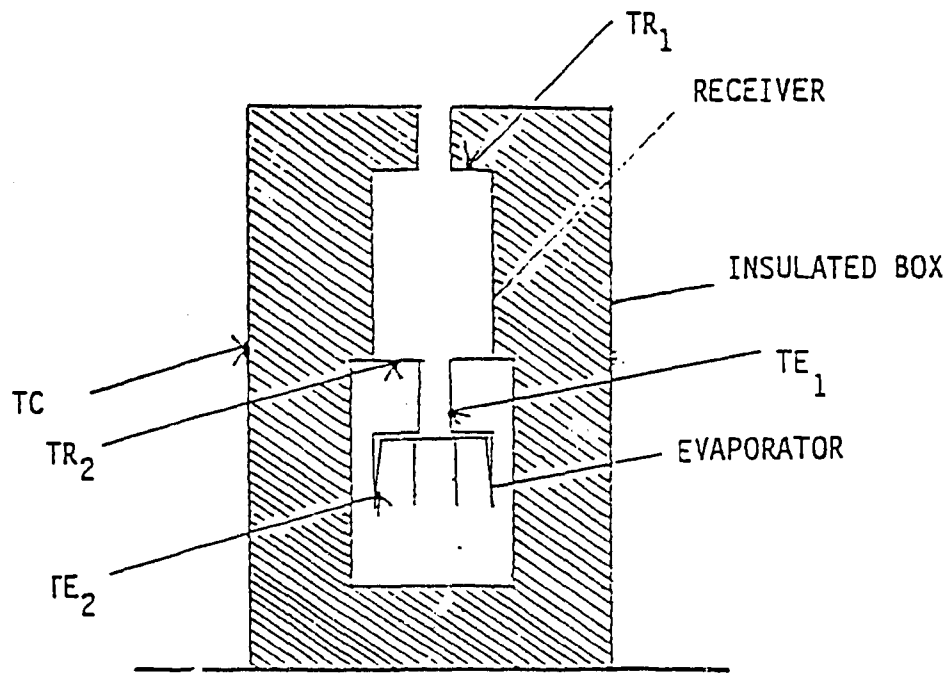

Fig. 5.6: Positions of sensors to determine Overall Heat Loss Coefficient.

$$U = (m_R\ C_R\ dTR/dt + m_E\ C_E\ dTE/dt + m_W\ C_W\ dTW/dt)/(3.6\ AC\ (TC - (TR + TE)/2) \quad (5.16)$$

The mean cover temperature of the cold box TC varies in a sinusoidal pattern, but for small time interval it was represented by the curve

$$TC = 33.65 - 0.44\ t + 0.01\ t^2, \quad (5.17)$$

where t is the time (h).

The temperature difference between the cover and the cold box decreases exponentially with time according to the Newton's law of cooling. The linear regression curves fitted are:

$$\ln\ (TC - TR) = 3.16 - 0.08\ t, \quad (5.18)$$

$$\ln\ (TC - TE) = 3.15 - 0.07\ t, \quad (5.19)$$

$$\ln\ (TC - TW) = 3.19 - 0.07\ t. \quad (5.20)$$

Thus from (5.17), and (5.18), (5.19) and (5.20) we get,

$$TR = 33.65 - 0.44\ t + 0.01\ t^2 - 25.57\ e^{-0.08\ t}, \quad (5.21)$$

$$TE = 33.65 - 0.44\ t + 0.01\ t^2 - 25.57\ e^{-0.07\ t}, \quad (5.22)$$

$$TW = 33.65 - 0.44\ t + 0.01\ t^2 - 24.29\ e^{-0.07\ t}. \quad (5.23)$$

Differentiating equations (5.21), (5.22), (5.23) with respect to time t and substituting in equation (5.16), the hourly values of overall heat loss coefficient can be computed. The computed values are shown in Table 5.2.

Table 5.2: Results of the Overall Heat Loss Coefficient Calculation for the Receiver/Evaporator Box.

Local Time, (Hr)	Time (Hr)	TR (C)	TE (C)	TW (C)	TC (C)	U (W/m^2-C)
16	1	11.98	12.41	11.86	33.73	0.14
17	2	13.13	12.88	12.40	32.77	0.15
18	3	13.89	13.19	12.91	31.83	0.15
19	4	14.85	13.99	13.80	31.60	0.14
20	5	15.42	14.45	14.25	31.57	0.14
21	6	15.99	14.79	14.60	31.55	0.13
22	7	16.94	16.09	15.85	31.32	0.13
23	8	17.91	17.01	16.83	30.86	0.14
24	9	18.29	17.47	17.27	30.47	0.14
1	10	19.26	17.93	17.90	30.02	0.14
2	11	19.82	18.92	18.84	29.79	0.14
3	12	20.58	19.43	19.42	29.33	0.15
4	13	20.98	20.07	19.99	29.33	0.15
5	14	21.35	20.45	20.37	29.13	0.15

5.2.3 Leak-tightness Tests

Prior to assembling, all the components, such as collector tubes, condenser, receiver/evaporator, were tested separately under pressure as well as under vacuum conditions. Once assembled, the solar collector was exposed to the sun and evacuated. The solar collector and condenser, and the receiver/evaporator were checked separately for vacuum tightness over the period of several days, isolating them with the help of isolating valves. The isolating valves and the methanol feeding arrangement are shown in Fig. 5.7.

5.2.4 Preparation of Charcoal for Test

As a first step to remove moisture adsorbed during transit, the charcoal was put into a vacuum oven at 150^{0}C for three days and evacuated with the help of a vacuum pump. The dry hot charcoal from the vacuum oven was filled into the collector tubes and the tubes were assembled. Degassing of the charcoal in the collector tubes was done by exposing the solar collector to the sun and evacuating it around the peak temperature, which reached up to 135°C on clear days. After several days, the charcoal was washed by letting it adsorb a small amount of methanol vapour from the methanol feeding bottle during the night, and by heating and evacuating it during the day. This was done to remove gases adsorbed into the deep pores of the charcoal and gradually replacing them by methanol. After a few such cycles, charcoal was finally ready for actual tests.

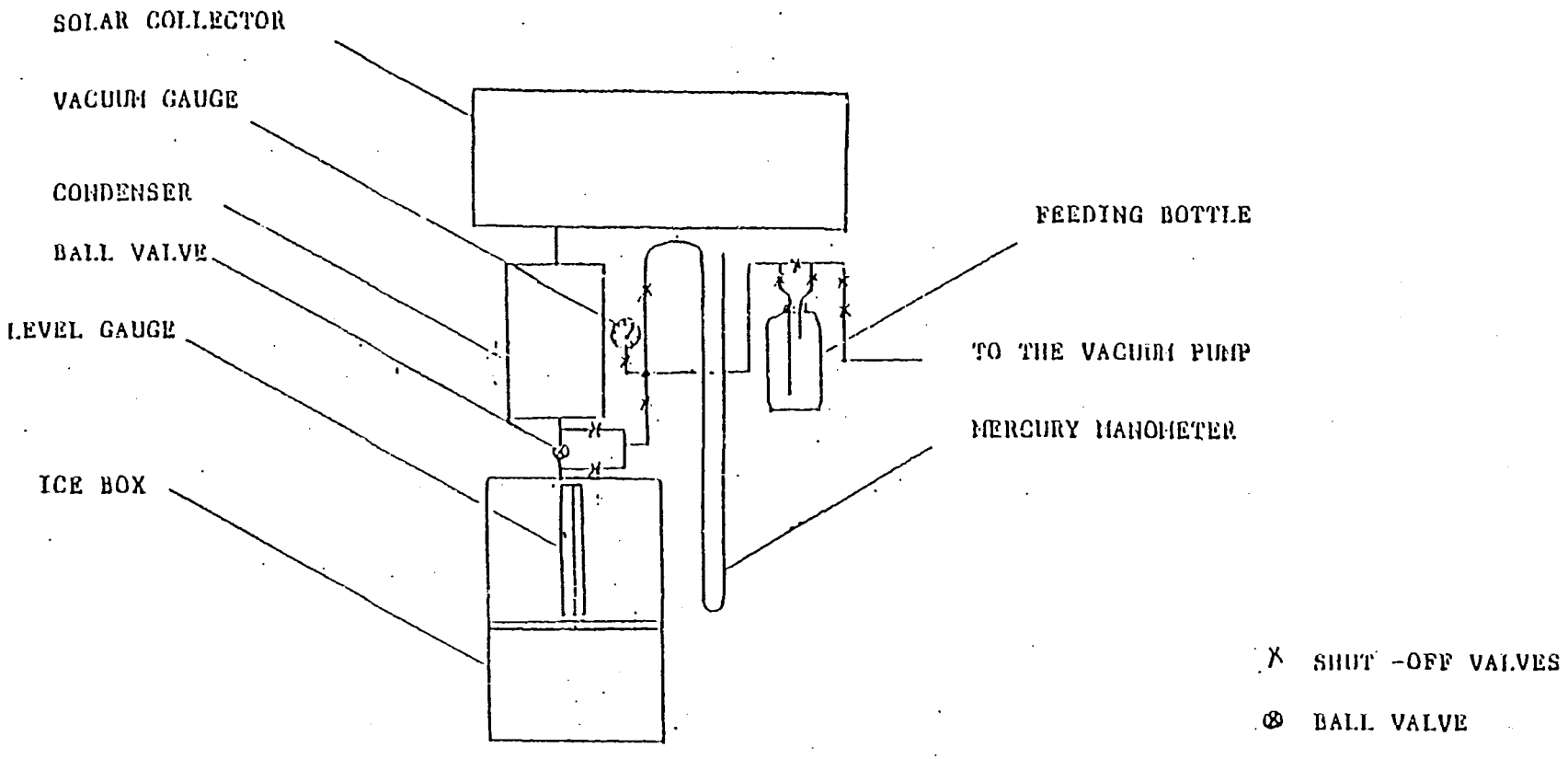

Fig. 5.7: The schematic diagram showing the isolating valves.

5.2.5 Charging of the System

Initially, the charcoal was allowed to adsorb methanol from the feeding bottle. But the adsorption from the feeding bottle was very slow and liquid methanol was therefore charged directly into the receiver/evaporator. The collector was covered during the day and the back insulation was lowered until the adsorption process was complete. The total methanol charged was four litres, all of which was adsorbed by the charcoal. The initial concentration of methanol in the charcoal was about 17.8 wt. % (dry basis).

5.2.6 Instrumentation

Temperature Measurement

The principal temperature measurements were made by twelve copper-constantan (T-Type) temperature sensors, which are designed for a temperature range between -88^0C and 370^0C. These thermocouples were calibrated against a standard mercury-in-glass thermometer having a precision of 0.1^0C. These temperature sensors were installed on the glass cover, top, inside and the bottom of the collector, the condenser, the receiver, the evaporator, and the water or ice temperature. One sensor was used to measure the ambient temperature. The positions of the sensors are shown in Fig. 5.8. These temperatures were recorded continuously by a Fuji chart recorder. Two calibrated k-type temperature sensors were used to measure condenser tube and the cooling water temperatures and those two values were read from the digital display.

Solar Radiation

A pyranometer attached to an integrator with digital display (Solar 118, Switzerland) was used to monitor the instantaneous and integrated values of solar radiation on a surface parallel to the solar collector. This pyranometer was calibrated against a standard pyranometer used at the meteorological station of the ET Park, AIT. The instantaneous and the integrated values of solar radiation were read manually.

Pressure

Besides an ordinary Bourdon gauge, a U-tube mercury manometer has been connected to the system through a system of isolating valves. The Bourdon gauge can be used to estimate the pressure range but the mercury manometer can be used to read the vacuum level to a resolution of 1 mm. One end of this manometer is exposed to the atmosphere. The atmospheric pressure can be read from the standard barometer installed at the ET Park, AIT. Thus, the system pressure at any time can be calculated.

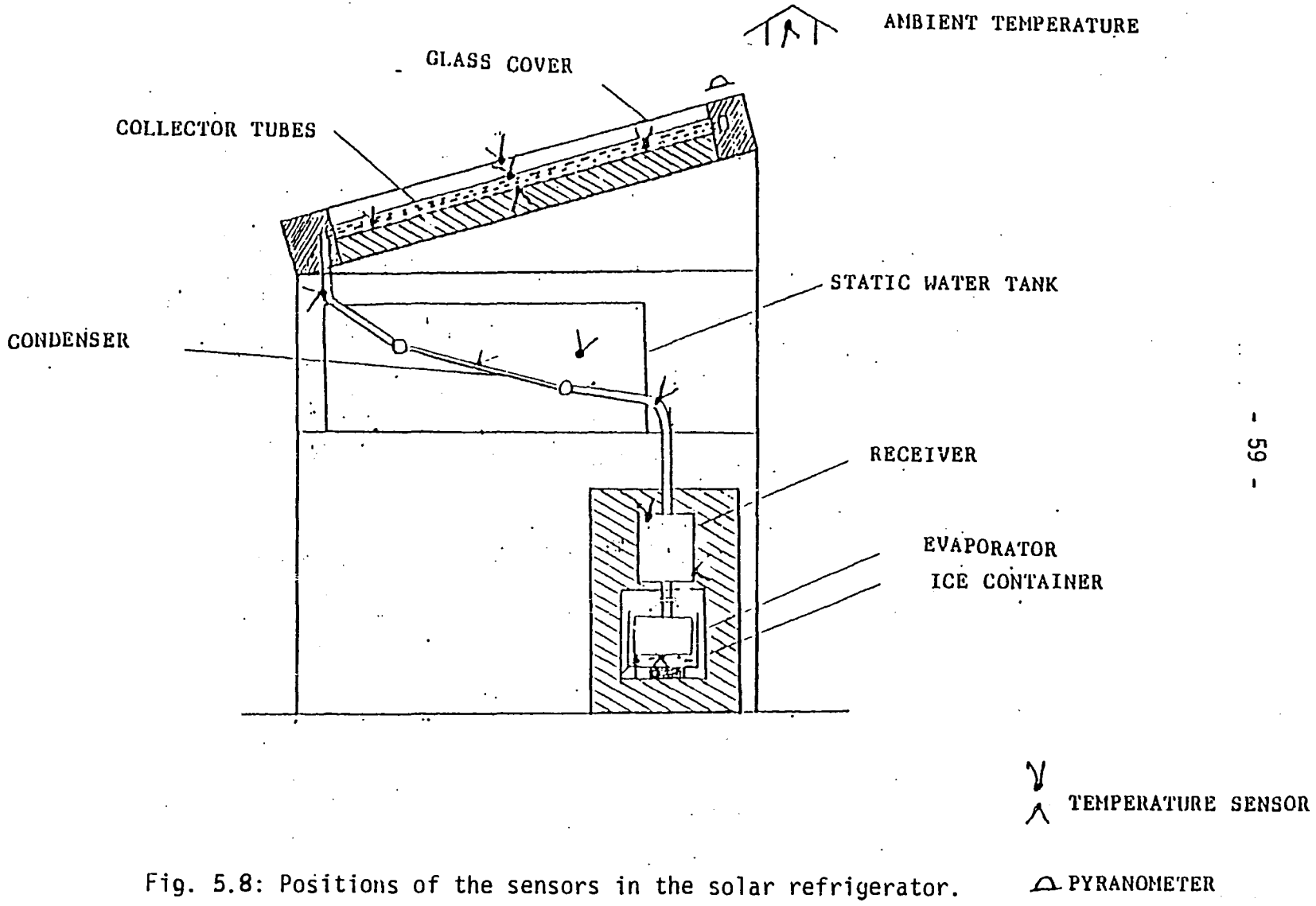

Fig. 5.8: Positions of the sensors in the solar refrigerator.

Liquid Level

The volume of the methanol can be read from the level glass attached to the receiver. Sine the density of methanol liquid is known from the property tables, the mass of methanol in the receiver, and thus the mass cycled, can be estimated.

5.3 Testing Procedure and General Observations

The performance of the above solar refrigerator has been monitored since the beginning of October, 1987. The the weather during October was highly variable, as there were a few exceptionally clear days, as well as some cloudy and some rainy days. The experimental observations for a few days are given in Tables 5.3 through 5.5.

5.3.1 Solar Radiation

The solar radiation incident on the surface of the collector during the period of the experimentation varied between 9.4 and 23.24 MJ/m^2-day. The daily solar radiation incident on the surface of the collector for the month of October is shown in Fig. 5.9.

5.3.2 Ambient Temperature

The minimum ambient temperature recorded during October was 20°C during a cool night, and the maximum value was 34°C during clear afternoons.

5.3.3 Collector Temperature

Five sensors (2 and 5 to measure top and bottom temperatures of collector tubes, 3 and 4 to measure charcoal temperatures from the top and bottom end of tubes, 1 to measure glass temperature) were used to measure collector temperatures. The collector reached 122°C during clear days, and the minimum collector temperature was 4 -- 6°C above the minimum ambient temperature, while the charcoal temperature was 1 -- 2°C above tube temperatures. The temperature profile of the collector during a clear day and including the ambient temperature are shown Fig. 5.10.

5.3.4 Condenser Temperatures

The water in the static water tank cools down to a temperature close to the minimum ambient temperature during the night as the tank is not insulated. The maximum water temperature was about 32°C and the condensation temperature was close to the ambient temperature.

Table 5.3: The Experimental Observations of the AIT Charcoal-Methanol Solar Refrigerator (17 October, 1987).

Local Time	Amb Temp.	Collector Temperatures					Condenser Temperatures				Receiver		Evaporator		Level Glass	Incident Radiation	Remarks
		Glass	Coll. Top	Coll. Bot	Char Top	Char. Bot	Vapour	Liquid	Tube	Water	Top	Bot.	Evap.	Ice			
(Hr)	(C)	(C)	(C)	(C)	(C)	(C)	(C)	(C)	(C)	(C)	(C)	(C)	(C)	(C)	(Cm)	(kJ)	
6.00	24.62	24.52	30.63	30.87	27.55	24.73	27.53	24.50	27.14	27.10	-8.80	-8.94	-2.85	-1.38	-	0.00	
7.00	26.15	27.55	32.15	30.87	32.10	32.38	27.53	26.02	27.14	27.10	1.91	-8.94	-2.85	-1.38	-	205.20	
8.00	26.15	33.61	41.24	40.05	38.16	38.50	33.59	26.02	27.34	27.10	11.09	0.24	-1.32	-1.38	-	962.20	
9.00	27.68	42.70	60.93	61.47	56.34	58.39	41.17	27.53	28.03	27.79	18.74	15.54	-1.32	-1.38	-	1809.80	
10.00	30.74	50.28	81.38	81.36	76.03	79.81	53.29	30.56	30.41	28.49	27.92	21.66	0.21	-1.38	4.00	2465.50	
10.50	33.04	54.06	86.99	87.79	80.58	85.93	60.10	30.56	31.40	28.98	27.92	19.37	0.98	-1.38	6.20	1452.30	
11.00	33.80	57.85	94.26	95.13	86.64	92.05	63.89	33.59	32.19	29.58	29.45	18.60	1.74	-1.38	9.00	1759.30	
11.50	30.74	51.79	89.72	90.54	88.15	92.05	51.77	31.32	31.40	30.17	27.92	18.60	4.80	-1.38	10.30	756.00	
12.00	30.74	45.73	85.17	85.95	85.12	87.46	47.23	30.56	31.10	30.37	26.39	17.07	4.80	-1.38	10.40	408.00	
12.50	32.27	48.76	92.75	92.07	91.18	93.58	55.56	32.08	31.60	30.66	28.69	17.84	7.10	-1.38	10.40	1101.30	
13.00	32.27	53.31	100.32	99.72	94.21	96.64	60.86	32.08	31.89	30.86	29.45	18.60	6.33	-1.38	11.90	1382.50	
13.50	33.80	57.85	106.38	105.84	100.27	104.29	63.89	33.59	32.49	31.36	30.22	26.25	7.86	-1.38	13.80	1642.20	
14.00	32.27	54.82	109.41	108.90	104.82	108.88	60.86	32.08	32.39	31.35	29.45	20.13	9.39	-1.38	15.30	1274.00	
14.50	33.04	63.91	113.20	113.49	104.82	113.47	63.89	32.83	32.78	32.15	27.92	20.13	9.39	-1.38	16.10	1340.40	
15.00	32.27	54.82	109.41	108.90	109.36	111.94	53.29	32.08	32.39	32.45	27.92	20.13	9.39	-1.38	16.60	930.80	
15.50	32.27	45.73	91.23	92.07	100.27	99.70	45.71	30.56	32.39	32.25	23.33	18.60	29.28	29.22	17.00	308.30	
16.00	29.21	45.73	80.63	79.83	86.64	87.46	44.20	29.05	-	-	15.68	17.07	20.10	21.57	15.60	653.30	
17.00	29.21	36.64	60.93	59.94	63.91	64.51	39.65	22.99	-	-	4.97	6.36	10.92	10.86	13.40	702.70	
18.00	29.21	33.61	50.33	50.76	53.31	53.80	36.62	21.47	-	-	-1.15	0.24	6.33	6.27	11.40	110.60	
19.00	29.21	30.58	42.75	43.11	45.73	46.15	33.59	24.50	-	-	-5.74	-4.35	1.74	1.68	10.10	0.00	
20.00	27.68	29.07	38.21	38.52	39.67	40.03	33.59	26.02	-	-	-5.74	-4.35	0.21	0.15	9.20	0.00	
21.00	27.68	27.55	36.69	35.46	38.16	38.50	32.08	26.02	-	-	-7.27	-5.88	-1.32	-1.38	8.30	0.00	
22.00	27.68	27.55	35.18	35.46	36.64	36.97	30.56	26.02	-	-	-8.80	-5.88	-1.32	-1.38	7.50	0.00	
23.00	26.15	26.04	35.18	35.46	36.64	36.97	30.56	26.02	-	-	-8.80	-7.41	-1.32	-1.38	6.50	0.00	
24.00	26.15	26.04	33.66	33.93	35.13	35.44	30.56	26.02	-	-	-8.80	-7.41	-2.85	-2.91	5.70	0.00	
1.00	26.15	26.04	32.15	32.40	35.13	35.44	30.56	26.02	-	-	-8.80	-7.41	-2.85	-2.91	-	0.00	
2.00	26.15	26.04	32.15	32.40	33.61	33.91	29.05	26.02	-	-	-8.80	-7.41	-2.85	-2.91	-	0.00	
3.00	26.15	26.04	32.15	32.40	33.61	33.91	29.05	24.50	-	-	-8.80	-7.41	-2.85	-2.91	-	0.00	
4.00	24.62	24.52	30.63	30.87	32.10	32.38	29.05	24.50	-	-	-8.80	-7.41	-2.85	-2.91	-	0.00	
5.00	24.62	24.52	30.63	29.34	29.07	29.32	29.05	24.50	-	-	-7.27	-7.41	-2.85	-2.91	-	0.00	
6.00	24.62	24.52	30.63	29.34	29.07	29.32	29.05	24.50	-	-	-1.15	-7.41	-4.38	-4.44	0.00	0.00[a]	

Total Incident Solar Radiation = 19265.0

[a] End of Adsorption.

Table 5.4: The Experimental Observations of the AIT Charcoal-Methanol Solar Refrigerator (27 October, 1987).

Local Time	Amb Temp.	Collector Temperatures					Condenser Temperatures				Receiver		Evaporator		Level Glass	Incident Radiation	Remarks
		Glass	Coll. Top	Coll. Bot	Char Top	Char. Bot	Vapour	Liquid	Tube	Water	Top	Bot.	Evap.	Ice			
(Hr)	(C)	(C)	(C)	(C)	(C)	(C)	(C)	(C)	(C)	(C)	(C)	(C)	(C)	(C)	(Cm)	(kJ)	
6.00	20.03	19.98	24.57	24.75	26.04	26.26	24.50	19.96	23.18	23.14	-11.86	-12.00	-5.91	-5.97	-	0.00	
7.00	24.62	21.49	26.09	26.28	26.04	26.26	24.50	21.47	23.87	23.93	0.38	-10.47	-7.44	-9.03	-	180.60	
8.00	26.15	26.04	33.66	32.40	32.10	33.91	27.53	22.99	23.97	23.93	6.50	-4.35	-4.38	-4.44	-	966.80	
9.00	27.68	35.13	53.36	53.82	50.28	50.74	36.62	24.50	27.64	25.22	15.68	12.48	-1.32	-1.38	-	1825.70	
10.00	29.21	44.22	76.08	76.77	69.97	73.69	48.74	26.02	28.63	25.52	24.86	20.13	-1.32	-1.38	3.90	2522.10	
10.50	29.21	47.25	82.14	82.89	76.03	79.81	53.29	26.02	29.12	26.01	23.33	15.54	-1.32	-1.38	5.80	1482.90	
11.00	29.21	50.28	88.20	89.01	82.09	85.93	56.32	27.53	29.32	26.51	23.33	14.01	-1.32	0.15	8.50	1577.50	
11.50	29.21	50.28	92.75	93.60	85.12	92.05	57.83	29.05	29.52	27.30	24.86	14.01	-1.32	0.15	11.20	1692.50	
12.00	29.21	50.28	97.29	98.19	91.18	95.11	59.35	29.05	29.12	27.60	24.86	14.01	0.21	0.15	13.90	1448.50	
12.50	29.21	47.25	98.81	99.72	95.73	99.70	53.29	29.05	29.22	28.09	24.86	14.01	-1.32	0.15	14.70	1307.30	
13.00	29.21	50.28	106.38	107.37	101.79	107.35	57.83	29.05	29.22	28.59	24.86	12.48	-1.32	0.15	16.10	1691.30	
13.50	29.21	51.79	112.44	113.49	109.36	113.47	57.83	29.05	29.12	28.68	24.86	12.48	-1.32	0.15	17.70	1635.50	
14.00	29.21	53.31	118.50	118.08	115.42	116.53	57.83	29.05	28.82	28.59	24.86	12.48	0.21	0.15	18.30	1520.10	
14.50	29.21	53.31	121.53	122.67	119.97	122.65	56.32	29.05	29.12	28.49	23.33	12.48	0.21	0.15	18.70	1368.60	
15.00	29.21	53.31	121.53	122.67	121.48	122.65	54.80	29.05	29.12	28.59	23.33	12.48	0.21	0.15	18.90	1187.50	
15.50	29.21	53.31	120.02	121.14	121.48	122.65	53.29	29.05	-	-	23.33	14.01	0.21	0.15	18.90	991.70	
16.00	29.21	53.31	113.96	115.02	116.94	118.06	53.29	30.56	-	-	23.33	17.07	15.51	15.45	16.80	797.90	
17.00	29.21	41.19	70.02	69.12	76.03	76.75	41.17	21.47	-	-	8.03	7.89	15.51	15.45	16.20	895.90	
18.00	26.15	32.10	51.84	50.76	57.85	58.39	36.62	15.41	-	-	-2.68	0.24	6.33	6.27	14.20	144.00	
19.00	26.15	27.55	42.75	41.58	45.73	46.15	33.59	19.96	-	-	-5.74	-4.35	0.21	1.68	13.10	0.00	
20.00	24.62	26.04	38.21	38.52	39.67	40.03	30.56	21.47	-	-	-7.27	-7.41	-1.32	1.68	11.60	0.00	
21.00	24.62	24.52	35.18	35.46	36.64	36.97	30.56	22.99	-	-	-8.80	-8.94	-1.32	-1.38	10.70	0.00	
22.00	23.09	23.01	33.66	33.93	33.61	33.91	29.05	22.99	-	-	-10.33	-10.47	-2.85	-1.38	8.90	0.00	
23.00	23.09	23.01	30.63	30.87	32.10	32.38	27.53	22.99	-	-	-10.33	-10.47	-2.85	-1.38	8.00	0.00	
24.00	23.09	23.01	30.63	30.87	32.10	32.38	27.53	22.99	-	-	-10.33	-10.47	-2.85	-1.38	7.30	0.00	
1.00	23.09	23.01	29.12	29.34	30.58	30.85	27.53	22.99	-	-	-10.33	-10.47	-4.38	-1.38	-	0.00	
2.00	23.09	23.01	29.12	29.34	30.58	30.85	27.53	22.99	-	-	-10.33	-10.47	-4.38	-1.38	-	0.00	
3.00	23.09	23.01	29.12	29.34	30.58	30.85	26.02	22.99	-	-	-10.33	-10.47	-4.38	-1.38	-	0.00	
4.00	21.56	21.49	27.60	27.81	30.58	30.85	26.02	21.47	-	-	-10.33	-10.47	-4.38	-1.38	-	0.00	
5.00	21.56	21.49	27.60	27.81	29.07	29.32	26.02	21.47	-	-	-10.33	-10.47	-4.38	-1.38	-	0.00	
6.00	21.56	21.49	26.09	26.28	27.55	27.79	24.50	21.47	-	-	-10.33	-10.47	-5.91	-1.38	0.00	0.00*	

Total Incident Solar Radiation = 23042.0

* End of Adsorption.

Table 5.5: The Experimental Observations of the AIT Charcoal-Methanol Solar Refrigerator (29 October, 1987).

Local Time	Amb Temp.	Collector Temperatures					Condenser Temperatures				Receiver		Evaporator		Level Glass	Incident Radiation	Remarks
		Glass	Coll. Top	Coll. Bot	Char Top	Char. Bot	Vapour	Liquid	Tube	Water	Top	Bot.	Evap.	Ice			
(Hr)	(C)	(C)	(C)	(C)	(C)	(C)	(C)	(C)	(C)	(C)	(C)	(C)	(C)	(C)	(Cm)	(kJ)	
6.00	24.62	24.52	29.12	29.34	29.07	29.32	26.02	22.99	25.16	25.12	0.38	-7.41	-5.91	-5.97	-	0.00	
7.00	24.62	23.01	29.12	29.34	29.07	29.32	27.53	22.99	25.46	25.52	4.97	-7.41	-4.38	-4.44	-	63.40	
8.00	24.62	26.04	32.15	32.40	32.10	32.38	29.05	24.50	25.46	25.52	8.03	-2.82	-2.85	-2.91	-	346.10	
9.00	26.15	35.13	50.33	50.00	47.25	47.68	35.11	26.02	25.75	25.62	15.68	9.42	-1.32	-1.38	-	1516.70	
10.00	27.68	41.19	73.05	73.71	68.46	70.63	45.71	27.53	27.04	26.11	27.92	27.78	0.21	0.15	3.90	2447.40	
10.50	29.21	44.22	79.11	79.83	73.00	76.75	48.74	27.53	29.02	26.51	26.39	18.60	-1.32	-1.38	5.80	1410.90	
11.00	30.74	47.25	85.17	85.95	80.58	84.40	51.77	29.05	29.62	26.80	24.86	17.07	-1.32	-1.38	6.70	1354.70	
11.50	30.74	47.25	86.69	87.48	83.61	85.93	51.77	29.05	30.41	27.89	24.86	15.54	-1.32	-1.38	8.80	1379.10	
12.00	30.74	50.28	94.26	95.13	88.15	92.05	56.32	29.80	30.51	28.19	26.39	15.54	-1.32	-1.38	10.40	1566.00	
12.50	30.74	50.28	94.26	95.13	91.18	95.11	54.80	29.80	30.11	28.68	26.39	15.54	0.21	0.15	12.00	1263.10	
13.00	30.74	51.79	98.81	99.72	95.73	99.70	56.32	30.56	30.41	29.28	26.39	15.54	3.27	3.21	13.00	1293.10	
13.50	30.74	54.82	103.35	104.31	100.27	104.29	56.32	30.56	30.31	29.58	26.39	15.54	4.80	4.74	14.00	1253.90	
14.00	30.74	53.31	104.87	105.84	103.30	105.82	54.80	30.56	30.11	30.37	26.39	15.54	3.27	3.21	15.00	1060.30	
14.50	30.74	57.85	110.93	111.96	107.85	110.41	60.86	32.08	31.10	30.37	27.92	15.54	4.80	4.74	16.50	1411.80	
15.00	30.74	56.34	112.44	113.49	110.88	113.47	56.32	32.08	30.90	30.76	26.39	17.07	6.33	6.27	17.00	1198.10	
15.50	30.74	51.79	109.41	110.43	110.88	111.94	50.26	30.56	-	-	26.39	17.07	7.86	7.80	16.90	748.60	
16.00	30.74	50.28	104.87	105.84	106.33	107.35	51.77	32.08	-	-	24.86	20.13	29.28	29.22	16.90	762.20	
17.00	29.21	39.67	69.51	67.59	74.52	75.22	41.17	24.50	-	-	9.56	9.42	15.51	15.45	14.50	534.30	
18.00	27.68	33.61	54.87	53.82	57.85	58.39	36.62	16.93	-	-	0.38	1.77	7.86	7.80	12.50	72.60	
19.00	27.68	30.58	45.78	44.64	47.25	47.68	35.11	16.93	-	-	-4.21	-2.82	3.27	3.21	11.00	0.00	
20.00	27.68	30.58	39.72	40.05	41.19	41.56	32.08	26.02	-	-	-4.21	-4.35	0.21	0.15	10.20	0.00	
21.00	26.62	27.55	35.18	35.46	36.64	36.97	29.05	24.50	-	-	-8.80	-7.41	-1.32	-1.38	9.20	0.00	
22.00	24.62	26.04	33.66	33.93	35.13	35.44	29.05	24.50	-	-	-8.80	-7.41	-1.32	-1.38	7.90	0.00	
23.00	24.62	24.52	32.15	32.40	33.61	33.91	29.05	24.50	-	-	-8.80	-8.94	-1.32	-1.38	7.00	0.00	
24.00	24.62	24.52	32.15	32.40	33.61	33.91	29.05	24.50	-	-	-8.80	-7.41	-2.85	-2.91	6.40	0.00	
1.00	23.09	23.01	30.63	30.87	30.58	30.85	27.53	24.50	-	-	-10.33	-10.47	-2.85	-2.91	-	0.00	
2.00	23.09	23.01	29.12	29.34	30.58	30.85	27.53	22.99	-	-	-8.80	-8.94	-2.85	-2.91	-	0.00	
3.00	23.09	23.01	29.12	29.34	30.58	30.85	27.53	22.99	-	-	-8.80	-8.94	-2.85	-2.91	-	0.00	
4.00	23.09	23.01	29.12	29.34	29.07	29.32	27.53	22.99	-	-	-8.80	-8.94	-2.85	-2.91	-	0.00	
5.00	23.09	23.01	29.12	29.34	29.07	29.32	27.53	22.99	-	-	-8.80	-8.94	-4.38	-4.44	-	0.00	
6.00	23.09	23.01	29.12	29.34	29.07	29.32	27.53	22.99	-	-	0.38	-8.94	-4.38	-4.44	0.00	0.00*	

Total Incident Solar Radiation = 19682.3

* End of Adsorption.

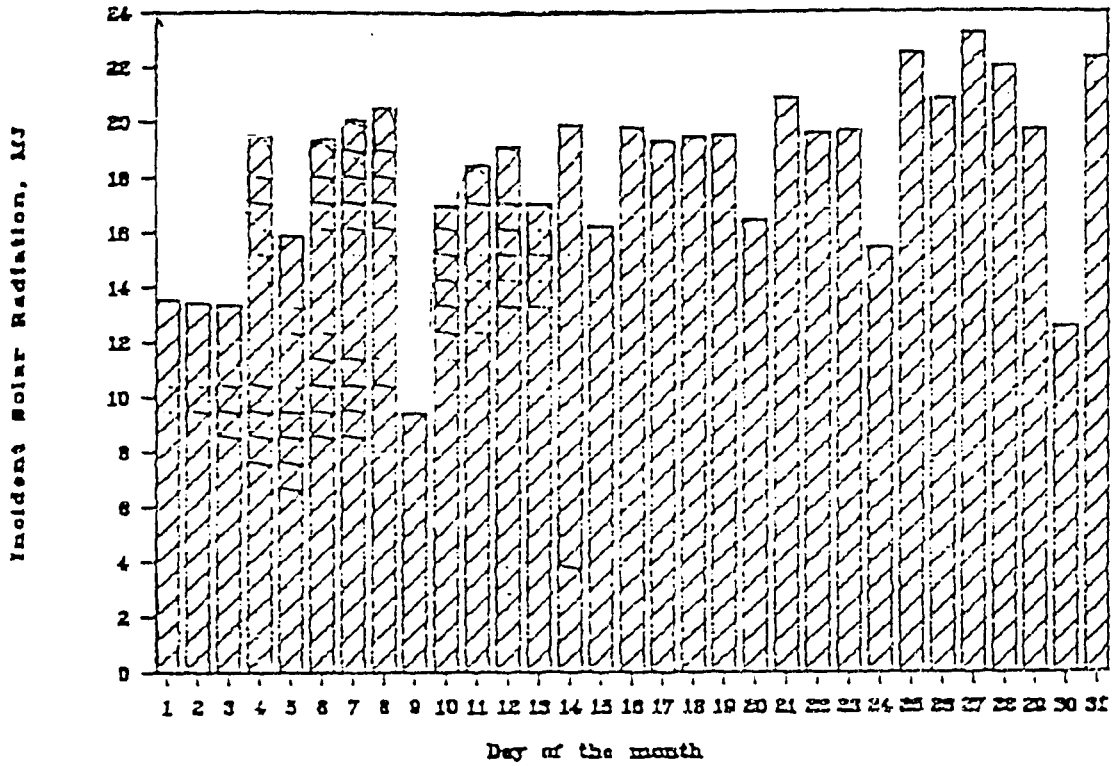

Fig. 5.9: The Incident Solar Radiation on the Surface of Solar Collector for the month of October, 1987.

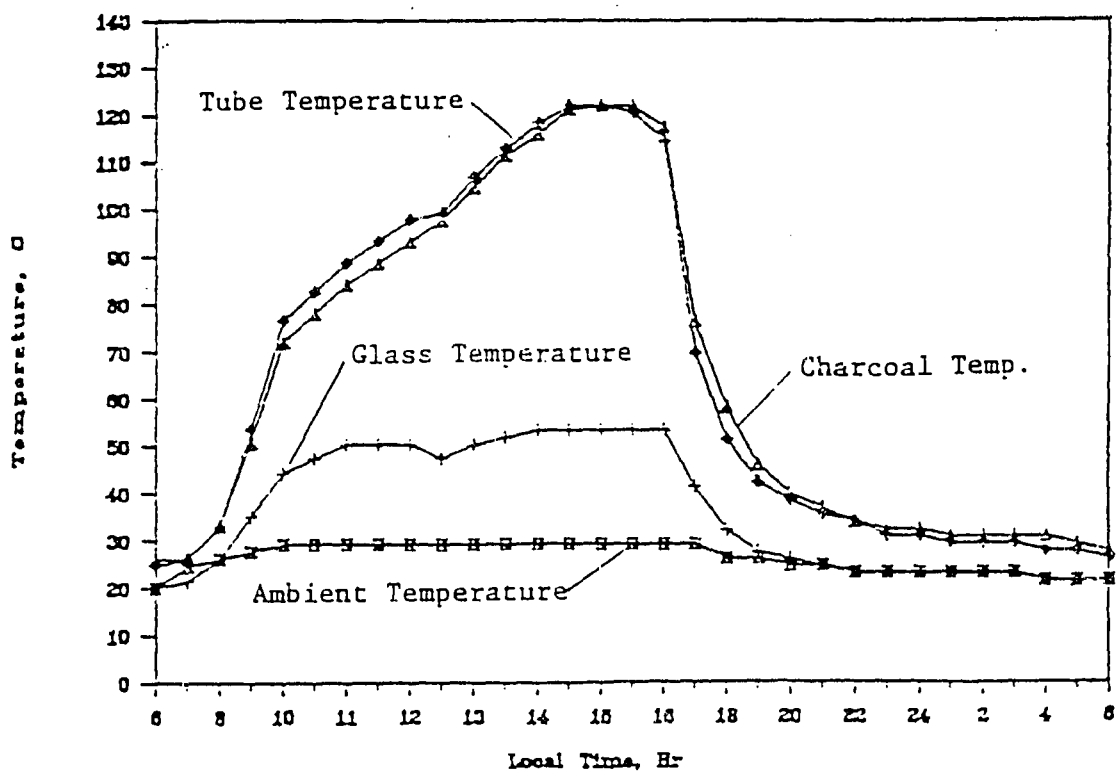

Fig. 5.10: The Temperature Profile of the Solar Collector during a Clear Day (27 October, 1987).

5.3.5 Receiver/Evaporator Temperature

Three temperature sensors(8, 9 and 10) were used to measure receiver/evaporator temperatures. The evaporator temperature is read by sensor 10, but during the cooling process it is immersed in the water and it reads a temperature intermediate between the evaporator and the water/ice temperature. The temperature measured by sensor 9, which is just above the evaporator, was taken as the evaporator temperature. The lowest evaporator temperature was -13.4°C. The temperature profile of the receiver/evaporator for a typical day is shown in Fig. 5.11. The condensation first starts in the receiver/evaporator as it is the coldest, and the temperature rises. This melts a small quantity of ice allowing the rest of the ice to be removed easily.

5.4 Experimental Data Analysis

5.4.1 Initial Analysis

The initial results calculated for the solar refrigerator were based on the heat balance at the end of desorption using the properties at the mean temperatures. The main assumptions are as follows:

1. The condenser temperature varies between 24°C and 32°C. But for this calculations, it was assumed equal to 31°C.

2. The temperature at state point 2 (beginning of the desorption), also called threshold temperature, cannot be determined accurately by observations as the first condensate collects in the evaporator and level cannot be read. So, this was determined from the p-T-x chart of the pair, and the value thus obtained was verified by calculations for T_2 using the mean properties by the Clausius Clapeyron equation as follows:

$$L(1/T_{ev} - 1/T_{con}) = H_{des}\,(1/T_1 - 1/T_2), \qquad (5.24)$$

where

T_{ev} = Evaporator Temperature, C,
T_{con} = Condenser, C,
T_1 = Temperature of charcoal at the end of adsorption, C,
T_2 = Threshold temperature, C,
L = Latent heat of evaporation, kJ/kg,
H_{des} = Heat of desorption, kJ/kg.

3. The methanol liquid is assumed to evaporate at -10°C with the latent heat of evaporation L constant.

The useful heat during desorption Q_u (from state point 1 to 3) is given as:

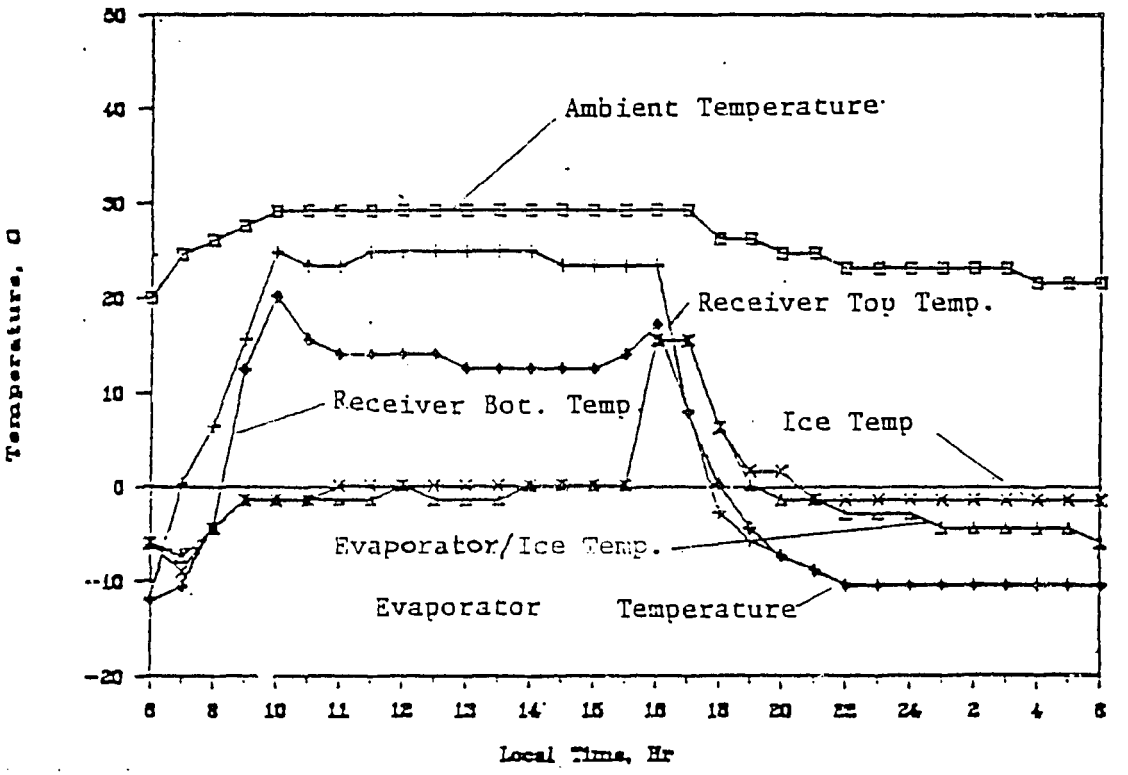

Fig. 5.11: The Temperature Profile of the Receiver/Evaporator Box (27 October, 1987).

$$Q_u = Q_{coll} + Q_{ch} + Q_{meoh} + Q_{des} \quad (5.25)$$

where

Q_{coll} = Total sensible heat used to raise the temperature of the collector, kJ,
Q_{ch} = Sensible heat used to heat the charcoal in the collector tubes, kJ,
Q_{meoh} = Sensible heat to the methanol liquid adsorbed in the charcoal, kJ,
Q_{des} = Total heat of desorption of the methanol, kJ.

If Q_{Ides} is the integrated value of the incident solar radiation on the surface of the solar collector at the end of desorption; then the average collector efficiency during desorption can be calculated as:

$$\text{Coll Eff.} = Q_u / Q_{Ides} \quad (5.26)$$

Based on the above assumptions, the cooling produced by the methanol during adsorption can be approximated as:

$$Q_c = m_r (L - CP_{meoh} (T_{con} + 10.0)), \quad (5.27)$$

where

m_r = Mass of the methanol cycled, kg,
CP_{meoh} = Specific heat of methanol, kJ/kg-K.

Thus, the integrated thermal coefficient of performance (COPIN) can be calculated as:

$$COPIN = Q_c / Q_u \quad (5.28)$$

Similarly, the two integrated COPs of the system based on the amount of incident solar radiation can be calculated as follows:

COPINS (until the end of desorption) $= Q_c / Q_{Ides}$ (5.29)

COPINS (over the day) $= Q_c / Q_{Iday}$ (5.30)

where Q_{Iday} is the total incident radiation.

The performance of the charcoal-methanol solar refrigerator for the period of initial testing is given in Table 5.6.

5.4.2 Detailed Analysis

The above analysis gives the average performance of the system, but detailed calculations were done to determine the performance over the particular day. This analysis is based on the heat balances of the collector during desortion, and heat balances of the receiver/evaporator during adsorption. The main assumptions for the calculations are as follows:

Table 5.6: Test Results of AIT Charcoal-Methanol Solar Refrigerator (2-12 October, 1987)

Day	Hours	Incident Solar Energy (kJ)	Temperatures Amb. (C)	Coll. (C)	Char. (C)	Cond. (C)	Methanol Cycled (kg)	Evap. Temps. (C)	Useful Heat (kJ)	Total Cooling (kJ)	Avg. Coll. Eff.	COPIH	COPIHS	Remarks
2/10/1987	6:00													
	13:30	12428.9	30.7	100.0	97.7	31.0	1.83	31.6	5340.8	1993.3	0.430	0.373	0.160	Clouded
	18:00	13404.6	23.1	26.9	26.9			-11.2					0.149	day
3/10/1987	6:00													
	15:00	11382.3	30.7	103.8	103.4	31.0	1.29	30.1	4649.0	1414.4	0.408	0.304	0.124	Clouded
	18:00	13315.0	26.2	28.8	29.2			-8.9					0.106	day
4/10/1987	6:00													Clear Morn.,
	15:00	16627.9	29.2	104.6	104.1	31.0	2.19	30.1	6005.7	2388.6	0.361	0.398	0.144	Rain
	18:00	19483.4	24.6	28.1	28.8			-10.9					0.123	After noon
5/10/1987	6:00													
	13:30	13398.9	31.5	109.2	105.7	31.0	2.05	30.1	5923.9	2232.8	0.442	0.377	0.167	Partially
	18:00	15844.4	23.1	28.1	28.0			-12.0					0.141	Clouded
6/10/1987	6:00													
	15:30	18523.9	33.0	116.8	116.7	31.0	2.44	29.3	6822.4	2660.4	0.368	0.290	0.144	Clear
	18:00	19307.9	24.6	27.7	27.6			-10.5					0.138	day
7/10/1987	6:00													
	14:30	18953.9	35.3	124.4	123.6	31.0	2.65	30.1	7337.3	2902.3	0.387	0.395	0.153	Clear
	18:00	20060.2	24.6	28.5	29.2			-9.7					0.145	day
8/10/1987	6:00													
	14:30	17444.8	27.6	108.0	107.6	31.0	2.40	27.8	6467.3	2636.6	0.371	0.407	0.151	Clear
	18:00	20513.8	23.9	27.7	28.0			-7.4					0.128	day
9/10/1987	6:00													
	14:30	9218.0	29.2	96.2	94.7	31.0	0.68	27.8	3466.4	746.7	0.375	0.215	0.081	Clouded
	18:00	9405.2	24.6	28.8	29.2			-8.9					0.079	day
10/10/1987	6:00													
	14:00	13288.4	33.8	109.2	105.3	31.0	1.77	27.0	5498.9	1946.2	0.414	0.354	0.146	Partially
	18:00	16905.5	23.1	28.4	24.4			-8.2					0.115	Clouded
11/10/1987	6:00													Rain
	14:00	15961.2	32.3	115.3	114.5	31.0	2.33	28.5	6543.0	2634.6	0.395	0.439	0.174	during
	18:00	18401.6	23.9	29.2	29.2			-8.9					0.138	Afternoon
12/10/1987	6:00													Clouded
	13:30	15166.3	32.3	98.5	97.3	31.0	2.40	27.1	5996.5	2634.6	0.395	0.439	0.174	Morning
	18:00	19087.0	24.6	30.8	30.7			-7.4					0.138	Clear Later

1. The methanol adsorbed in the charcoal is assumed to be at the mean charcoal temperature.

2. The properties of the collector tubes and the charcoal were assumed constant.

3. The properties of the methanol were computed as a function of temperature from the regression formulas based on published tables (Liley, 1982).

4. The heat of desorption was computed as a function of the charcoal temperature T and concentration x as follows:

$$H_{des} = (P(T)\,\mathcal{V}(T)/T) \quad \text{slope}(x), \tag{5.31}$$

where

P(T) = Saturation pressure of the methanol vapour at temp. T, bar,

slope = Slope of the isosters calculated from the Clausius diagram for the charcoal-methanol based on the laboratory tests.

For the slopes for different concentrations of methanol in charcoal, x (wt. %) was represented by the following regressions:

$$\text{slope} = 4977.84 - 3776.07\,x \qquad 0.15 \leq x \leq 0.21,$$

$$\text{slope} = 11076.1 - 43996.0\,x \qquad 0.10 \leq x \leq 0.15,$$

$$\text{slope} = 7206.6 - 5366.9\,x \qquad 0.02 \leq x \leq 0.10.$$

The specific volume $\mathcal{V}$ of the saturated methanol vapour can calculated as:

$$\mathcal{V}(T) = 21780.3 \quad \exp(-0.0304\,T),\ m^3/kg \tag{5.32}$$

The saturation vapour pressure of methanol was calculated using the Harlacher equation(Reid and others, 1977) as follows:

$$P(T) = \exp(HARA + HARB/T + HARC\ \ln(T) + HARD * P(T)/T^2) \tag{5.33}$$

5. Other Properties of methanol were calculated as follows:

$$CP_{meoh} = 3.96 - 0.152\,T + 0.000035\,T^2 \tag{5.34}$$

$$\rho_{meoh} = 947.7 - 0.1152\,T - 0.0014\,T^2 \tag{5.35}$$

$$h_l = 121.07 + 0.7115\,T + 0.003\,T^2 \tag{5.36}$$

$$h_v = 1120.35 + 3.383\,T - 0.00401\,T^2 \tag{5.37}$$

here

CP_{meoh} = Specific heat, kJ/kg-K,
ρ_{meoh} = Density, kg/m^3,
h_l = Specific enthalpy of methanol liquid, kJ/kg,
h_v = Specific enthalpy of methanol vapour, kJ/kg,
and T = Temperature, K.

6. For the COP calculations during desorption, the methanol was assumed to evaporate at -10°C with a constant latent heat L.

Desorption Period

The temperature at the state point 2 at the beginning of desorption was estimated by the method described earlier. The first heat balance starts when the methanol level can be read from the level glass. The heat used during the sensible heating up to 2, and the desorption until value could be read, were estimated from the experimental data. The heat balance of the solar collector was calculated every half an hour until the end of desorption.

The useful heat dQUsed for each period can be calculated as:

$$dQUsed = dQTube + dQChar + dQMeoh + dQDes, \quad (5.38)$$

where

dQTube = Sensible heating of the collector tubes during the interval, kJ,
dQChar = Sensible heating of the charcoal in the tubes, kJ,
dQMeoh = Sensible heating of mean mass of methanol, kJ,
dQDes = Heat of desorption, kJ.

If dQRad is the incident radiation, during the same interval, the collector efficiency can be calculated as:

$$Coll.\ Eff = dQUsed/\ dQRad \quad (5.39)$$

Similarly if dQEv is the cooling that could be produced by the methanol desorbed calculated as shown earlier, the thermal coefficient of performance of the system during the period is:

$$COP_{In} = dQEv/dQUsed \quad (5.40)$$

The coefficient of performance for the same period based on the incident solar radiation is

$$COP_{Ins} = dQEv/dQRad \quad (5.41)$$

The accumulated value of thermal coefficient of performance up to the particular period can be calculated as:

$$COP_{Intg.} = \sum dQEv / \sum dQUsed \qquad (5.42)$$

Similarly, the accumulated coefficient of performance based on the solar radiation up to that period is :

$$COP_{Intgs.} = \sum dQEv / \sum dQRad \qquad (5.43)$$

The concentration of methanol in the charcoal was calculated reading the methanol level from the level glass, and the corresponding values calculated using Dubinin the equation and the performance of the solar refrigerator during the desorption period for a clear day is shown in Table 5.7.

Adsorption Period

The net cooling produced during the adsorption was calculated by performing hourly heat balances of the receiver/evaporator. The methanol level generally could not be read after 24:00 hours (midnight). But the end of adsorption was estimated from the temperature profile of the receiver/evaporator, which generally occurred after 2:00 a.m. The evaporator temperature remains constant during the period after midnight. The last heat balance covers the time period between midnight and the end of adsorption. In each case, the properties of the methanol were evaluated at the mean temperature for the period. The net cooling produced by the system dQNet during each period can calculated as:

$$dQNet = dQc - (dQRec + dQEvap + dQLIq + dQLoss), \qquad (5.44)$$

where the heat values for the components during the period are:

dQc = Cooling produced by the methanol cycled during the period (kJ),
dQRec = Sensible heating/cooling of the receiver (kJ),
dQEvap = Sensible heating/cooling of the evaporator (kJ),
dQLiq = Sensible heating/cooling of the mean mass of the liquid in the receiver/evaporator (kJ),
dQLoss = Heat lost from the receiver/evaporator box (kJ).

Thus the net solar COP, also called the overall coefficient of performance of the refrigerator, can be calculated as:

$$\text{Net Solar COP} = \sum dQNet / \sum dQRAd, \qquad (5.45)$$

where $\sum dQNet$ is the net cooling produced during adsorption period, and $\sum dQRad$ is the total incident solar radiation during the day.

The performance of the system during the adsorption period is shown in Table 5.8.

Table 5.7: The Performance of the AIT Charcoal-Methanol Solar Refrigerator during a Clear Day (29 October, 1987).

Local Time (Hr)	Amb. Temp. (C)	Mean Temp. Coll. (C)	Mean Temp. Char (C)	Exp. MEOH Conc.	Theo. MEOH Conc.	dQTube (kJ)	dQChar (kJ)	dQMeoh (kJ)	dMeoh (kg)	dQDes (kJ)	dQUsed (kJ)	dQRad (kJ)	dQEV (kJ)	Coll. Eff.	Coeff. of Performances In	Ins	Intg.	Intgs.	Remark
6.00	24.6	29.2	29.2	.178															
10.00	27.7	73.4	69.5	.144	0.164	703.0	502.8	645.9	0.61	623.5	2475.2	4373.6	673.8	0.57	0.00	0.00	0.27	0.15	
10.50	29.2	79.5	74.9	.128	0.159	97.0	66.4	37.2	0.28	344.4	545.0	1410.9	314.1	0.39	0.58	0.22	0.33	0.17	
11.00	30.7	85.6	82.5	.120	0.142	97.0	94.9	49.5	0.13	182.2	423.5	1354.7	147.1	0.31	0.35	0.11	0.33	0.16	
11.50	30.7	87.1	84.8	.103	0.129	24.2	28.4	13.6	0.31	462.9	529.1	1379.1	336.8	0.38	0.64	0.24	0.37	0.17	
12.00	30.7	94.7	90.1	.090	0.119	121.2	66.4	27.8	0.23	376.3	591.8	1566.0	251.1	0.38	0.42	0.16	0.38	0.17	
12.50	30.7	94.7	93.1	.077	0.106	0.0	37.9	13.9	0.23	378.7	430.6	1263.1	250.1	0.34	0.58	0.20	0.39	0.17	
13.00	30.7	99.3	97.7	.069	0.095	72.7	56.9	18.6	0.14	236.1	384.3	1293.1	155.1	0.30	0.40	0.12	0.40	0.17	
13.50	30.7	103.8	102.3	.061	0.083	72.7	56.9	16.8	0.14	234.4	380.8	1253.9	154.1	0.30	0.40	0.12	0.40	0.16	
14.00	30.7	105.4	104.6	.054	0.074	24.2	28.4	7.5	0.14	232.5	292.6	1060.3	153.2	0.28	0.52	0.14	0.40	0.16	
14.50	30.7	111.4	109.1	.042	0.068	97.0	56.9	12.6	0.21	341.6	508.0	1411.8	225.4	0.36	0.44	0.16	0.41	0.16	
15.00	30.7	113.0	112.2	.038	0.061	24.2	37.9	7.1	0.07	113.3	182.7	1198.1	75.3	0.15	0.41	0.06	0.41	0.16	
Total						1333.2	1033.9	850.4	2.49	3525.9	6743.5	17564.6	2736.0						
As % of Incident Radiation						7.6	5.9	4.8		20.1	38.4								
Total % of Heat Used						19.8	15.3	12.6		52.3									

Table 5.8: The Performance of the AIT Solar Refrigerator during Adsorption Process (29 October, 1987).

Local Time (Hr)	Amb. Temp. (C)	Mean Temp. Rec. (C)	Mean Temp. Evap. (C)	dQRec (kJ)	dQEvap (kJ)	dQLiq (kJ)	dQloss (kJ)	dQC (kJ)	dQNet (kJ)	Remarks
15.00	30.7	21.7	17.1							
15.50	30.7	14.4	17.07	0.00	0.00	0.00	7.14	-25.25	-32.40	
16.00	30.7	20.3	20.13	0.59	2.36	4.78	4.55	20.28	8.00	
17.00	29.2	19.2	9.42	10.01	8.25	75.46	9.43	389.56	286.41	
18.00	27.7	8.5	1.77	6.48	5.89	41.72	17.46	308.93	237.37	
19.00	27.7	2.2	-2.82	3.53	3.53	19.93	22.31	245.87	196.56	
20.00	27.7	-1.1	-4.35	0.59	1.18	3.01	25.16	134.38	104.44	
21.00	24.6	-3.4	-7.41	2.95	2.36	13.83	25.83	174.06	129.10	
22.00	24.6	-4.7	-7.41	0.00	0.00	0.00	25.66	232.15	206.49	
23.00	24.6	-4.9	-8.94	0.59	1.18	2.15	25.83	163.26	133.52	
0.00	24.6	-5.3	-7.41	0.59	1.18	1.94	26.16	109.07	79.20	
6.00	23.1	-4.9	-8.94	2.95	1.18	4.65	150.94	1226.94	1067.22	
Total				28.27	27.10	167.5	340.5	2979.2	2415.9	

Net Solar COP = 0.123

5.5 Results and Conclusions

The average efficiency of the collector varied between 33 and 44% and the peak collector temperature reached 122°C during clear days. The collector temperature was above 90°C even during cloudy days. The thermal coefficient of performance of the system was about 40% including the thermal mass of the components. The system can cycle up to 14 % wt. of methanol out of the 17.8% initially charged into the system. The integrated solar COP over the day was in the range 15%; but the net solar COP of the system during clear days including all the thermal losses in the receiver/evaporator was above 10% and reached up to 12.3%. This result is comparable to the contemporary French results. The evaporator temperature during most days was below -7°C but during some nights, it was as low as -12°C. This system was able to produce up to 4 kg of ice during clear days and the ice produced was subcooled to -4°C; most of the ice produced was removable. It was found that the heat losses in the evaporator were very high mainly due to the large heat transfer area of the box, and the longitudinal heat transfer through the connecting tubes. The solar refrigerator has outperformed our design expectations.

5.6 Cost and Economics of the System

5.6.1 Cost of the System

Table 5.9 shows the cost of the experimental unit built and tested at AIT. The cost of this unit does not contain the cost of the valves and other measuring equipments which are not needed in finished product. It is seen that the major cost of this refrigerator is the cost of the solar collector which accounts for about 60% of total costs. The break down of the solar collector cost shows that cost of the collector tubes and fittings was 31.6%, while the cost of charcoal was 22.5%, assuming the charcoal was acquired by surface mail. The other major cost is the labour cost which was assumed 25% of the material cost and is about 20% of the total cost. The total cost of the solar refrigerator was about US$ 1000.0, in December 1987. The cost of this solar refrigerator could be easily reduced using other cheaper materials such aluminum tubes or sections, and also using the locally manufactured charcoals. It must be mentioned here that the cost of imported charcoal was about ฿ 316.0/kg while the local charcoal is about seven times cheaper. The quality of the local charcoals can be tailor made for this particular application, and hopefully the cheaper local charcoals will help to reduce system costs significantly.

5.6.2 Economic Evaluation

A detailed economic evaluatiation of the solar refrigerator would be premature at this stage since this system is yet to reach a form suitable for commercial production. But a

Table 5.9: The Cost of the Experimental System.

Items	Cost (Bahts)	Cost (% of total)
1. Solar Collector		
Solar collector	8005.0	31.6
Activated Charcoal	5700.0	22.5
Selective Surface	1460.0	5.8
2. Water-cooled Condenser with static water tank	2490.0	9.8
3. Receiver/Evaporator	1260.0	5.0
4. Miscellaneous		
Methanol	500.0	2.0
MS Steel frame	840.0	3.3
Labour Cost	5064.0	20.0
Total Cost	25319.0 (about US $ 1000.0)	100.0

preliminary assessment of economic feasibility has been made using two simple economic indicators: the pay-back period, and the cost:revenue ratio.

The annual revenue from the unit is assumed to come from the sales of ice produced at the current local market prices. The retail price of ice in Bangkok is 3 bahts per kilogram, but in remote areas ice can be sold at twice the Bangkok price. So prices of 4, 5, and 6 bahts per kilogram are also considered. Although the system with slight improvement of the evaporator should be able to produce about 5 kg of ice during clear days, an average ice production of 3 kg per day has been taken for all calculations.

Table 5.10 shows the cost to revenue ratios for assumed lives of the unit from 10 years to 20 years, and assumed interest rates on the borrowed money from 10% to 17.5%. For all calculations a general inflation rate of 7% has been taken. The price of ice for this calculation is assumed to be 3 bahts per kilogram. The cost to revenue ratio varies from 0.52:1 under the most favorable conditions to 1.26:1 under the worst conditions.

Table 5.11 shows the pay-back period of the system using the break even point method. For all calculations only the initial

Table 5.10: Costs and Revenues.

Interest Rate (%)	Machine Life (years)	Initial Cost (bahts)	Present Value of Revenues (bahts)	Ratio
10.0	10.0	25319.0	27917.0	0.91
	15.0		39234.0	0.65
	20.0		49089.0	0.52
12.0	10.0	25319.0	25421.0	0.99
	15.0		34386.0	0.74
	20.0		41521.0	0.61
15.0	10.0	25319.0	22263.0	1.14
	15.0		28641.0	0.88
	20.0		33089.0	0.77
17.5	10.0	25319.0	20069.0	1.26
	15.0		24909.0	1.02
	20.0		27940.0	0.91

Table 5.11: Pay-Back Periods.

Interst Rate (%)	Pay Back Period (years)			
	Selling Price of Ice			
	3 bahts/kg	4 bahts/kg	5 bahts/kg	6 bahts/kg
10.0	8.94	6.49	5.10	4.20
12.0	9.95	7.01	5.42	4.41
15.0	12.17	8.00	5.99	4.79
17.5	15.55	9.14	6.58	5.17

cost of the equipment has been considered (maintenance not included) and present values were calculated at the general inflation rate of 7% per year.

5.6.3 Cost Comparison with the Photovoltaic Refrigerators

This solar refrigerator without much modification can be used for vaccine storage and freezing icepacks. Thus, it is reasonable to compare the cost of our system with the cost of photovoltaic refrigerators. The cost of the photovoltaic refrigerators used in the Expanded Programme of Immunization producing about 1.2 to 2 kg of ice per day range from US$ 4000.0 up to US$ 8000.0. Compared with our system these solar refrigerators are expensive. Moreover instances of failure of photovoltaic systems in field conditions have been encountered due to various reasons, such as failure of the photovoltaic panels due to temperature and wind induced stresses (Srivastava, 1987). Thus there is a great need for some cheap, reliable and robust systems, such as the system developed here.

5.7 Recommendations for the Future Work

The charcoal in the solar refrigerator is cycling more methanol compared to the sample of the same type tested in our test rig. This can be seen from the the theoretical concentrations calculated from the Dubinin equation (see Theo. MEOH Conc. in Table 5.7) and the actual values based on the experimental results (see Exp MEOH Conc. in Table 5.7). Due to the excellent methanol cycling capacity of the charcoal in the solar refrigerator, the receiver/evaporator has been undersized. At this stage, the system is partially charged, and any additional methanol charged into this system cannot be measured during clear days. So, the first improvement should be to redesign the receiver/evaporator. This receiver/evaporator should be larger in capacity, there should be a better level glass arrangement to measure the methanol cycled accurately. Moreover the receiver/evaporator box should be well insulated but compact. Some arrangements should also be made to reduce the longitudinal heat leak through the connecting tube into the receiver/evaporator. With these improvements, the system should be tested to evaluate its long term performance.

This system has performed satisfactorily during tests carried out so far. But long term performance of this system during different seasons must be monitored before possible commercial exploitation of such system in this region.

References

Bechec, M., G. Dhenain, J. Fontaine, G. Marsin, and D. Royer (1981). A Solar Ice Making and Cold Storage Machine With Intermittent Adsorption Cycle. In: Hall, D. O., and J. Mortan (Eds.). Solar World Forum, Vol. 2, Pergamon Press. pp. 1066.

Boon-Long, P. (1983) 'Crop Processing Systems in Northern Thailand', In: Devapriya, D.S. (1984), 'Location Modelling for Post-Harvest Handling Chain ' case of Perishable Crops grown in Northern Thailand' Research Study, Asian Institute of Technology, Bangkok. pp. 1-3.

Breck, D. W. (1974). Zeolite Molecular Sieve. John Wiley and Sons, New York. p. 771.

Chantavorapap, S. (1979) 'Development of Solar Energy in Thailand' Application of Solar Energy in Southeast Asia', Asian Institute of Technology, Bangkok. pp. 142.

Critoph, R. E., and R. Vogel (1986). Possible Adsorption Pairs for Use in Solar Cooling. International Journal of Ambient Energy. In press.

Derrik, A., and J. M. Durand (1986). Photovoltaic Refrigerators for Rural Health Care-Experiments. In: McNelis, B., and J. Morton (Ed.) Solar Energy for Developing Countries Power for Villages. ISES, U. K. Section. pp. 19-25.

Devapriya, D.S. (1984) 'Location Modelling for Post-Harvest Handling Chain' case of Perishable Crops grown in Northern Thailand' Research Study, Asian Institute of Technology, Bangkok. pp. 1-3.

Dubinin, M. M., and V. A. Astakhov (1970). Adv. Chem. Ser. 102. p.72.

Exell, R.H.B., and K. Saricali (1976). The Availability of Solar Radiation in Thailand, Research Report 63, Asian Institute of Technology, Bangkok, Thailand. 85 p.

Exell, R. H. B., and S. Kornsakoo (1981). Design and Testing of of a Solar Powered Refrigerator Research Report No. 126, Asian Institute of Technology, Bangkok. p. 60.

Exell, R. H. B. (1983). The Theory of Simple Solar Refrigerator. Renewable Energy Review Journal, Vol. 5, No. 2. pp. 1-17.

References (Contd.)

Expanded Programme of Immunization (1986). EPI Technical Series The Cold Chain Product Information Sheets. WHO/UNICEF/EPI.TS/86.1. pp. 9.

Food and Agriculture Organization (1984). Design and Operation of Cold Stores in Developing Countries, WHO, Rome. pp. 1.

Grenier, Ph., and M. Pons (1984). Experimental and Theoretical Results on the Use of an Activated Carbon CH_3OH Intermittent Cycle for Application to a Solar Powered Ice Maker. In S. V. Szokolay (Ed.) Solar World Congress, Vol. 1. Pergamon Press. pp. 500-506.

Guilliminot, J. J., F. Meunier, G. Marsin, and D. Royer (1981). In: Reider, D. (Ed.). Proc. of the EC Contractors Meeting, Athens. pp. 93-100.

Holman, J. P. (1981). Heat Transfer. McGraw-Hill International Book Company. pp. 283.

Kasemsap, M. (1985), Personal Communications.

Kirk, H. J. C. (1962). The Geology and Mineral Resources of the Simporna Peninsula North Borneo. Geological Survey Department British Territories in Borneo, Kuching, Sarabak. pp. 40-118.

Liney, P. E. (1982). Thermodynamic Properties of Methanol. Chemical Engineering, pp. 50-51.

Marel, H. W. van der, and H. Beutelspacher (1976). Atlas of the Infrared Spectroscopy of Clay Minerals and their Admixtures. Elsevier Scientific Publishing Company. pp. 292-298.

Meunier, F. and B. Mischler (1979). Solar Cooling through Cycles using Microporous Solid Adsorbents. In: Boer, K. W, and B. H. Glenn (Eds.), SUN II, Pergamon Press. pp. 676-680.

Meunier, F., Ph. Grenier, J.J. Guilleminot, and M. Pons (1986). Solar Powered Refrigeration Using Intermittent Solid Adsorption Cycles. To be published in the J. Solar Energy Engineering.

Minato, H., and T. Tamura (1978). Production of Oxygen and Nitrogen With Natural Zeolites. In: Sand, L. B., and F. A. Mumpton (Eds.). Natural Zeolites, Occurrences, Properties, Use. Pergamon Press Ltd. pp. 509-516.

References (Contd.)

Noh, J. H., and S. J. Kim (1986). Zeolites from Tertiary Tuffaceous Rocks in Yeongil Area, Korea. In: Murakami, Y., A. Iijima, and J. Ward (Eds.). New Developments in Zeolite Science Technology. Proc. of 7th International Conference.

Ota, S., and T. Sudo (1949). Studies in Oya-ishi Part 2, Mineralogical Composition. In: Sand, L. B., and F. A. Mumpton (Eds.). Natural Zeolites, Occurrences, Properties, Use. Pergamon Press Ltd. pp. 451-470.

Perry, R. H., and C. H. Chilton (1973). Chemical Engineer's Handbook. McGraw-Hill Kogakusha Ltd. pp. 5-22.

Polayani, M. (1970). Verh. deut. phys. Ges. In: Smisek, M., S. Cerney (Auths.). Active Carbon Manufacture, Properties and Applications. Elsevier Publishing Company. pp. 71-162.

Reid, R. C., J. M. Prausnitz, and T. K. Sherwood (1977). The Properties of Gases and Liquids. McGraw-Hill Book Company. pp. 629-679.

Saisithi, P. (1982) Present Status of Food Technology in Thailand Country Report, Institute of Food and Product Development, Kasesart University. pp. 23.

Smisek, M., S. Cerny (1970). Active Carbon Manufacture, Properties and Applications. Elsevier Publising Company. pp. 71-162.

Sridhar, K. (1987). Studies on Activated Carbon-Methanol Pairs with Relevance to Ice Making. M. Eng. Thesis, Asian Institute of Technology, Bangkok (Unpublished). p. 84.

Srivastava, N. K. (1987). Private Communications.

Tchernev, D. I. (1978). Solar Energy Application of Natural Zeolites. In: Sand, L. B., and F. A. Mumpton (Eds.). Natural Zeolites, Occurrences, Properties, Use. Pergamon Press Ltd. pp. 479-485.

Tchernev, D. I. (1984). Use of Natural Zeolites in Solar Refrigeration. ASSET, 6, NO. 5. pp. 21-24.

Uppal, A. H., B. Norton, S. D. Probert, and J. C. McVeigh (1986). Solar Adsorption-Cycle Refrigerator for Vaccine Storage. In: McNelis, B., and J. Morton (Ed.) Solar Energy for Developing Countries Power for Villages. ISES, U. K. Section. pp. 28-36.

References (Contd.)

Vandendriessche, H. (1976) 'Tropical Fruit Processing Industry: A Case studies of the industry in Developing Countries' Developing Centre of the Organisation for Economic Cooperation and Development, Paris. pp. 31-32.

Vaughan, D. E. W. (1978). Properties of Natural Zeolites. In: Sand, L. B., and F. A. Mumpton (Eds.). Natural Zeolites, Occurrences, Properties, Use. Pergamon Press Ltd. pp. 353-371.

Wadia, D. N. (1975). Geology of India. Tata McGraw-Hill Publishing Co., New Delhi. pp. 281.

Worek, W. M. (1986). Personal Communication.

World Health Organisation (1981). Specifications for Photovoltaic Refrigerator WHO EPI/9.81/CC.

Zhu, Z. (1987). Testing of a Solar Powered Zeolite-Water Refrigerator. M. Eng. Thesis, Asian Institute of Technology, Bangkok (Unpublished). p. 95.

APPENDIX A

Design Calculations

The solar collector consists of 38 kg of copper, 3.85 kg of brass. The total amount of charcoal that can be filled in the generator/collector is 17.8 kg. From the p-T-x diagram, it is clear that the rich concentration of methanol is 15% and the weak concentration will be 7% if the generator temperature reaches 100°C. If the system follows the ideal cycle, the collector, charcoal and the methanol adsorbed in the charcoal have to be sensibly heated to 86°C. Thus the heat to be supplied during the sensible heating process from initial temperature of 30° to 86°C is:

$$Q_{1-2} = (38 \times 0.38 + 3.85 \times 0.385)\ (86 - 30) + (17.8 \times 0.7 + 17.8 \times 0.15 \times 2.55)\ (86 - 30) = 1970.7 \text{ kJ.}$$

Similarily, the heat supplied during the generation process from a temperature of 86°C to the maximum generator temperature of 100°C when the concentration of methanol in the charcoal decreases to 7% is:

$$Q_{2-3} = (38 \times 0.38 + 3.85 \times 0.385 + 17.8 \times 0.7 + 17.8 \times (0.15 + 0.07)/2 \times 2.55))\ (100 - 86) + 17.8 \times 1500 \times (0.15 - 0.07) = 2603.3 \text{ kJ.}$$

So the total heat to be supplied by the collector is the sum of Q_{1-2} and Q_{2-3}, and is equal to 4573.9 kJ. The total heat needed to heat the container from the state 1 to 3 is 1114.6 kJ, which is approximately 24.4% of the total heat that has to be supplied to the system.

If we assume the average efficiency of the solar collector equal to 30%, the total incident solar energy on the surface of the collector has to be 15.25 MJ. But if the efficiency of the solar collector is 35%, the above amount reduces to 13.07 MJ. Since the average solar radiation for Bangkok is about 16 MJ/m^2, the peak being approximately 20 MJ/m^2 (Exell and Sarikari, 1976) the solar collector has sufficient area to supply the required amount of heat to the system.

Estimation of the Cooling Produced

If we negelet the thermal mass of the receiver, the evaporator, and heat leak, the net cooling produced by the evaporation of about 1.4 kg of methanol is 1537.2 kJ. Thus the thermal coefficient of performance of the system is 33.6% but the overall coefficient of performance will be between 10 to 11.7%. But the thermal mass of the receiver, evaporator and the heat leak to the receiver/evaporator box will reduce this

performance further. The overall coefficient of performance of the system is expected to be around 10% and the system is expected to produce about 3 kg of ice from water initially at 30°C.

Estimation of Heat Lost by the collector during Adsorption

After the generator passes the highest temperature for the day, the back insulation of the collector can be lowered to cool the generator and the charcoal contained in it. If we assume half of the circumference of each tube to be exposed to the ambient air the total heat transfer area is approximately 1.5 m^2. The heat loss from the back of the collector will be mainly by three modes of heat transfer (i) natural convection, (ii) forced convection due to wind, and (iii) radiation.

(i) Heat Loss by Natural Convection

For a heated plate facing downward the Nusselt number Nu is given by Holman (1981) as follows:

$$Nu = 0.56\ (Gr\ Pr\ \cos\theta)^{1/4}.$$

But the Grashof number $Gr = g\,\beta\,(T_w - T_\infty)\,x^3/\nu^2$,

where

- β = Volume coefficient of expansion = 1/T, where T is in kelvins,
- T_w = Wall temperature(K),
- T_∞ = Free stream temperature(K),
- x = Length of the plate(m),
- ν = Kinematic viscosity of air = μ/ρ , (m^2/s),
- μ = Dynamic viscosity (kg/m-s),
- Pr = Prandl number = ν/α, and $\alpha = k/\rho\, c_p$,
- k = Conductivity of air (W/m-K),
- α = Diffusivity (m^2/s),
- θ = Angle made by the heated plate with the vertical, (degrees).

In the above equation T is calculated as:

$$T = T_{\infty} + 0.25\ (T_w - T_{\infty}).$$

Other properties are evaluated at temperature T_1 which is given as:

$$T_1 = T_w - 0.25\ (T_w - T_{\infty}).$$

Assuming the wall temperature equal to 35°C and the free stream temperature of 30°C, β is equal to 1/304.4 and the fluid properties have to be evaluated at 29°C. This gives Gr Pr equal to $687E10^6$. Thus the convective heat tranfer coefficient

can be calculated as:

$$h_c = Nu\ k/x.$$

The above equation gives a convective heat tranfer coefficient due to natural convection h_c for 1.2 m long tube equal to 1.39 W/m^2-K.

(ii) Heat Tranfer due to Wind

Assuming the average wind speed of 1 m/s and applying the empirical relation of Watmuff, Charter and Procter (Exell, 1983), the convective heat tranfer coefficient due to wind flowing over the plate is:

$$h_w = 2.8 + 3.0 = 5.8\ W/m^2\text{-}K.$$

Thus the total heat lost by natural convection and the wind blowing across the exposed area of 1.5 m^2, assuming the average temperature difference of 5°C between the back of the collector plate and ambient, is equal to 53.92 W.

(iii) Radiation

Assuming a temperature difference of 5°C between the collector and the ambient at 30°C, and emissivity of the back of the coated collector equal to 0.8, the heat transfer through the surface area of 1.5 m^2 is:

$$q_r = \epsilon \sigma (T_w^4 - T_a^4) A$$
$$q_r = 0.8 \times 5.669 \times 10^{-8} (308.15^4 - 303.15^4) \times 1.5$$
$$= 39.5\ W.$$

Thus the total heat lost by the back of the collector by above three modes of heat transfer is equal to 93.4 W. If the time to release the heat is 12 hours, the total heat that can be lost is equal to 4036 kJ. The heat to be lost during adsorption period is equal to 2731 kJ. Thus the back of the collector can dissipate the heat during adsorption. It must be remembered that heat will also be lost from the top of the collector.

PHOTOGRAPHS

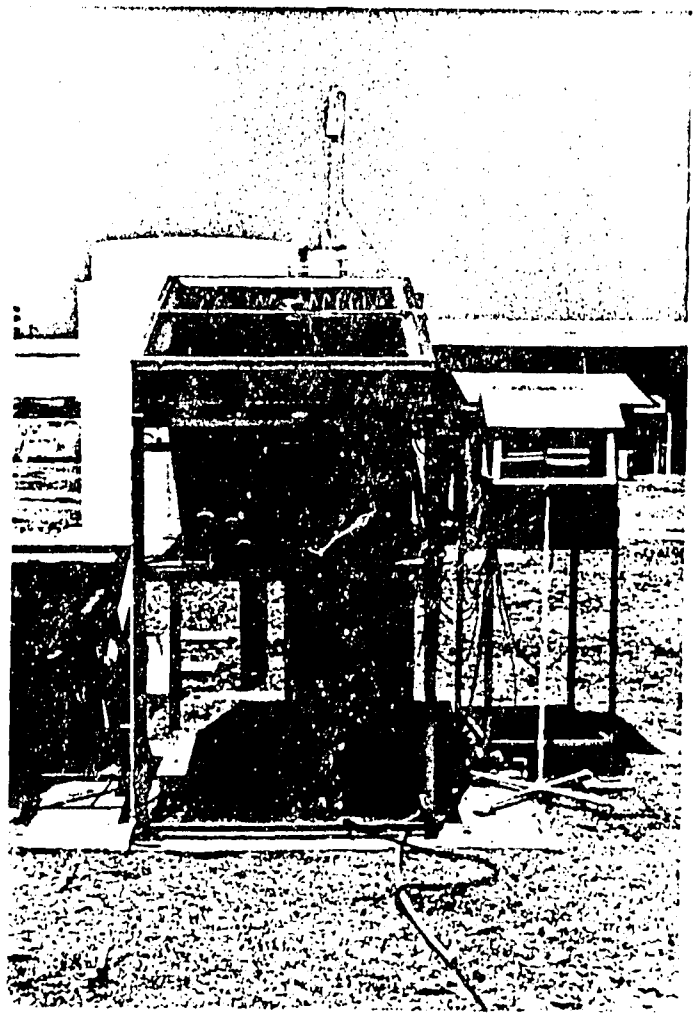

Front view of the solar refrigerator.

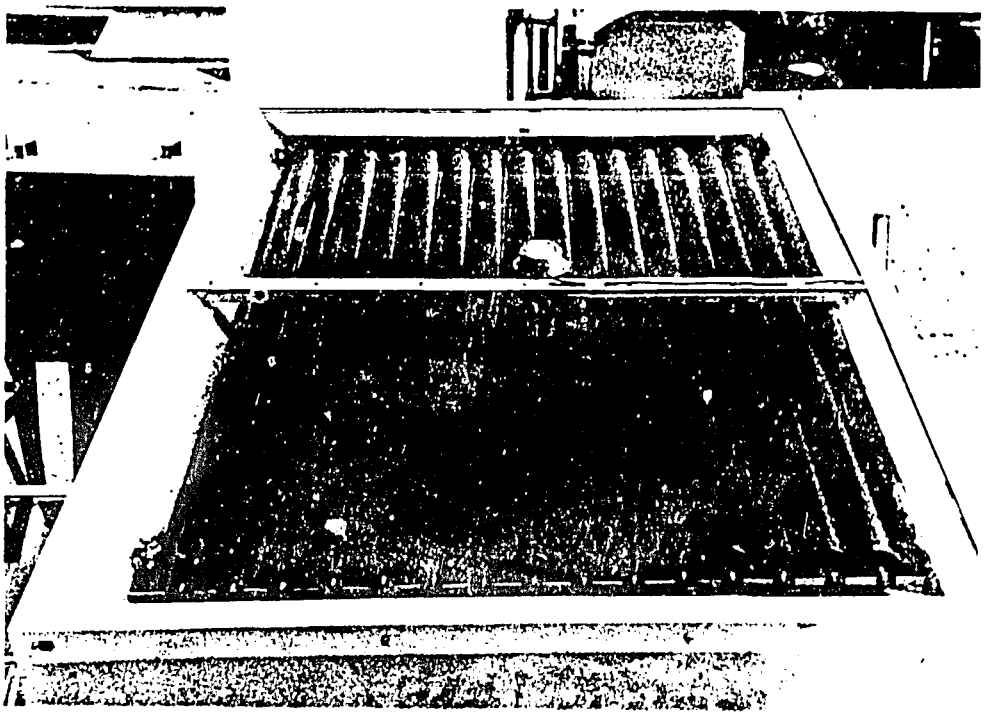

Solar collector.

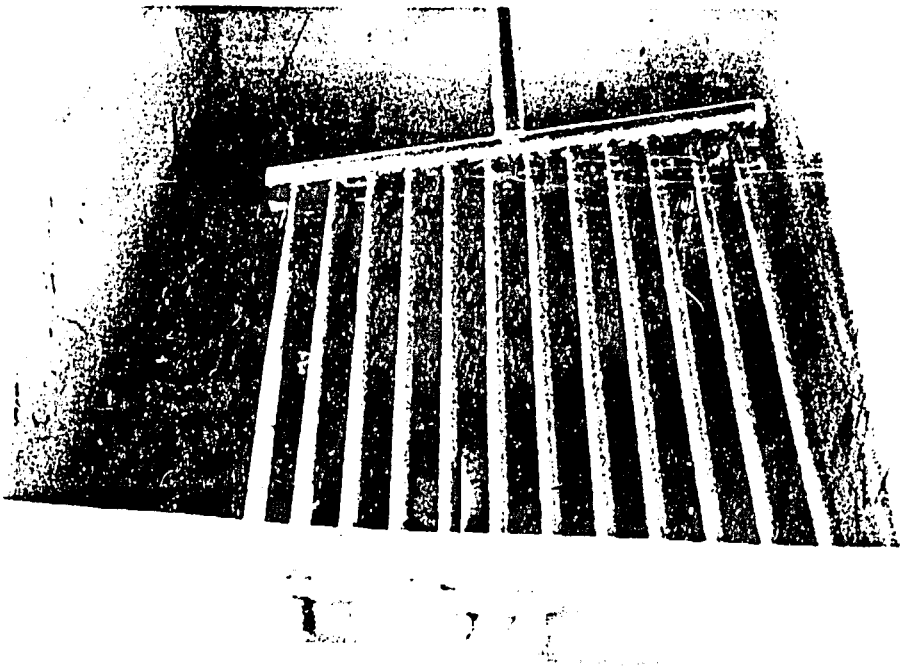

Condenser

Isolation valves and ice box

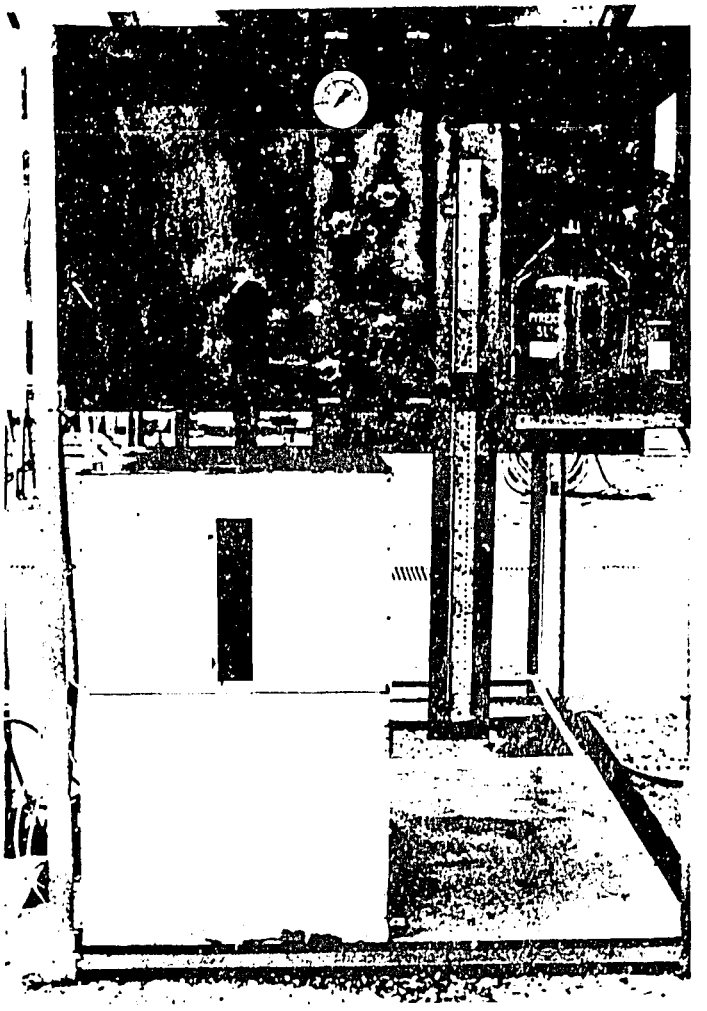

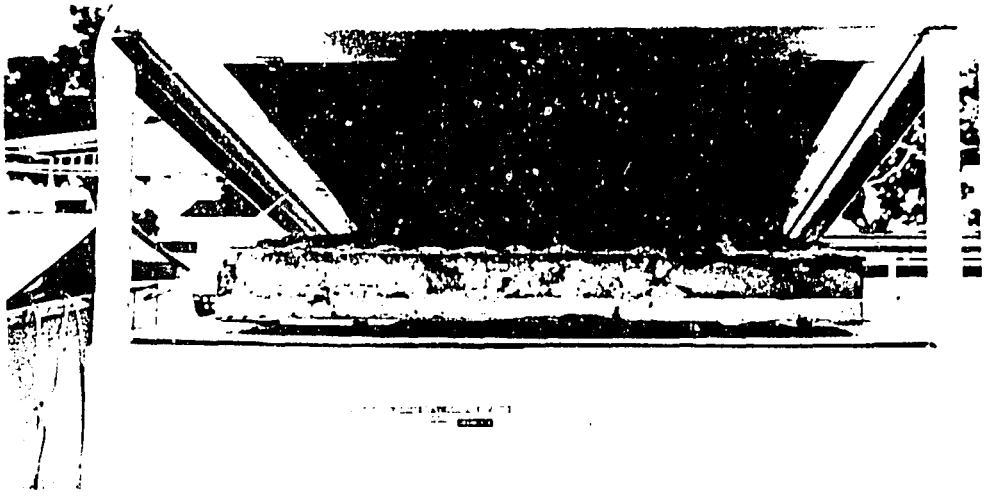

Back of the solar collector showing insulation lowered.